Application of Adverse Outcome Pathway framework in assessing nanogold exposure to *Daphnia magna*

A Mbangatha

orcid.org/0000-0001-9307-8226

Dissertation submitted in fulfilment of the requirements for the degree *Master of Science in Environmental Sciences* at the North-West University

Supervisor: Dr TL Botha

Co-supervisor: Prof V Wepener

Graduation May 2022

29294746

Acknowledgements

- I would like to express my gratitude to the following people:
- I would like to thank God Almighty for the love and support that HE has shown during this process, having an opportunity to work with considerate and thoughtful individuals that I will mention.
- My dearest supervisor, Dr Tarryn Lee Botha (I normally call her Dr T), pursuing this master's degree was because of your consistent persuasion. Thank you for your kind encouraging words and continuous support, I will be forever grateful. Thank you for mothering me, you are family (believe that). You are one of best people I have come across in my life, I am completely blessed to have met you and I appreciate you.
- My co-supervisor, Prof Victor Wepener, who will be forever smiling. Thank you for the opportunity you have given me to be a co-supervisor for the honours student 2021 and while I was doing my master's degree. Thank you for trusting and believing. I am completely blessed to have met you and I appreciate you. You are gentle and kind.
- To my supervisors (Dr T and Prof), it was an honour and privilege to work with you. You are indeed a blessing from God for me.
- I would like to thank the North-West University for the opportunity to study in this institution.
- I would like to thank MINTEK for supplying the Gold nanomaterials for this study.
- I would like to thank the financial assistance of NRF (National Research Foundation) of South Africa. Opinions, findings and conclusions or recommendations expressed are that of the author(s), and not of the NRF.
- I would like to thank NABF (National aquatic bioassay facility) for access of advanced resources/equipment.
- Thank you, Dr Josie South (Lecturer in ecology at the University of Leeds) for assisting with functional response in analysing data and sharing expert skills to carry out the functional response experiments in this study.
- Thank you, Suanne Bosch for assisting with characterization and dissolution.
- Thank you, Hannes Erasmus for assisting in dissolution samples to be analysed using GFAAS (Graphite furnace atomic absorption spectrometer) in this study.
- Thank you Makolobe Mabotja, Bianca Van der Linde, Armagh Cook and Hanro Pearson for assisting with media preparation, inoculation of algae and daphnia culture during this study.

- To my dearest best twin sister, Asavela Mbangatha (best friend) thank you for your encouraging wise words and forever supporting me in everything I do.
- I would like to express my gratitude to my parents (Zolile Measurement Zwelinzima Mbangata and Batandwa Mbangata), family and friends for your love and support.
- To my roommate (Eva Marumo), your constant positive words and advice during this study have been handful. Our long conversations at the kitchen were a stress reliever for me personally.

Abstract

Nanotechnology has found its way into almost all aspects of technology, science and every-day life and is a promising field for future advancements. Nanomaterials (NMs) are regarded as materials where one dimension has a size range between 1- 100 nm, and they may occur in several different elemental cores and shapes with different surface coatings. The developmental of gold nanomaterials (nAu) has become advantageous as it is applicable for medicinal diagnosis (rapid test kits), imaging and as a drug delivery vector. Once NMs are released into the aquatic environment, at all stages of their product lifecycle, they have potential to cause harmful effects on aquatic organisms. However, there is limited information regarding harmful effects of these NMs especially at the molecular level. *Daphnia magna* is a planktonic crustacean known to be a filter feeder ingesting particles, microorganisms, and many other unicellular and filamentous algae species found in aquatic environment. *Daphnia magna* is an internationally recognized test organism thereby making them an important species in bioassays and have internationally standardized Organisation for Economic Co-operation and Development (OECD) protocols for toxicity testing. The adverse outcome pathway (AOP) consists of a molecular initiating event (MIE), collective key events (KEs) that can be measured which lead to an adverse outcome (AO), that needs to have a regulatory consequence. The AOP framework will be utilized in this study to address adverse effects of nAu (CTAB capped rod shaped nAu and citrate capped spherical nAu) and their ionic bulk Au on *D. magna* at different levels of biological organisation.

The first aim of this study was to determine the acute and chronic toxicity of nAu and ionic Au using *D. magna* as indicator organism. The first objective was to determine the physico-chemical characteristics of the two nAu's and ionic Au in the environmental media to explain the acute and chronic responses observed in *D. magna*. Secondly, to determine the LC10, LC20 and LC50 of nAu and ionic Au based on mortality data using the OECD202 protocol. The second aim was to use the AOP framework to determine the sub-lethal effects of nAu and ionic Au on *D. magna*. The objectives were as follow: To determine the MIE at the molecular level (metabolomics), KE at the whole organism level (physiological changes based on swimming behaviour, heart rate, and respiration) and AO at community level (functional response and reproduction). To propose an AOP for nAu and ionic Au based on the MIE, KEs and AO, *D. magna* were exposed to sub lethal concentrations of CTAB capped rod shaped nAu [LC10 (2 µg/L) & LC20 (4 µg/L)] and citrate capped nAu [LC10 (2 mg/L) & LC20 (20 mg/L)] and ionic Au [LC10 (1 µg/L) & LC20 (4 µg/L)], following OECD protocol. Metabolites and associated pathways disrupted were quantified using

Gas chromatography coupled with time of flight mass spectrometry (GCxGC-TOF-MS). Multivariate analyses was done using MetaboAnalyst software to statistically identify the unique metabolites produced following exposure to the nAu and ionic Au and determine which metabolic pathways (MIE) were influenced The KEs were measured as follows: After 48 h exposure video recordings were taken and the heartbeat of *D. magna* was counted manually by playing the video clip in slow motion including the use of a pen and paper to tap the beats, respiration was measured using a 24 well sealed Loligo Systems® microplate chamber with PreSens precision sensing to measure oxygen consumption. CytoViva® dark field hyperspectral imaging was conducted in this study to examine the accumulation of nAu and physical biological damage of ionic Au exposure of daphnids. Individual and community behavioural recordings were taken at 0 h and at 48 h using a Basler monochrome GigE video camera and videos were analysed using Ethiovision X14 software. The exposed daphnids response to predation was quantified using functional response with fish (*Danio rerio*) used as a predator fed different prey densities and monitored for 30 minutes. CTAB capped rod shaped nAu had a size of ± 40 nm with an LC50 of 12.1 µg/L and had the highest acute toxicity of all compounds tested. The reproduction of *D. magna* was significantly influenced with decrease amino acids, therefore increasing energy requirement reserves resulting *D. magna* to have adverse effects (e.g. decline in reproduction) affecting physiological changes (heart rate, respiration, and behaviour). Citrate capped nAu had a size of ± 20 nm and were spherical in shape with a LC50 of >100 mg/L while ionic Au had a LC50 of 57 µg/L. The study revealed different physiological responses between exposure groups compared to the control. Only the highest exposure concentrations (LC20) resulted in significant ($p<0.05$) physiological changes with increased heart rate and corresponding decrease in oxygen consumption in *D. magna*. Both exposure concentrations of the nAu groups increased significantly ($p <0.05$) when compared to the control. However, ionic Au exposure groups showed a significant decrease ($p < 0.05$) when compared to the control.

This study revealed that a nano-specific response can be observed and the AOP framework can be utilized to determine the effect of two different nAu and ionic Au in an aquatic ecosystem using *D. magna* as a model organism.

Keywords: Adverse outcome pathway, *Daphnia magna*, Swimming behaviour, Respiration, Heart rate, Functional response, Reproduction.

List of Abbreviations

A

AgNPs	Silver nanoparticles
ANOVA	Analysis of variance
AOP	Adverse Outcome Pathway
AO	Adverse outcome
Au	Gold
AuNPs	Gold nanoparticles

C

CTAB	Cetrimonium bromide

D

DLS	Dynamic light scattering
DNA	Deoxyribonucleic acid

E

EC	Effective concentration

F

FR	Functional response

G

GCxGC-TOF-MS	Gas chromatography coupled with time of flight mass spectrometry
GFAAS	Graphite furnace atomic absorption spectrometer
GLM	Generalized linear model

K

KEs	Key events

KEGG	Kyoto Encyclopedia of Genes and Genomes
K-M	Kaplan-Meier survival curves
L	
LC	Lethal concentration
LOWESS	Locally weighted scatterplot smoothing
M	
MIE	Molecular initiating event
MLE	Maximum likelihood estimation
MS	Mass spectrometry
N	
NABF	National Aquatic Bioassay Facility
NAD	Nicotinamide adenine dinucleotide
NADP	Nicotinamide adenine dinucleotide phosphate
nAu	Gold nanomaterials
nAu	(CTAB rod shaped nAu and citrate capped nAu)
NMs	Nanomaterials
NMR	Nuclear magnetic resonance
NOAEL	No observed adverse effect level
NPs	Nanoparticles
NRF	National Research Foundation
O	
OECD	Organisation for Economic Co-operation and Development
P	
PCA	Principal Component Analysis

PLS-DA	Partial least squares-discriminant analysis
R	
RNA	Ribonucleic acid
RO	Reverse osmosis
ROS	Reactive oxygen stress
S	
SDR	Sensor Dish Reader
SE	Standard error
T	
TDS	Total dissolved solids
TEM	Transmission Electron Microscopy
TiO2	Titanium dioxide
V	
VIP	variable importance in projection

Table of Contents

List of Tables

List of Figures

Chapter 1

General Introduction

Chapter 1: General Introduction

1.1 *Daphnia magna* as a test organism

Daphnia magna is a planktonic crustacean genus that is found in freshwater. They belong to the phylum **Arthropoda**, subphylum **Crustacea**, class **Branchiopoda**, order **Cladocera** and family **Daphniidae**. *Daphnia* spp. are also known as water fleas (Carpenter et al., 1987; Dodson and Hanazato, 1995a; Tessier et al., 2000). This is due to their saltatory (hopping- two legs move together without changing) swimming behaviour. *Daphnia magna* are an internationally recognized test organisms thereby making them an important species in bioassays. When conducting bioassays, the standard Organisation for Economic Co-operation and Development (OECD202) protocol guideline for testing of chemicals (OECD, 2004) specific to daphnia is followed. Factors making them ideal indication species are their reproductive abilities, limited lifespan, simple cultivation within a laboratory (Gökçe et al., 2018) and they are an important source of food for fish and other aquatic organisms in an ecosystem and therefore are a vital part of the aquatic food web (Dodson and Frey, 1991; Dodson and Hanazato, 1995b; Ignace et al., 2010). Moreover, these species are transparent allowing the measurements of other physiological functions such as heart rate (Baumer et al., 2002; Pirow et al., 2004). *Daphnia magna* are filter feeders (Wong and Ward, 1972) which allows them to take up food particles and as a consequence they may also ingest nanoparticles with a size range between 240- 640 nm from the water column. With a capability of filtering up to 400 mL of water daily the chances of ingestion of nano-contaminants are high (Botha et al., 2016; Wray and Klaine, 2015). However, once the *D. magna* are exposed to nanoparticles, studies indicate that these particles remain in the external compartments such as the external surface of the gut or on the carapace (Botha et al., 2016; García-Cambero et al., 2013; Wray and Klaine, 2015).

1.1.1 Life cycle of species of *D. magna*

Asexual reproduction

The environment of daphnids changes with season and they are adopted to these changes. During spring, female daphnids begin to grow, and they may have one egg or as many as forty eggs (clutch of eggs) in the brood pouch (dorsally beneath the carapace) (Ebert, 2005). These eggs grow without fertilization and all become female daphnids (asexual mode of reproduction)

(Figure 1.1). No males are produced until autumn. For three days, the eggs (diploid asexual eggs) develop, at first there are only dark spheres but, after a few hours the spheres begin to take the shape of daphnids at 20°C. After a day, some of the body structures are formed and neonate daphnids may move in the brood pouch and will resemble the adult daphnia (Wetzel, 1975). After two days, the heart of the unborn neonate is visibly beating. After three days, there are many matured and fully formed neonate daphnids. The asexual reproduction reaches its climax as the embryonic neonate struggle free of the brood pouch via ventral flexion (Dewey and Parker, 1964). After they emerge, they lie quietly in the water until their tissue is filled with moisture and expand. At first, they are soft, but soon their exoskeleton hardens, and they can no longer grow. The neonates repeatedly molt (cast off their exoskeletons) until their carapace hardens (Anderson and Jenkins, 1942). This process of growth and shedding continues for about 15 days until neonates mature and begin to develop their own eggs (Ebert, 2005).

Sexual reproduction

As winter approaches or conditions grow less favourable, a change takes place in the daphnids life cycle. The male daphnids appear, and female produce a new kind of egg (haploid eggs- sexual eggs), which the male daphnids fertilize (sexual mode of reproduction) (Figure 1.1). The haploid eggs are enclosed in a thickened and darkly pigmented shell called an ephippium. These fertilized eggs are known as winter eggs and are capable of surviving the environmental change (shortage of food supply; increased population of the culture; reduced temperature) without damage (Banta, 1939; Stross and Hill, 1965). Most of the daphnids die and sink to the bottom with their winter eggs which remain dormant. These resting eggs are surrounded by a protective ephippium structure. This structure assists in melanisation of the two large eggs that undergo a diapause period before female offspring will hatch from them). When spring warms the air and water, the winter eggs will hatch and grow into female offspring. Daphnids are valuable to man because by studying them, scientist made discoveries that can be applied to human life (Ebert, 2005; Ward and Whipple, 1959).

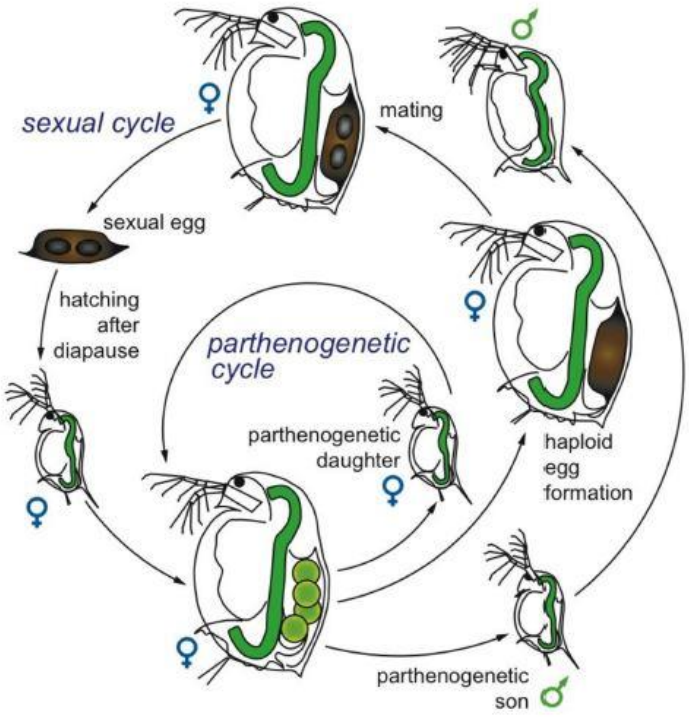

Figure 1. 1: Life cycle of a parthenogenetic *Daphnia magna*. This diagram shows the sexual and asexual life cycle of *D. magna* (after Ebert, 2005).

1.2 Gold nanomaterials (nAu)

Nanotechnology has become prominent in the world of science and technology. This is because of its potential revolutionary advances in the production and applications of nanomaterials and the impact of its use in several fields such as microelectronics and i.e. energy storage units and therapeutics (Karatzas et al., 2020). Furthermore, these NMs are being developed for application in medicinal diagnosis, imaging and as a drug delivery vector (Riediker et al., 2019). Nanomaterials are regarded as materials where one dimension has a size range between 1- 100 nm and they may occur in several different shapes with different surface coatings (OECD, 2020). The NMs are widely used in many products, however, the harmful effects of these NMs are unknown. It is known that NMs may get released into aquatic ecosystems (Oleszczuk et al., 2015) but there is limited information on the behaviour and toxicity of these NMs in aquatic food webs (Kabir et al., 2018; Gökçe et al., 2018; Oleszczuk et al., 2015).

Gold nanomaterials (nAu) are known to be stable and consist in different shape and structures. These include nanospheres, nanorods, nanocubes, nanocages, nanoshells, and nanoflowers. They have different synthetic approaches that need to be followed (Li et al., 2015; Xiao et al.,

2019). The optical properties of nAu are dependent on surface plasmon resonance. This explains the interaction of electrons between negative and positive charges at the surface (Ramalingam, 2019). The size of nAu dictates the characteristics of the nanoparticles and the functions that it performs. Small sized nAu (2 nm - 15 nm) are usually applied in immunohistochemistry, microscopy (light and high magnification Transmission Electron Microscopy - TEM) and as biomarkers. Medium sized nAu (20 nm - 60 nm) are used in environmental detection and purification, drug delivery, biomarkers, chemical sensors, and DNA (Deoxyribonucleic acid) detection. Large sized nAu (80 nm - 250 nm) are applied in forensic science, electronic devices, and optical mammography (Hu et al., 2020; Pissuwan et al., 2019; Shah et al., 2014). The focus of this study is on two different forms of nAu with two different functionalized groups attached to assist with the stabilization of the nanomaterials in aqueous suspension. The materials studied were: nanorods capped with cetrimonium bromide (CTAB) and citrate-capped nanospheres.

1.3 The Adverse outcome pathway (AOP)

Adverse Outcome Pathways (AOP) will be used as a framework to address adverse effects of nAu and their ionic bulk elemental Au on *D. magna* at different levels of biological organisation. Adverse Outcome Pathway utilises pathway-based concepts that specify specific modes of action (Ankley et al., 2010). The **Mode of action** can be defined as a “common set of biochemical, physiological, or behavioural responses that characterize an adverse biological response” (Borgert et al., 2004; European Centre For Ecotoxicology And Toxicology Of Chemicals (ECETOC) 2007). Adverse Outcome Pathways consist of collective key events (KEs) that can be measured and lead to an adverse outcome (AO), that needs to have a regulatory consequence. The first event of an AOP is the molecular initiating event (MIE) where the initial chemical interaction takes place. An AOP is referred to as chemically-agnostic indicating an exposure-response relationship that could result from environmental stimuli where chemical or non-chemical stressors influence the MIE (Ankley and Edwards, 2018; Villeneuve et al., 2014). However, an AO could be prevented by the organism through homeostatic mechanisms (Bossuyt and Janssen, 2005). The key events that were utilised in this study were sub-cellular metabolomic responses, whole organisms physiological responses (heart rate, respiration and swimming behaviour) and ecological predator-prey interactions (functional response). The AO considered in this study was the influence of nAu and ionic Au on on Daphnid reproduction.

1.4 Research question

Can the AOP framework be used to determine the effects of nAu (CTAB capped rod shaped nAu and citrate capped nAu) and ionic Au to aquatic ecosystems using *D. magna* as the indicator organisms?

1.5 Problem statement

The shape and functional group of nanomaterials will have an effect on the toxicity of nAu to *D. magna*. The AOP framework will be used to determine how the two different types of nAu (CTAB capped rod shaped nAu and citrate capped nAu) and an ionic Au (traditional metal ion) affect *D. magna.*

1.6 Research aims and objectives

The aims and objectives of the study are as follows:

Aim 1: To determine the acute and chronic toxicity of nAu and ionic Au using *D. magna* as indicator organism.

Objectives:

- To determine the physico-chemical characteristics of the two nAu's and ionic Au in the environmental media to explain the acute and chronic responses observed in *D. magna*.
- To determine the LC10, 20 and 50 of nAu and ionic Au based on mortality data using the OECD202 protocol.
- To determine the effects of nAu and ionic Au on the reproduction of *D. magna* using the standardized OECD211 protocol.
- To visualize the uptake and distribution of nAu by *D. magna* using CytoViva Hyperspectral Darkfield Imagery.

Aim 2: To use the AOP framework to determine the sub-lethal effects of nAu and ionic Au on *D. magna*.

Objectives:

- To determine the MIE at molecular level (metabolomics) and KEs at whole organism level (physiological changes based on swimming behaviour, heart rate, and respiration).

- To determine the AO (functional response and reproduction).
- To propose an AOP for nAu and ionic Au based on the KEs and AO.

1.7 Basic hypothesis

Ho: The AOP framework is not suitable to determine the effect of two different nAu and ionic Au in aquatic ecosystems using *D. magna*.

HA: The AOP framework is suitable to determine the effect of two different nAu and ionic Au in aquatic ecosystems using *D. magna*.

1.8 Outline of the dissertation

Chapter 1 introduces the key concepts of the study with the study hypotheses, aim and objectives.

Chapter 2 provides the characterization results of the two NMs used in the study and reports on the acute and chronic toxicity of the nAu and ionic Au using the OECD202 and OECD211 standardized protocols, respectively. The LC10, LC20 and LC50 concentrations were derived from the acute mortality-based data. The chronic effect of nAu and ionic Au exposure on reproduction of *D. magna* was expressed as the concentration where 50% of the reproduction was inhibited, i.e. the growth EC50. The LC10 and LC20 concentrations that were derived from the acute toxicity tests were used as the subsequent exposure concentrations to determine the effects at different levels of biological organization (Chapters 3 and 4).

Chapter 3 presents the results of the metabolomics and physiological (heart rate, respiration) responses in *D. magna* following exposure to sublethal concentrations of nAu and ionic Au.

In **Chapter 4** the individual and social behavioural (swimming) and functional responses of *D. magna* are presented following exposure to sublethal nAu and ionic Au concentrations.

The data produced in Chapters 2 to 4 are integrated into a proposed nAu AOP for *D. magna* in the conclusions **Chapter 5**. Recommendations for future studies to further refine the AOP are also provided in this chapter.

Chapter 6 presents the references cited in the dissertation.

Chapter 2

Acute and Chronic Exposures

Chapter 2: Acute and Chronic Exposures

2.1 Introduction

Gold is a soft, malleable transition metal with the symbol Au represented by electron configuration of (Xe) 4f145d106s1 (Shah et al., 2014; Yang et al., 2015). Gold nanoparticles (nAus) are widely used for molecular applications such as genomics, immunoassays, and clinical chemistry. They serve as an important component in medicinal applications such as detection and photothermolysis of microorganisms and cancer cells (Vicky et al., 2010). The size of AuNPs dictates the characteristics of the nanoparticles and the functions that it performs. Nanogold can exist in various shapes such as nanospheres, nanocubes, nanostars, nanoshells, nanoclusters and rod-shaped (Khan et al., 2014). Gold colloid is quasi-spherical shape known as Au nanospheres. It consists of a single-crystal structure together with a circular projection under TEM imaging. Gold nanospheres do not have sharp corners on the surface. The size of Au nanospheres might be influenced by the alteration ratio of citrate and Au. However, Au nanorods consists of anisotropic shape (the materials characteristic features are direction-dependent, i.e. permitted to change with more than one structural framework to depict them (Das et al., 2011; Yang et al., 2015). Both spherical and rod-shaped nanogold are applied in biosensing, photothermal therapy, bioassays, biomedical imaging, drug delivery and more recently in solar cell development which could lead to environmental release (Kozanoglu et al., 2013; Qiao et al., 2011).

Characterization is an essential aspect in nanoscience since the effect of a NMs can be directly linked to its shape, size, agglomeration, and metal ion dissolution (Khan et al., 2019). Composite analysers such as a Malvern Zetasizer Nano series can be used to measure particle surface charge (zeta potential) and size (dynamic light scattering - DLS). Dynamic light scattering has been utilized with coherent light sources such as commercial lasers to measure macromolecules and small particles in dilute suspension. It is important to note that DLS for particle sizing is proficient in providing estimated averaged particle size in suspension. The data acquisition is fast, effective and can be accessed in the wide submicron range of particle sizes (Hassan et al., 2015; Verma et al., 2014). Transmission electron microscopy can visualize nanomaterials and provide a highly magnified image using a particle beam of electrons transmitted through an object. They have the ability to magnify objects by up to 2 million times allowing for visualization of primary particle sizes and agglomeration of nanomaterials in the nanometer range. By observing changes

in NMs physico-chemical characteristics, it is possible to get a better understanding of the contribution that these factors make to the toxicity of NMs in the environment and which nanomaterial characteristics should be changed or addressed to make them less hazardous (Bozich et al., 2014).

Acute toxicity is an adverse change(s) that normally occurs within a limited period following the exposure of an organism to a single dose range of a substance which is expected to cause fifty percent death of the treated population (Lorke, 1983). On the other hand, chronic toxicity can be defined as adverse change(s) that usually occur within months or years following exposure of an organism to multiple doses of a substance. Acute and chronic toxicity aims in obtaining information at the whole organism level of the chemical's hazard without acquiring knowledge into its mechanism of action. Chronic toxicity aims in determining the effects of a substance following prolonged and continuous exposures and is therefore not aimed to observe no observed adverse effect levels (NOAEL), but rather to progressively damage one or more critical target organs. The data generated through acute and chronic toxicity testing are utilized for risk assessment management and identification and handling of hazardous chemical products (Mohammadpour et al., 2019; Walum, 1998). Both bioassays (acute and chronic toxicity) are conducted following OECD, internationally recognized, standard protocols. Botha et al. (2015) successfully utilized standard toxicity protocols to determine the hazard (i.e. calculation of LC50 values) of spherical nAu to *D. magna* and freshwater fish species. Other studies also used *D. magna* to show reproductive effects following long-term exposures to pristine and wastewater-borne AgNPs and TiO_2NPs (Hartmann et al., 2019). *Daphnia magna* is known to be a lower invertebrates, poses no risks as it was ethically approved in this study with ethics number 01425-20-A9.

In the present study the aim was investigate, (i) the acute toxicity of nAu and ionic Au to *D. magna*, (ii) the contribution of nAu and ionic Au to *D. magna* toxicity, (iii) the longer-term reproductive effects of nAu and ionic Au on *D. magna*.

2.2 Materials and methods

2.2.1 Nanomaterial stock solution

Two shapes of nanogold with different functional groups were selected for this study: citrate capped spherical nAu (14 ± 2 nm) and CTAB capped rod shaped nAu (14 ± 2 nm). Both stock solutions were prepared and supplied by MINTEK (South Africa). The nAu stock solutions were

made up of a concentration of 1 g/L, which was further diluted using MilliQ water. The nAu's product code was TMU14G and batch numbers (20130304FKP49b; 20130308FKP52; 20140905BM001). The stocks were prepared by standard citrate reduction techniques and were sterilised using the filtration method (Frens, 1973; Murphy et al., 2008). The ionic Au was purchased at Sigma- Aldrich/Merck with product code 254169- 500MG (Gold(Iii) Chloride Hydrate, 99.995% Trace metal basis). Exposure and therefore characterization of both citrate capped nAu and CTAB capped rod shaped nAu was done in a M7 medium (OECD, 2004; OECD, 2012). The M7 medium consists of 26 salts that contain nutrients and vitamins. Dilutions were made for both citrate capped nAu and CTAB capped rod shaped nAu in a 50 mL falcon tube. Samples were sonicated for one hour at 25°C in a sonication bath filled with 450 mL reverse osmosis water, where after characterization was performed to determine size, agglomeration, and charge (zeta potential). The nominal concentrations were characterized for both were 5, 20, 60 and 100 mg /L for citrate capped nAu and µg/L for CTAB capped rod shaped nAu respectively. Characterization was carried out at time intervals 0 - and after 48-hours in the M7 medium.

2.2.2 Characterization of nAu in M7 exposure media

The size of the NMs at each concentration was measured in a 1 mL cuvette and surface charges were measured in a 1 mL folded capillary zeta cell using electrophoretic mobility on the Zetasizer instrument (Dynamic light scattering; Malvern Zetasizer Nano series, NanoZS). Transmission electron microscopy (TEM) (FEI Tecnai G2) was used to quantify the nAu diameter and particle aggregation patterns of both citrate capped nAu and CTAB capped rod shaped nAu. One drop respectively of both citrate capped nAu and CTAB capped rod shaped nAu medium was dropped onto a carbon coated copper grid and allowed to settle for a few minutes. The excess water was removed using a filter paper by touching only the edge of the droplet and the grid was allowed to dry before examination at high resolution (200 kV) and images were taken using a digital micrograph (FEI company) (Botha et al., 2015).

In order to determine ionic metal dissolution rates for the nAu, a dialysis method was used (Handy et al., 1989). Briefly three replicates of each concentration of citrate capped nAu, CTAB capped rod shaped nAu and ionic nAu were placed in M7 media. The concentrations were as follows for citrate capped nAu (20 and 100 mg/L), CTAB capped rod shaped nAu (20 and 100 µg/L) and ionic nAu (1 and 4 µg/L). Dialysis tubing (artificial semi-permeable membrane tubing that facilitates the flow of tiny molecules in solution based on differential diffusion) with a length of 10 cm was prepared by sealing the end of the dialysis tubing with a medi-clip to make a bag which

was filled with 8 mL of nAu nanomaterial solution using a pipette and sealing off the dialysis bag with a second clip. The external surface of the dialysis bag was thoroughly rinsed with Milli-Q water to avoid cross contamination before placing in a glass beaker filled with 500 mL M7 media. Control dialysis bags were filled with 8 mL M7 media that did not contain any NMs were also prepared. The solution in the beakers were stirred with a multipoint magnetic stirrer for 48 h at room temperature. Samples were taken after 48 h from the solution in the beaker to assess the Au ions that were released from the NMs in the dialysis bag. A volume of 13 mL M7 media was collected and acidified using 0.5 mL nitric acid and 1.5 mL hydrochloric acid prior to further processing. The samples were stored at room temperature prior to analysis.

Gold concentrations were measured using a graphite furnace atomic absorption spectrometer (PerkinElmer AAnalyst 600 GFAAS) that is equipped with a transversely heated graphite tube atomizer and equipped with Zeeman-effect background correction. The calibration was performed using 10 mL of an aqueous solution of the appropriate concentrations of standards. Samples were analysed in triplicate and where dilutions were required, 1% of nitric acid was used. The instrument parameters are presented in Table 2.1.

Table 2. 1: Instrumental parameters used in the determination of Au by means of graphite furnace atomic absorption spectrometer (GFAAS).

Wavelength		242.8 nm		
Slit width		0.7 nm		
Temperature program				
Step	Temperature (◦C)	Ramp time (s)	Hold time (s)	Flow
Drying	110	1	30	250
Pyrolysis	160	15	30	250
Auto zero	1 100	10	20	250
Atomization	2 200	0	5	0
Cleaning	2 450	1	3	250

2.2.3 Daphnia culture maintenance

Daphnia magna (clone MBP996-ToxSolutions Kits and Services) were maintained at the National Aquatic Bioassay Facility (NABF) at the North-West University and cultured in 5 L ISO medium

(OECD, 2004). The Standard ISO media contained calcium chloride ($CaCl_2 \cdot 2H2O$); magnesium sulphate ($MgSO_4 \cdot 7H_2O$); sodium bicarbonate ($NaHCO_3$) and potassium chloride (KCl). The media was aerated using an air stone and diffuser for 24 h prior to use (OECD, 2004; Truter, 1994) and media was replaced weekly. *Daphnia magna* cultures were kept at 20-22°C in a temperature-controlled room with a light cycle of 16 h light: 8 h dark, at a stocking density of 20-100 daphnia per litre. The daphnids were fed 1.17×10^6 cells/mL unicellular algae (*Raphidocelis subcapitata*) three times per week (Figure 2.1).

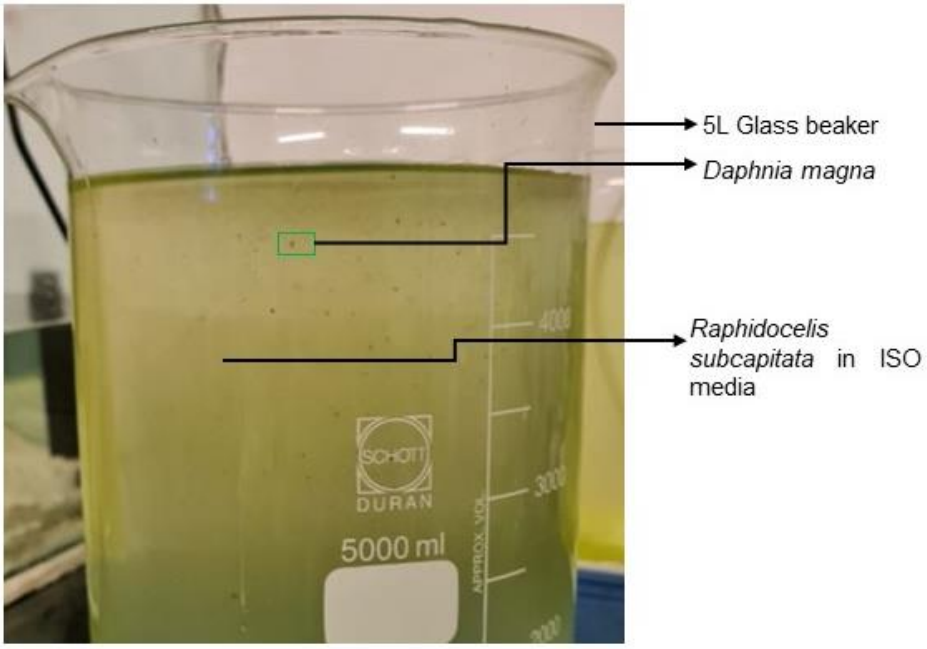

Figure 2. 1: The *D. magna* culture in 5 L glass beakers at the NABF after feeding with 1.17×10^6 cells/mL unicellular algae (*Raphidocelis subcapitata*).

2.2.4 *Raphidocelis subcapitata* culture maintenance for feeding daphnia

Primary algae cultures were kept at 22-23°C in a BG-11 media prepared using 250 mL Erlenmeyer flasks under low light intensity (Stanier and Cohen-Bazire, 1977). In order to determine the cells per mL, cells were counted using a hemocytometer. Feeding cultures were prepared by removing 100 µL cell suspension of algae from the Erlenmeyer flasks and placed in an Eppendorf and diluted by adding 100 µL of Trypan blue solution. The dye assists in distinguishing between living and dead cells. The dye passes through a membrane of dead cells so they will appear blue under a microscope while living cells exclude the dye and will appear mostly clear.

Both chambers of the hemocytometer were loaded by pipetting suspension of algae under the cover slip and the hemocytometer was placed under the microscope. Each chamber was divided into a grid pattern consisting of nine large squares. Each square has the same dimensions and contained 10^{-4} mL of suspension. The laboratory rule stated that cells should be counted into four corner squares and into the centre square. Cells counted included the cells that touched the top and left boundaries and excluded the cells that touched the bottom and right boundaries. Both living (viable) and dead (non-viable) cells were counted. Non-viable cells appeared to be dead, blurry and did not have a defined shape. Again, some cells appeared to be clumped (they were counted as two cells) or in small groups.

The calculations were conducted in replicates to get an average of total cell number per mL.

% of viable cells: Viable cells/ Total no. of cells ×100

Average no. of cells/ square: Viable cells/ Squares

Dilution factor: Final volume/ Volume of cells

Concentration (viable cells mL): Average no. of cells/square × Dilution factor × 10^4

Once calculated, subcultures at 1.17×10^6 cell/mL were stored in 50 mL falcon tubes at -20 °C in a freezer and were used to feed daphnia cultures three times per week.

2.2.5 Bioassays

Acute toxicity test

A standard daphnia Immobilization test (OECD, 2004) protocol was used to determine the LC50 of the two shapes of nAu NMs and ionic Au. The 14 nm NMs (citrate capped nAu and CTAB capped rod shaped nAu) and ionic Au were used for the exposure studies on *D. magna* from a healthy culture. The test on *D. magna* was done over a period of 48 h, at a temperature of 20 - 21°C. For acute toxicity testing neonate daphnia were hatched from ephippia according to protocols as outlined in ToxSolutions Kits and Services and one day old neonates were used for acute toxicity testing (Chapman et al., 2011).

Daphnids were placed in M7 media for 24 h prior the exposure test. The exposure tests consisted of three replicates of seven (7) neonate daphnids per beaker (n=21) including a control of M7 media and three replicates of seven (7) daphnids per beaker which contained 50 mL of exposure media. Exposures were tested across an increasing range of concentrations, i.e. for citrate

capped nAu (1, 2, 5, 10, 20, 40, 80, 160 and 240 mg/L), CTAB capped rod shaped nAu (0.5, 1, 2, 5, 10, 20, 40 and 80 µg/L) and ionic Au (1, 2, 3, 5, 10, 20 and 50 µg/L). Concentration ranges were selected following initial range finding tests. Immobilization and physico-chemical water parameters (temperature, TDS, conductivity, pH,) were noted at 24 h intervals from 0 h until completion of the test at 48 h. Any immobile daphnia were removed from the test beaker using a plastic pipette (OECD, 2004). Immobility was defined as animals that are not able to swim within 15 s after gentle agitation of the test vessel (even if they can still move their antennae) according to the OECD202 protocol.

Chronic toxicity test

The *D. magna* 28 days reproduction test was conducted following an OECD211 guideline for chronic toxicity testing with the species (OECD, 2012). The temperature was maintained between 20 - 21°C with a photoperiod of 16 h light: 8 h dark. The exposure medium and concentrations were renewed at 48 h time intervals. In addition, each beaker was supplied with 1.17×10^6 cells/mL unicellular algae (*R. subcapitata*) during media and concentration renewal. Ten first generation daphnids per concentration were individually placed in 50 mL glass beakers. The selected concentrations were below the LC50's. The concentrations were as follows: for citrate capped nAu (0.5, 1, 5, 10, 25 and 50 mg/L), for CTAB capped rod shaped nAu (0.5, 10, 40, 50, 100 and 500 ng/L) and for ionic Au (0.125, 0.25, 0.5, 1, 2 and 4 µg/L). The number of juveniles and molts produced were counted, removed, and noted daily per beaker (n=10 per concentration). Behaviour changes observed were noted each 24 h for the duration of the test.

2.2.6 Statistical analyses

The statistical analysis after acute testing was conducted using ToxRat® Solutions Software to determine the LC10, LC20 and LC50 for both ionic Au and nAu NMs. The software used a Probit analysis using linear maximum likelihood regression with immobility at 48 h. The daily counts of molts and juveniles released by *D. magna* at each concentration during the duration of the test were observed and taken into consideration. The data sets were checked for normality of distribution using D'Agostino and Pearson omnibus normality test. If the data set was normally distributed, one-way ANOVA was conducted, and the Tukey's Multiple Comparison Test was used to determine significance between groups. However, if data sets were not distributed normally, the Kruskal–Walis Test using Dunn's Multiple Comparison Test was performed to determine significance. Significance was regarded as $p < 0.05$ (Botha et al., 2016; Kelpsiene et al., 2020).

2.3 Results

2.3.1 Characterization of nAu

There was an increase in the dynamic particle diameter for all the exposure concentrations from the 14 nm (in the dispersion solution) to >200 nm in the M7 exposure media (Table 2.2). Notably the aggregation increased over exposure time with the lowest and higher concentrations of both CTAB capped rod shaped nAu (5 and 20 µg/L) and citrate capped nAu (5 and 100 mg/L) displaying larger agglomerates than at 0 h. At the mid-concentration levels there appeared to be a slight dis-aggregation with the average diameter of the NM particles reducing slightly. The Zeta potential was negative across all exposure concentrations (Table 2.2). After 48 h, it was noted that both nAu increased in charge except for CTAB capped rod shaped nAu at 100 µg/L. Both nAu NMs (Figure 2.2a) showed different sizes and shapes with the CTAB capped rod shaped nAu displaying different other shapes present (spheres and stars) while the spheres were uniform in shape (Figure 2.2b).

Table 2. 2: Size distribution (nm) and zeta potential (mV) of CTAB capped rod shaped nAu, in daphnia M7 medium across exposure concentrations.

Nominal concentration	**Size distribution (nm)**		**Zeta potential (mV)**	
CTAB capped rod shaped nAu	0 h	48 h	0 h	48 h
5 µg/L	128.8	353.7	-14.2	-15.1
20 µg/L	276.0	93.6	-20.8	-15.0
60 µg/L	100.4	190.4	-11.2	-14.1
100 µg/L	232.8	225.6	-11.6	-9.6
Citrate capped nAu				
5 mg/L	178.1	300.0	-11.5	-14.6
20 mg/L	191.6	279.0	-13.2	-13.9
60 mg/L	157.8	125.0	-12.6	-14.2
100 mg/L	127.0	254.5	-11.1	-14.0

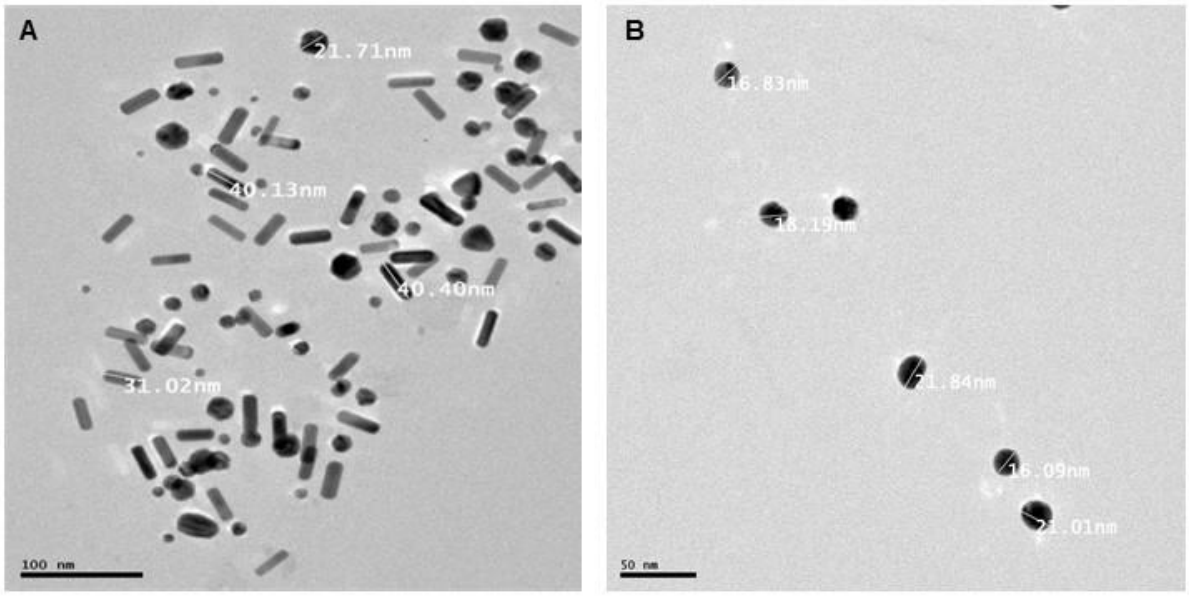

Figure 2. 2: A TEM photograph of a drop of CTAB capped rod shaped nAu (A) and citrate capped nAu (B) at 1 mg/L in MilliQ water.

2.3.2 Dissolution of Au from NMs

An accurate calibration curve was obtained with an RSD of 0.999 (Figure 2.3). The actual measured concentrations of ionic Au were within 30% of the nominal concentrations added to the exposure media (Table 2.3). Although the dissolution observed for CTAB capped rod shaped nAu was greater than for citrate capped nAu it was still very low at 1% and less (Table 2.3).

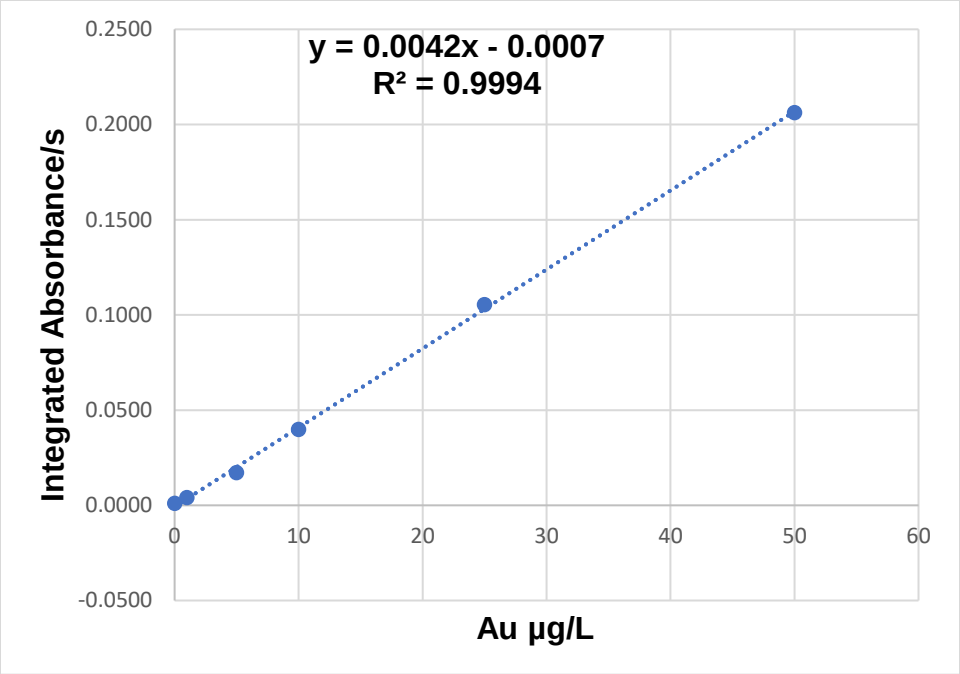

Figure 2. 3: Gold aqueous standard calibration curve used for nAu and ionic Au measurements. The dotted line represents the calibration curve (least-squares method) obtained for the aqueous standards.

Table 2. 3: Percentage recovery of ionic Au and percentage dissolution of Au ions in M7 daphnid media from CTAB capped nAu and citrate capped nAu after 48 h.

	Gold added (µg/L)	**Recovery and percentage dissolution (%)**
Ionic Au (Chloro-auric acid)	1	77.1 ± 7.2
Ionic Au (Chloro-auric acid)	6	111 ± 4.2
CTAB-capped nAu	20	1 ± 0.07
CTAB capped nAu	100	1.01 ± 0.26
Citrate capped nAu	20	0.42 ± 0.26
Citrate capped nAu	100	0.37 ± 0.3

2.3.3 Acute toxicity bioassay

The physico-chemical parameters remained stable for the duration of the test (data not presented). A dose dependent response was seen for immobilization of *D. magna* exposed to CTAB capped rod shaped nAu (Figure 2.4 A) and ionic Au (Figure 2.4 C) but not for citrate capped nAu (Figure 2.4 B). The LC50 values for ionic Au was 57 µg/L and 12.1 µg/L for CTAB capped rod shaped nAu and were more toxic compared to the citrate capped nAu (>100 mg/L) (Table 2.4).

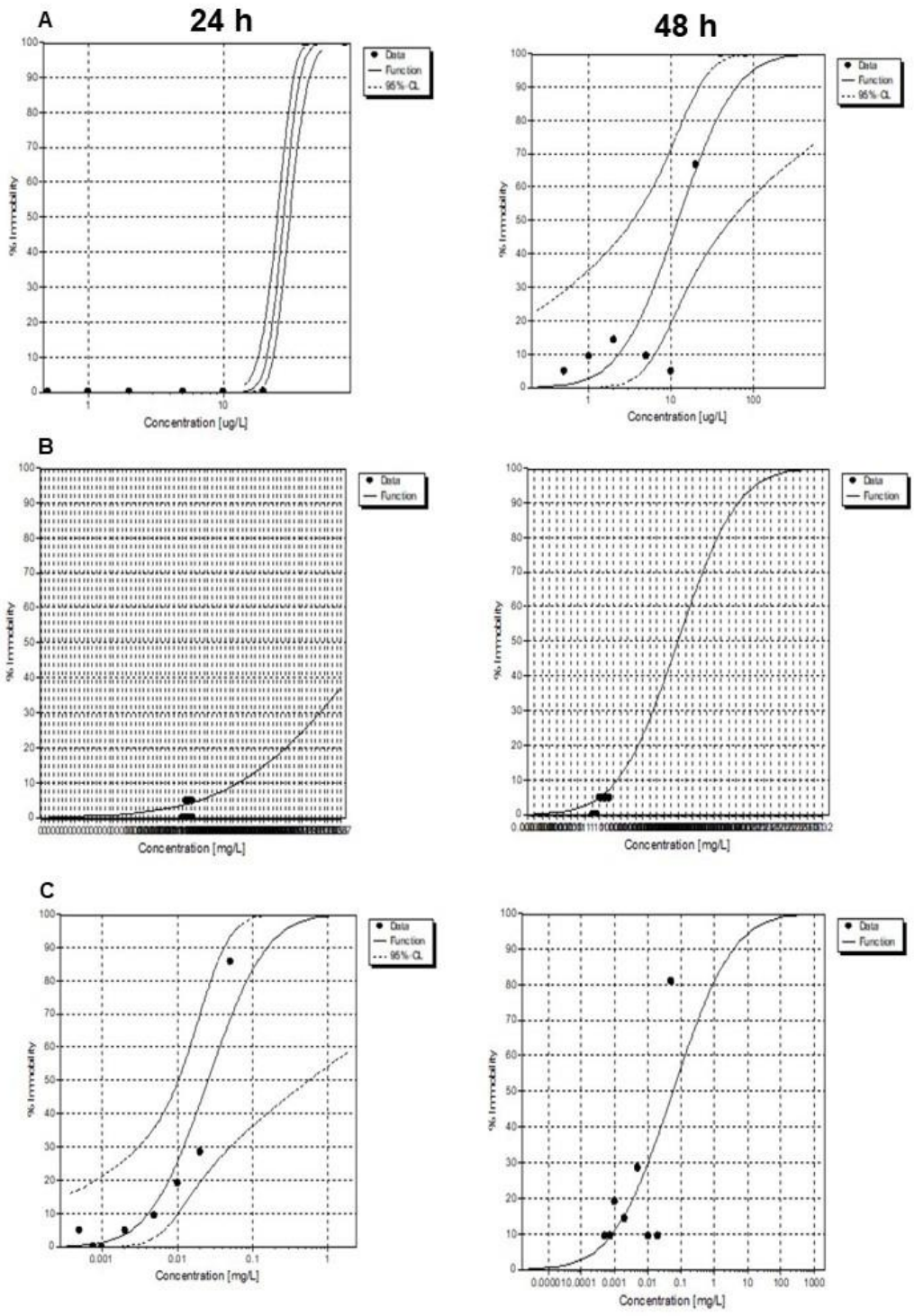

Figure 2. 4: Concentration-effect curve showing cumulative immobility in *D. magna* following exposure to CTAB capped rod shaped nAu (A), citrate capped nAu (B) and ionic Au (C) after 24 h and 48 h.

Table 2. 4: Results of the Probit analysis for immobility of *D. magna* following exposure at 48 h to CTAB capped rod shaped nAu, citrate capped nAu and ionic Au. Selected effective concentrations (LC10, LC20 and LC50) and their 95%-confidence limits (cl) were calculated according to Fieller`s theorem. Not determined is indicated by n.d.

CTAB capped rod shaped nAu			
	Concentration (µg/L)	Lower cl	Upper cl
LC10	2	0.02	6.4
LC20	4	0.15	10.3
LC50	12.1	3.4	53.4
Citrate capped nAu			
	Concentration (mg/L)	Lower cl	Upper cl
LC10	2	n.d.	n.d.
LC20	20	n.d.	n.d.
LC50	70	n.d.	n.d.
Ionic nAu			
	Concentration (µg/L)	Lower cl	Upper cl
LC10	1	n.d.	n.d.
LC20	4	n.d.	n.d.
LC50	57	n.d.	n.d.

2.3.4 Chronic toxicity test

The OECD211 test requires that mortality in the control group must be less than 20% and that there should be more or equal to 60% number of offspring produced per parent animal surviving at the end (i.e. after 28 days) of the test for the test to be valid. Although the test was repeated on three different occasions, these conditions could not be met. However for the puposes of the project we still present the data since control mortalities were lower than exposure mortalities and offspring produced higher than in the exposure groups.

The survival of *D. magna* showed that all three Au exposure groups (represented by Kaplan-Meier survival curves in Figure 2.5) decreased compared to the control group over the exposure time. Based on the K-M survival curves more than 50% of the *D. magna* population will not survive longer than 20 days when exposed to 5 ng/L CTAB capped rod shaped nAu and 1 mg/L citrate capped nAu (Figure 2.5 A and B). The majority of the *D. magna* populations (>80%) will survive (i.e. exposure duration of 28 days) at all nAu exposure concentrations. However, survival following exposure to ionic Au is lower when compared to the nAu. There were no significant differences in the number of molts between the different exposure concentrations for the nAu and ionic Au groups (Figure 2.6 A, B, C). Notable however was that all of the CTAB capped rod shaped nAu exposure groups were more than the control regarding the number of molts (Figure 2.6 A), while the the lowest citrate capped nAu exposure concentrations had the lowest number of molts per day (Figure 2.6 B). All of the ionic Au exposure groups had lower numbers of molts when compared to the control (Figure 2.6 C). For the CTAB capped rod shaped nAu (Figure 2.7 A) the 50 ng/L exposure group produced significantly more offspring, while the 0.5, 10 and 500 ng/L exposure groups produced significanly less offspring. All the citrate capped sphere nAu exposure and ionic Au concentrations produced significantly less offspring than the control (Figure 2.7 B and C). Additional observations noted within the exposure tests, the parents that gave birth to six juveniles at a time will not survive, but the offspring had high chance of survival. The exposure of ionic Au was noted that survived offsprings were rapidly spinning forward and in circular motion.

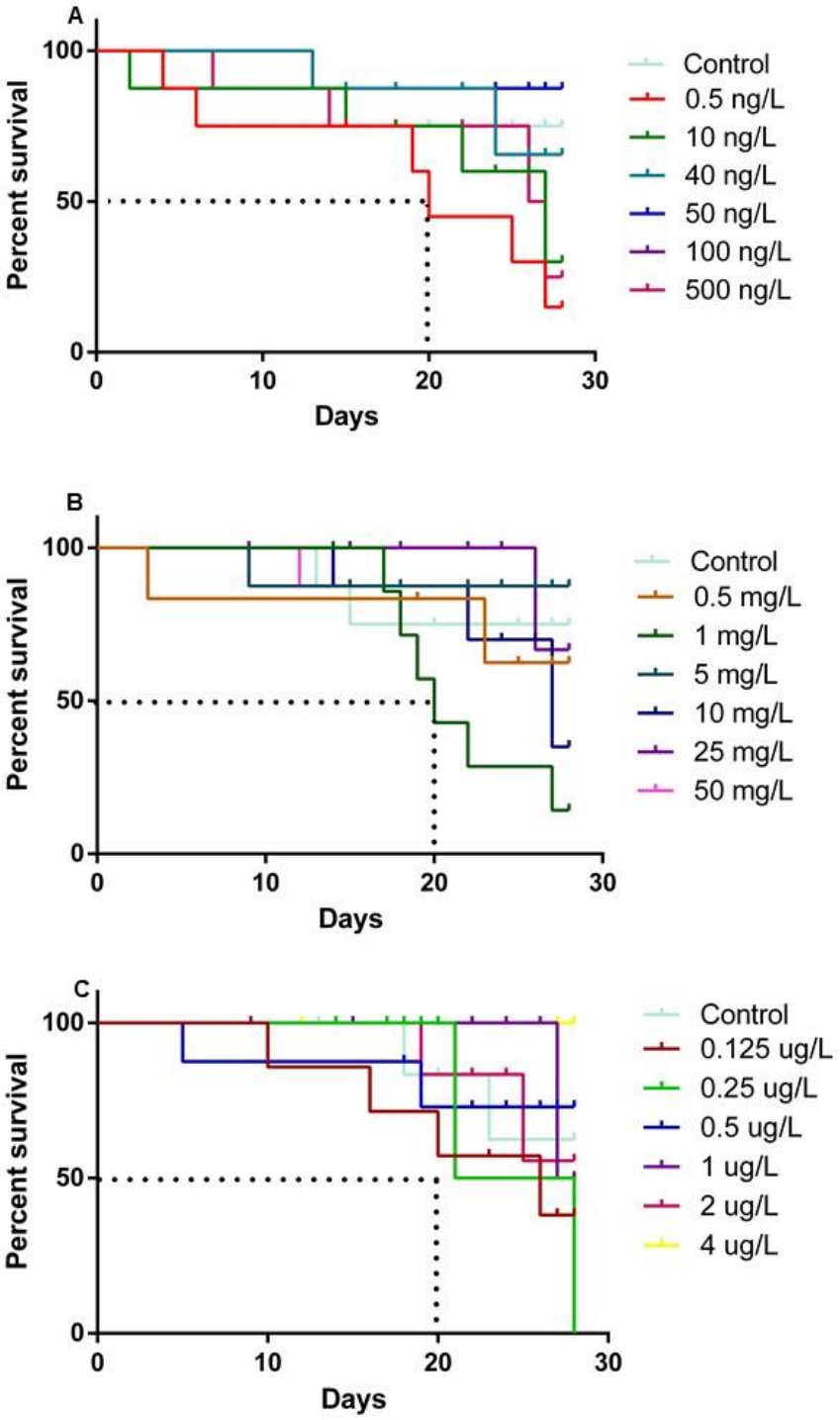

Figure 2. 5: Kaplan Meier survival curves for *D. magna* exposed to different concentrations of CTAB capped (A) nAu, citrate capped nAu (B) and ionic Au (C) throughout their life-time. The intersect of the dotted lines with an exposure concentration represents 50% survival of the population after 20 days of exposure.

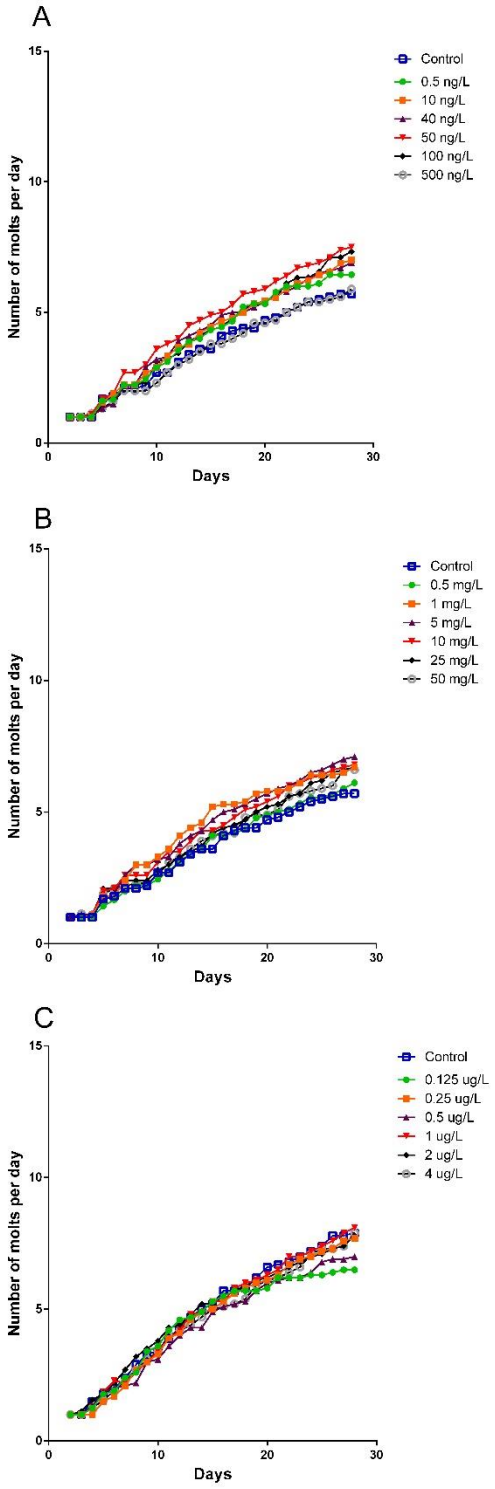

Figure 2. 6: The number of molts released following exposure of *D. magna* to CTAB capped rod shaped nAu (A), citrate capped nAu (B) and ionic Au (C). Each exposure concentration represents a pooled sample of ten *D. magna* adults. The asterisk * indicates significant ($p < 0.05$) difference ($p<0.05$) from the control.

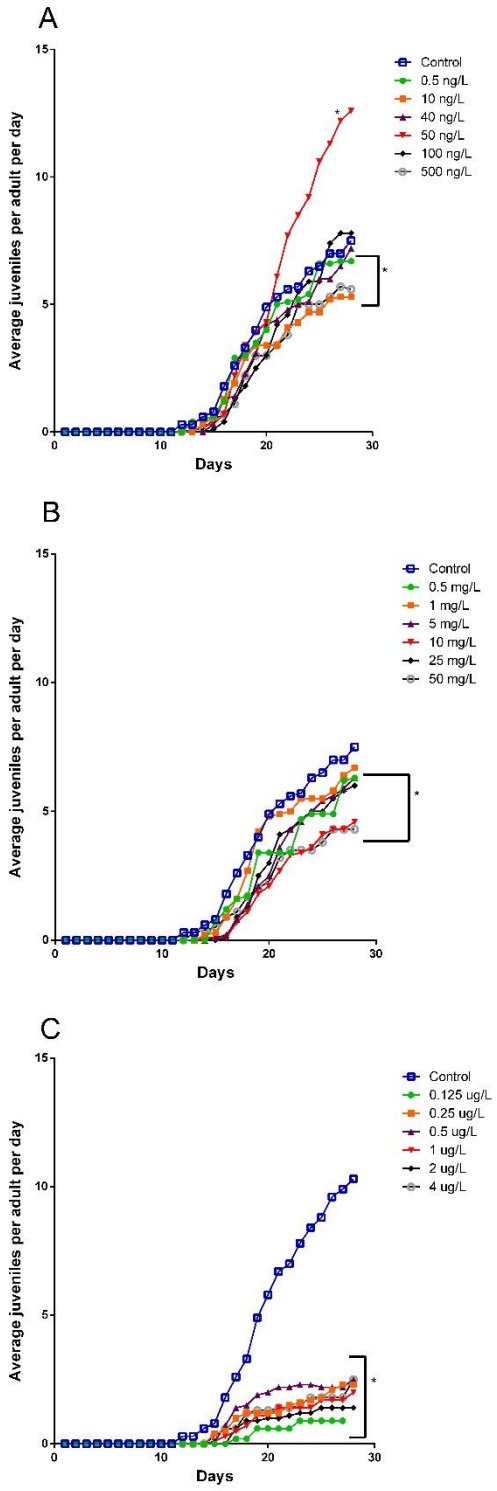

Figure 2. 7: The average juveniles per adult per day following exposure of *D. magna* to CTAB capped rod shaped nAu (A), citrate capped nAu (B) and ionic Au (C). Each exposure concentration represents a pooled sample of ten *D. magna* adults. The asterisk * indicates significant ($p < 0.05$) difference ($p<0.05$) from the control.

2.4 Discussion

Nanoparticle ecotoxicity includes numerous aspects relating to particle characterization, i.e. the size of the particle, the capping agent, how particles aggregate in an aquatic medium, and the surface charge that exists. The size and surface coating may have an effect in the NMs bioavailability, accumulation, and toxicity (Barreto et al., 2020; Barreto et al., 2015). The nAus with negatively charged ligands showed to be less toxic than the positively charged ligands (Bozich et al., 2014; Lee and Ranville, 2012; Mattsson et al., 2018). The CTAB capped rod shaped nAu are more positively charged than the citrate capped nAu, which explains why the CTAB capped rod shaped nAu are more toxic than the citrate capped nAu. However, both nAu NMs at 0 h were already negatively charged, indicating particle interaction with the M7 medium (Römer et al., 2013) despite the physico-chemical parameters remaining stable for the duration of the test. The stability of NMs can also be altered in the media by forming a protein corona on the surface (Mattsson et al., 2018). Negative zeta potentials have the potential to decrease aggregation (Botha et al., 2015; Griffitt et al., 2008; Weinberg et al., 2011) but the opposite was seen in this study as nAu became less negative over 48 h while agglomeration increased. Citrate capped nAu increase in their size either by aggregation or agglomeration which was observed in this study; the primary particle size was 14 nm while agglomerations of up to 300 nm were observed. The same phenomenon was observed for CTAB capped rod shaped nAu which further agglomerated over time. Therefore, smaller sized nAu might react better with other compounds present in the medium resulting in a "size-dependent aggregation/agglomeration of nAu's" (Barreto et al., 2020, Barreto et al., 2015; Iswarya et al., 2016). According to Botha et al. (2015), increased concentration of nAu tend to increase agglomeration causing the charge to be less negative in the media. According to Lee and Ranville (2012), sedimentation rates of NMs in hard water are reliant on the particle concentrations but when citrate-stabilized nAu's are added to hard water, aggregates form more rapidly. This implies that the ingested nAu's are probably in a steady-state, which remain within *the D. magna*. According to Kim et al. (2015) there was a decrease in bioaccumulation of heavy metals in *D. magna*. This suggested the uptake of c-AgNPs affected acute toxicity of heavy metals and further explained that AgNPs (can take up cationic heavy metals) interact with other pollutants specifically heavy metals in a medium.

The CTAB capped rod nAu's displayed multiple shapes (spheres and stars) while the citrate capped nAu were uniformly spherical in shape. This is because star-shaped Au NPs are formed under the exact same growth conditions that normally produce nAu rods (Nehl et al., 2006). The

proportion of small nAu rods increases with an increase in the seed size used for nanorod synthesis (Gole and Murphy, 2004). The procedure involves synthesis of citrate-stabilized Au nanoparticles to be used as the seeds, and overgrowth of the seeds into nanorods with the assistance of a surfactant such as CTAB (Yang et al., 2015).

The toxicity of NMs is related to their contact with the cell membrane which triggers a response resulting in uptake, translocation, accumulation, and death of a cell (Wang et al., 2013). The higher toxicity of the more positive CTAB capped rod shape nAu is likely due to the high affinity towards negatively charged surfaces of cell membrane which increases the cellular uptake of the particle resulting in cell death (Bozich et al., 2014; Wang et al., 2013). Since, negatively charged citrate capped nAu are unable to accumulate in the tissue of an organism, this NM has a much lower toxicity. This supports the findings by Li et al. (2015) and Botha et al. (2015). The results from this study also support the findings by the aforementioned authors that the toxicity of ionic Au was orders of magnitude higher than the nAu toxicity.

In a previous study, *D. magna* was exposed to citrate capped nAu with size ± 14 nm for 14 days at concentrations ranging from 0.5 - 20 mg/L. There were no mortalities and no effects observed in reproduction (Botha et al., 2016). This is further supported by similar finding by Pacheco et al. (2018). However, the aforementioned authors used ISO media and not M7 media which contains serveral additional salts and vitamins. In the current study, which made use of M7 media and an exposure period of 28 days, recorded parental mortality with increased number of total offspring. It was found that parents that produced six juveniles at a time did not survive, but the offspring had high chance of survival as observed.

Molting is an important process that plays a crucial role in daphnid development. This is necessary for growth and to excrete or eliminate any externally accumulated metals (Dabrunz et al., 2011; Nasser et al., 2016). The ingested NMs remain in external compartments such as the gut or adsorbed to the external carapace surface of *D. magna* (Botha et al., 2016; García-Cambero et al., 2013; Wray and Klaine, 2015). Failure to successfully molt in *D. magna* can cause adverse effects in the regulation of internalized metal concentrations. Thus the lower occurance of molting can cause an increase in the nAu body burden (Botha et al., 2016) which has a negative effect on higher order responses (see Chapters 3 and 4). Previous studies showed that selenium inhibited molting proccesses completely which resulted in decreased survival rate and population decline of *D. magna* (Bodar et al., 1990; Nasser et al., 2016).

The desired media which are suitable for prolonged culture of *D. magna* are the M4 and M7 media (OECD, 2012). This is because both media contain the chelating agent EDTA. The toxicity of cadmium was much lower when conducting the reproduction test in both M4 and M7 media than in media that does not contain EDTA. This is due to the chelation effect that the EDTA in M4 and M7 media has on metals. The alternative media to use when testing chemicals that contain metals, is ISO media (hard fresh water) since it does not contain EDTA with added seaweed extract.

Chapter 3

Metabolomics and physiology

Chapter 3: Metabolomics and physiology

3.1 Introduction

Daphnids are often used as ecotoxicological model organisms since there is a good understanding of their complex physiological processes and how stress induced molecular responses link with whole organism responses (Heckmann et al., 2008). To overcome environmental stress, they are characterized with a short life span, quick maturation, and reproduction (Kaas et al., 2009). The heart rate of *D. magna* is an endpoint that is mostly observed to measure the toxicity effect of chemicals such as cardiovascular drugs (Dzialowski et al., 2006) and pesticides (Kish, 2017). The heart of *D. magna* is different to that of mammals, arthropods, and other crustaceans (Villegas-Navarro et al., 2003) but does however, respond to most toxic chemicals in comparable to key mechanisms (Allen et al., 2019; Leatherman et al., 2009). The heart of daphnia consists of thin membrane and spots that are mostly found in one cell thick (Allen et al., 2019; Pirow et al., 2004; Zang et al., 2019). The daphnid heart is both myogenic (i.e. each contraction of the heart muscle regulates the flow of blood in the form of a pulse or heart rate) and neurogenic (i.e. some form of neural control, which allows it to respond well to different known stimulants of heart rate and heart rhythm) (Bekker and Krijgsman, 1951; Campbell et al., 2004; Kaas et al., 2009; Postmes et al., 1973; Villegas-Navarro et al., 2003). Thoracic limbs play a crucial role in feeding and ventilation in daphnids since they create water currents for food particles to be filtrated and oxygen supply around the body (Bownik et al., 2019a; Lari et al., 2017; Pirow et al., 1999a). Daphnids have a well-adapted respiratory system that can be altered by physiological processes such as feeding, predator activity or by physical and chemical stressors (Paul et al., 2004; Schmoker and Hernández -León, 2003; Weider and Lampert, 1985). The impact of feeding on metabolic rate assists in understanding the cost of feeding and cost the species fitness. This can be affected in two ways: firstly, the concentration of the food can affect the feeding behaviour by changing the mechanical cost of food and handling, thus affecting respiration rate. Secondly, the concentration of the food can affect the assimilation rate by changing the biochemical processing of food. There was a positive linear correlation between assimilation rate and respiration rate of *D. magna* (Bohrer and Lampert, 1988; Jensen and Hessen 2007; Robison et al., 2018). Energy flow production relies on the gas exchange between oxygen and carbon dioxide at the cellular level of an organism and its environment. Moreover, integumentary respiration of daphnia takes place because of its thin walled integument

and large surface area. It has been found that when the movement rate of the daphnids thoracic limbs remain constant, the ambient oxygen concentration declines, which supports that respiratory gas exchange occurs via different routes (i.e. gill breathing, intestinal respiration, and also integumentary respiration) (Pirow et al., 1999a; Pirow et al., 2004). Epipodites occurs when respiratory gas exchange occurs within the inner wall of the carapace of *D. magna* (Pirow et al., 1999a).

Metabolites are intermediate end products of metabolism and can be influenced by internal biological changes, e.g. genetics and external environmental changes (Fiehn, 2002). Metabolites vary in structure and in chemical composition illustrating different energy levels (Idle and Gonzalez, 2007; Stitt and Fernie, 2003). Metabolomics is the scientific study of complete, high-throughput analysis of multi-faceted data of metabolites present within an organism, cell or tissue set under limited conditions whereby producing a biochemical profile called a metabolome (Gomez-Casati et al., 2013). This assists in acknowledging relations of multi-faceted molecules in biological systems (Hall et al., 2002; Idle and Gonzalez, 2007). Metabolomics represent continuous large-scale analysis at the systems level of RNA and proteins metabolites (Bino et al., 2004; Weckwerth, 2003). Methodologies such as mass spectrometry (MS) and nuclear magnetic resonance (NMR) spectroscopy are used for the highly advanced and multi-faceted identification of molecular metabolites (Gomez-Casati et al., 2016; Lei et al., 2011). When comparing metabolomic studies with genomics or proteomics, it reflects alterations in a specific phenotype of a species, cell, or tissue just as effectively (Griffin and Shockcor, 2004; Spratlin et al., 2009). There are two types (untargeted and targeted metabolomics) of metabolomics characterization. The untargeted metabolomics can be used to characterize all molecules in a sample and is the approach used in this study. The targeted metabolomics can be used to analyse a particular set of identified chemical metabolites that are characterized, for example lipids, amino acids, nucleotides, or steroids (Bonvallot et al., 2014). When comparing between MS and NMR, the MS is more sensitive than the NMR technique, measuring metabolites at picograms per millilitre level while the NMR distinguishes metabolites at micrograms per millilitre (Bonvallot et al., 2014). *Daphnia magna* has been used in metabolomic studies to examine the mode of action with regard to exposure to specific ranges of continuous harmful organic pollutants and metals within the environment (Han et al., 2006; Jansen et al., 2011; Sarma and Nandini, 2006; Woermann and Sures, 2020). A few studies have been conducted on the influence of NMs on the metabolomics of daphnia, e.g. the effect of hormesis on oxidative stress following exposure of *Daphnia pulex* to fullerene crystals (nC60) was assessed using transcriptomics and metabolomics (Wang et al., 2019). *Daphnia similis* was evaluated during a 21 day's chronic exposure to determine

physiological effects of silver nanoparticles (AgNPs) exposed to two ambient encountered concentrations (0.02 and 1 ppb) (Wang et al., 2018).

To show exposure – response relationships and to understand the mechanisms of NM action, it is essential to have an indication of whether NMs are taken up and internalized (Galdiero et al., 2017). CytoViva hyperspectral darkfield imagery has successfully been used to show the presence of NMs in tissues of organisms following exposure. The uptake of Au nanomaterials in *D. magna* can cause chemical change such as oxidative stress or physical changes by causing increased release of the external carapace (Nasser et al., 2016). An increased uptake and toxicity of titanium dioxide (TiO2) nanoparticles (NPs) in *D. magna* can lead to high oxidative stress injury (Liu et al., 2019). *Daphnia magna* showed an increase adhesion of nAu to the external carapace, ingestion, and uptake in the gut. There was no significant effect observed on reproduction and moulting patterns. In addition, the uptake and surface adsorption of nAu can be caused by interaction of nAu in the ISO media and charge of the particle (Botha et al., 2016).

The aims of this chapter was to i) determine the effect of ionic Au and two different types of nAu (citrate capped nAu and CTAB capped rod shaped nAu) on the metabolomic profile of *D. magna,* ii) to determine which metabolic pathways were altered in each treatment, iii) to evaluate changes in heart rate and respiration as key events of the *D. magna* exposed to ionic Au and two different types of nAu and (iv) to determine whether these responses could be related to the uptake of the particles using CytoViva.

3.2 Materials and methods

3.2.1 Test and exposure solution preparation

Adult *D. magna* were placed in a clean 5 L beaker with oxygenated M7 media for 24 h prior the exposure test at 20-21°C.

Dilutions were conducted for both nAu and ionic Au as outlined in Chapter 2. The concentrations selected were based on the LC10 and LC20 values calculated in Chapter 2. For CTAB capped rod shaped nAu and ionic Au the exposure concentrations were LC10 (2 µg/L) and LC20 (4 µg/L),

while for citrate capped nAu the concentrations were LC10 (2 mg/L) and LC20 (20 mg/L) and these values were obtained from literature (Li et al., 2010).

3.2.2 Heart rate

For each treatment, three replicates of ten adult daphnids (n=30) were placed in 250 mL beakers using plastic pipette (the tips of the plastic pipette were cut with scissors as not to crush the adult daphnids). The treatments of nAu and ionic Au were spiked to the predetermined concentrations. After 48 h exposure test, adult daphnids were individually placed in an indented slide filled with M7 medium using a plastic pipette and covered with a coverslip. The indented slide was placed on a Zeiss (Carl Zeiss Microscopy GmbH; Carl-Zeiss-Promenade 10) compound microscope and a three minute video recording were taken with an Axiocam (Axiocam 506) at 25 frames per second using an iPad connected to the router (Figure 3.1). This was done for all the concentrations and the control of nAu and ionic Au. The highest magnification of 40x was used for video recording. This was to ensure the heartbeat of the *D. magna* is visible for counting later on (Campbell et al., 2004). The heart is situated above the brooding chamber (Figure 3.2). The heartbeat of *D. magna* was counted manually by playing the video clip in slow motion (Park et al., 2019) including the use of a pen and paper to tap the beats (Greene et al., 2017). The frequency of appendage movement was not counted from the recorded video clips.

Figure 3. 1: Video recording of *D. magna* heart rate after 48 h.

Figure 3. 2: The arrow indicates the position of the *D. magna* heart.

3.2.3 Respiration

The exposure conducted followed that of the heart rate exposures as outlined above. After a 48 h exposure period, adult daphnids were individually placed in a 24-well sealed Loligo Systems® microplate respirometer chamber (Figure 3.3) with oxygenated M7 medium (at least 70% saturation). The readings were noted for one hour in 15 seconds intervals at 20-21°C.

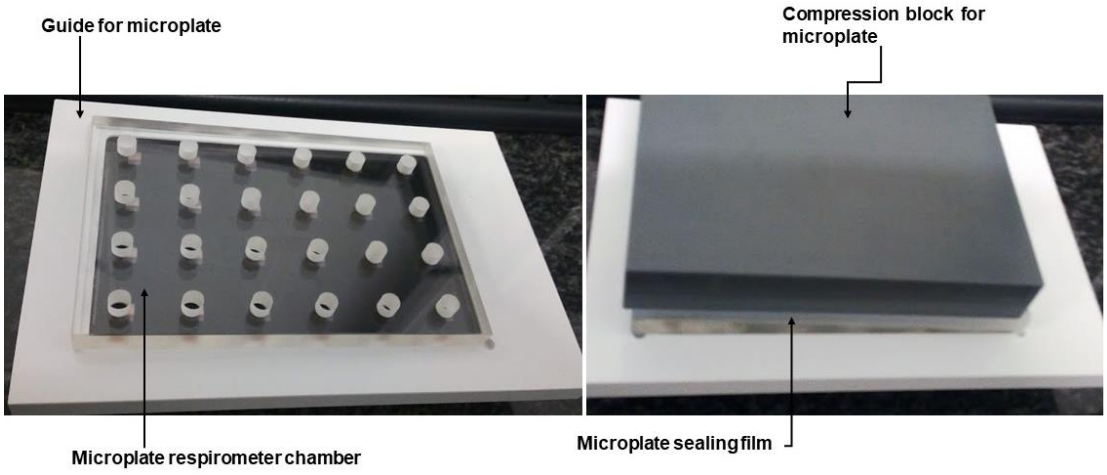

Figure 3. 3: The 24-well sealed Loligo Systems® microplate respirometer chamber. The right picture indicating sealed microplate respirometer chamber.

After the analysis, daphnids were placed in petri dishes using a plastic pipette according to their exposure groups (control; LC10 and LC20 for both nAu and ionic Au). Daphnids were blotted dry on a paper towel and weighed as a group (n = 30) on an ultrafine Mettler Toledo scale (Figure 3.4). The weights obtained were used to calculate the rate of oxygen consumed per mg daphnid using the software SDR Version 4 (Figure 3.5).

Figure 3. 4: Ultrafine Mettler Toledo scale used to accurately weigh the *D. magna*.

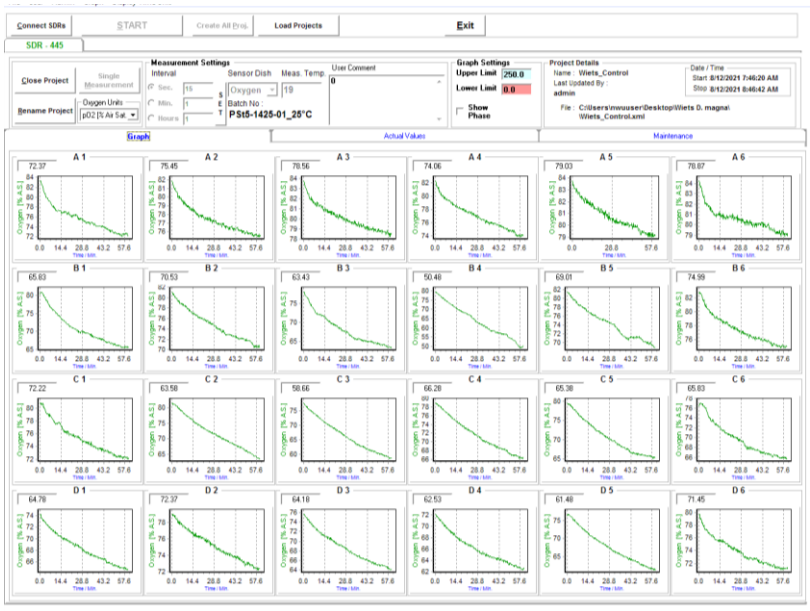

Figure 3. 5: An example of the calculation of oxygen consumption rates using the software SDR Version 4.

3.2.4 Metabolomics

Ten replicates of ten adult daphnids (n=100) were placed in 50 mL beakers using a plastic pipette and exposed to the LC10 and LC20 concentrations as described above. After 48 h exposure, adult daphnids were placed in a 2.5 mL Eppendorf tube (snap cap tube) after excess media was removed and flash frozen using liquid nitrogen to halt enzymatic activity. The samples were kept at -80°C. The samples were weighted before and after the drying process then the freeze dried samples were later extracted.

For the extraction of the whole metabolome from the *D. magna*, a single-phase extraction method (Beukes et al., 2019) was applied to all experimental groups (control, CTAB capped rod shaped nAu, citrate capped nAu and ionic Au). Freeze dried samples were transferred to a 1.5 mL Eppendorf tube and 50 µL of the Internal Standard (3-Phenylbutyric acid 50 ppm) and 1 mL extraction solution mixture composed of chloroform, methanol & water (1:3:1) was added. After the addition of a 3 mm tungsten carbide bead, the sample mixtures were shaken in a vibration mill at 30 Hz for five minute and consequently centrifuged at 12 000 rpm for five minutes at 4°C. The supernatant was transferred into a GC vial and dried under a gentle stream of nitrogen at 40°C for 20-30 minutes. For derivatisation purposes, 50 µL methoxyamine HCl (150 mg in 10 mL pyridine) was added followed by and incubation step at 50°C for 90 minutes. Hereafter, 40 µL BSTFA + 1% TMCS (N,O-Bis(trimethylsilyl)trifluoroacetamide with trimethylchlorosilane) from Sigma Aldrich (St. Louis, MO, USA) was added, and the extract was re-incubated at 50°C for 60 min. The extracts were then transferred to a 250 µL sample vial and capped prior to gas chromatography coupled with time of flight mass spectrometry (GCxGC-TOF-MS) analysis. A quality control sample was prepared by combining extractions from each sample.

3.2.5 CytoViva® Hyperspectral Dark Field Imagery

CytoViva® dark field hyperspectral imaging was conducted in this study to examine the adsorption or accumulation of nAu and ionic Au to the external carapace or internal structures of daphnids. This will assist on determining whether nAu remain on the external surface or accumulate in internal tissues and thus link the metabolic and physiological changes (heart rate and respiration) to particle activity. After a 48 h of exposure time, adult *D. magna* were collected and placed onto

a microscope slide using plastic pipette then blotted dry using paper towel. Cryopreserve gel (Tissue-Tek® OCT Compound) was used to mount adult daphnia onto the microscope slide. Slides were carefully covered with a cover slip to prevent the gut content from being pushed out of the organism prior to imaging. Visualization was done using a CytoViva® 150 Unit integrated onto an Olympus BX43 microscope. Images of the exposed *D. magna* were captured using the Dagexcel X16 camera and DAGE Exponent software at 10X magnification (Botha et al., 2016). This was conducted for all treatment groups (CTAB capped rod shaped nAu, citrate capped nAu and ionic Au) as well as the control group.

3.2.6 Statistical analysis

For the respiration and heart rate, the data sets were checked for normality of distribution using D'Agostino and Pearson omnibus normality test. For normally distributed data, one-way ANOVA was conducted using Tukey's Multiple Comparison Test to determine significance between groups ($p < 0.05$). However, if data sets were not distributed normally, the Kruskal-Walis Test using Dunn's Multiple Comparison Test was performed to determine significance. Significance was regarded as $p < 0.05$ (Botha et al., 2016; Kelpsiene et al., 2020).

For the metabolomics data, Leco Corporation ChromaTOF software (version 4.50) was used for peak finding and mass spectral deconvolution at an S/N ratio of 100, with a minimum of 3 apexing peaks. Using the mass fragmentation patterns generated by the MS, together with their respective GC retention times, the identities of these peaks were determined by comparing it to commercially available NIST spectral libraries (mainlib, replib).

The concentrations of the *D. magna* metabolites were determined by generating calibration curves using external standards and metabolite data was further analysed (Jeong and Simpson, 2020; Wu and Li, 2016). The metabolite concentration data (.csv format) were imported into MetaboAnalyst (version 5.0) MetaboAnalystR (Xia Lab, Montreal, QC, Canada). The data were filtered prior to analyses in order to identify and remove variables that are unlikely to be of use when modelling the data based on the interquartile range (Chong et al., 2018a; Pang et al, 2020; Castillo et al., 2011). In addition, the values found within the quantification range and removed outliers (variables that are unlikely to be of use when modelling the data) were replaced using the half minimum integer representing the quantification range in the metabolite data (Chong et al., 2018a; Chong et al., 2019; Sun and Weckwerth, 2012). The metabolite data were individually

normalized with the sum of the total concentrations for each sample. The normalized concentration data points were then scaled using the autoscaling function (Pang et al, 2020; Chong and Xia, 2018b). The above method has been conducted in previous studies using metabolomics with varying contaminants and target organisms (Jeong and Simpson, 2019; Jeong and Simpson, 2020; Kapoore and Vaidyanathan, 2016; Rusilowicz et al., 2016).

After normalization of the metabolite data, statistical analyses were performed using MetaboAnalyst (version 5.0) MetaboAnalystR (Xia Lab, Montreal, QC, Canada) (Chong and Xia, 2018b). The data were first analysed using univariate (T-test) and multivariate [Principal Component Analysis (PCA) and Partial Least Squares - Discriminant Analysis (PLS-DA)] statistical analyses which generated a matrix of scores for the top 15 principal components. Multivariate analysis methods are the most commonly used methods used for exploratory data analysis. PCA is an unsupervised method aiming to find the directions that best explain the variance in a data set (X) without referring to class labels (Y). PLS-DA is a supervised method that uses multivariate regression techniques to extract via linear combination of original variables (X) the information that can predict the class membership (Y). Moreover, PLS-DA was assessed to observe any separation among exposed groups. This was conducted using an average of PLSDA plots. A one-way analysis of variance (ANOVA) was performed to note statistical significance using $p < 0.05$. Metabolite percent changes were calculated using the average metabolite concentration of the compound exposure group relative to the average of the unexposed control group (Southam et al., 2011).

Furthermore, the metabolites that showed statistical differences for each treatment were subject to pathway analysis using MetaboAnalyst (version 5.0) (Chong et al., 2018a). The global test algorithm was applied to the KEGG pathway libraries to uncover pathways in *D. magna*. The pathway library for *Drosophila melanogaster* was used as a reference invertebrate (Kovacevic et al., 2016) since *D. magna* has the most in common with *D. melanogaster* characteristics. Pathway analysis allowed for a rapid determination of which biochemical pathways were significantly impacted during sub-lethal exposure to select nAu and ionic Au.

3.3 Results

3.3.1 Heart rate

Although all the heart rate in all of the exposure groups increased relative to the control, only the LC20 of citrate capped nAu and ionic Au (Figure 3.6 B and C) increased significantly ($p < 0.05$). However, CTAB capped nAu showed no increased significance ($p < 0.05$) at LC20 (Figure 3.6 A).

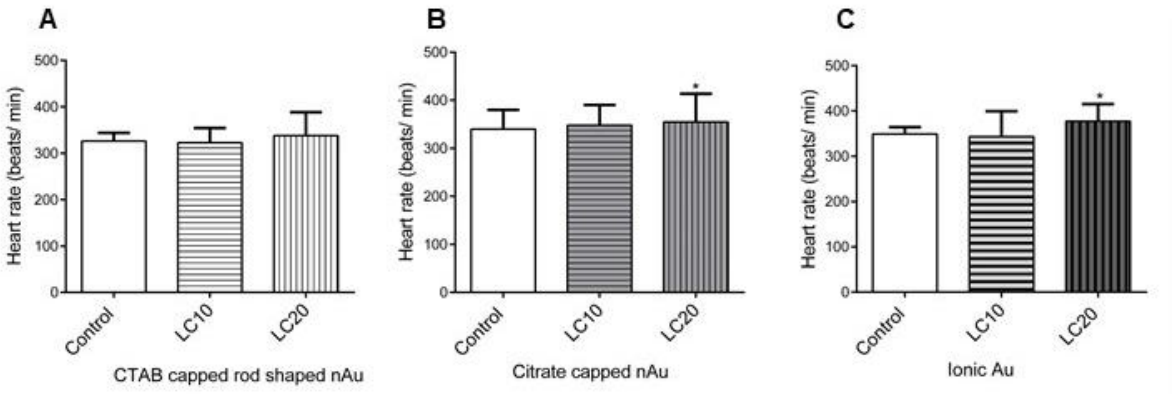

Figure 3. 6: The mean [± standard error (SE)] heart rate of *D. magna* (beats per minute) following 48 h exposure to CTAB capped rod shaped nAu (A), citrate capped nAu (B) and ionic Au (C). The * indicates significance ($p < 0.05$) from the control.

3.3.2 Respiration rate

The respiration rate of both exposure concentrations of the nAu groups (Figure 3.7 A and B) increased significantly ($p < 0.05$) when compared to the control. In contrast the two ionic Au exposure groups showed a significant decrease ($p < 0.05$) when compared to the control group (Figure 3.7 C).

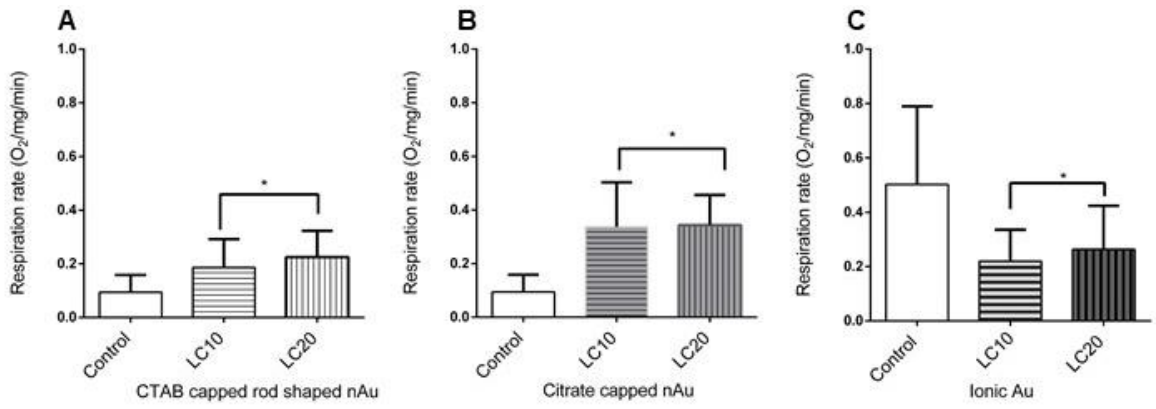

Figure 3. 7: The mean (± SE) respiration rate of *D. magna* (O_2 / mg daphnid / min) following 48 h exposure to CTAB capped rod shaped nAu (A), citrate capped nAu (B) and ionic Au (C). The * indicates significance ($p < 0.05$) from the control.

3.3.3 Metabolomic profiling using untargeted analysis

CTAB capped rod shaped nAu

When one-way Anova analysis was conducted, the metabolites Chloro Dimethoxyphenethylamine, Cyclohexanebis methylamine and Dimethoxy nitrophenethylamine showed significant decrease when compared to the control. However, Decanamine and Tetradecanamine showed significant increase when compared to the control (Figure 3.8 A). There was separation of CTAB capped rod shaped nAu LC20 from the control but an overlap was observed between LC10 and LC20 when compared to the control (Figure 3.9 A). The variable importance in projection (VIP) (top 15 metabolites) responsible for variance in the metabolome including Chloro Dimethoxyphenethylamine, Cyclohexanebis methylamine, Dimethoxy nitrophenethylamine, Decanamine and Tetradecanamine after exposure to CTAB capped rod shaped nAu (Figure 3.10 A).

Citrate capped nAu

When one-way Anova analysis was conducted- the following metabolites, which were also altered in CTAB capped rod shaped nAu, showed statistical significance, that is, Cyclohexanebis, Chloro Dimethoxyphenethylamine methylamine showed significant decrease while Decanamine showed significant increase when compared to the control (Figure 3.8 B). There is an indication of separation of citrate capped nAu LC20 from the control (Figure 3.9 B). The results demonstrated

the VIP top 15 metabolites responsible for variance in the metabolome including Cyclohexanebis, Chloro Dimethoxyphenethylamine methylamine and Decanamine after exposure to citrate capped nAu (Figure 3.10 B).

Ionic Au

When one-way Anova analysis was conducted, the same trend was observed as with both nAu groups. Cyclohexanebis methylamine and Chloro Dimethoxyphenethylamine showed a significant decrease when compared to the control, while metabolite Decanamine showed significant increase when compared to the control (Figure 3.8 C). There was an overlap between ionic Au LC10 and ionic Au LC20 when compared to the control (Figure 3.9 C). The results demonstrated the VIP top 15 metabolites responsible for variance in the metabolome including Cyclohexanebis methylamine, Chloro Dimethoxyphenethylamine and Decanamine (Figure 3.10 C).

Effect of concentration

Clustering analysis revealed that when the top 25 metabolites were clustered according to concentrations there was a separation between control and exposed- this separation became more pronounced as the concentration increased (Figure 3.11 and Figure 3.12). The metabolites included unknown analytes which are still to be characterized. The LC10 and LC20 groups compared to control showed an overlap in the following metabolites: metabolite Chloro Dimethoxyphenethylamine, Cyclohexanebis methylamine, Dimethoxy nitrophenethylamine, Decanamine, Tetradecanamine, Glucose, Hydroxybutyric acid and Octopamine. While the LC10 group exclusively had Citruline, Benzyl alcohol, Azeliac acid, L Isoleucine, two of Acetic acid, Xylose and Trimethylsilylmeth compared to the LC20 which exclusively had Pyran bromomethyl, Triethanolamine, Propanol ethoxy, Diethylene glycol, Butanedioic acid, Octanoic acid, Undecene chloro, Nonenol, Tagatose, Fructose, Gluconic acid and Glyceryl glycoside. Moreover, the LC10 had 36 % Analyte compared to the LC20 which exclusively had 20 % Analyte out of 25 metabolites.

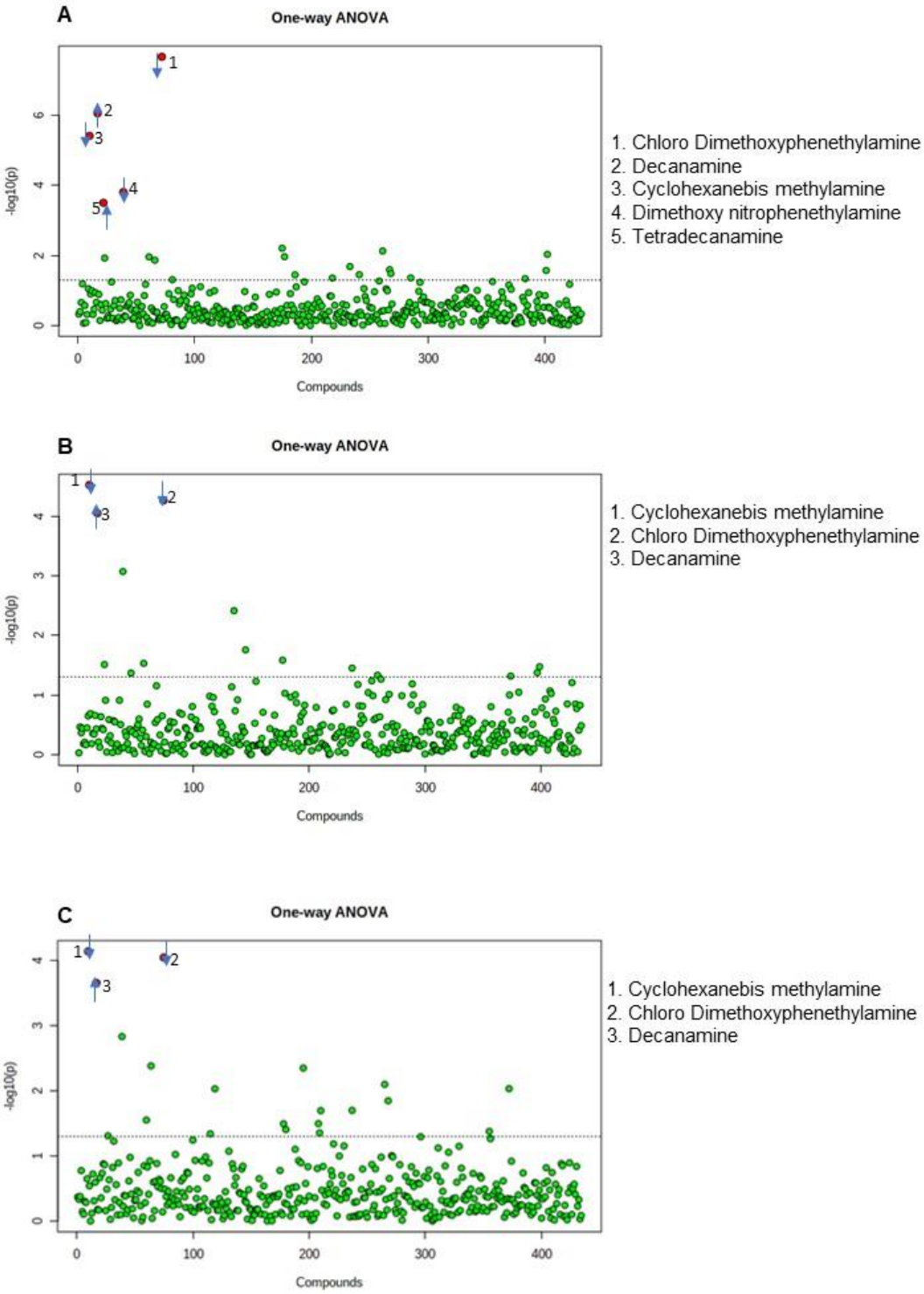

Figure 3. 8: A one-way analysis of variance (ANOVA) plots of averaged (n = 9) metabolite data sets for CTAB capped rod shaped nAu (A), citrate capped nAu (B) and ionic Au (C). Red dots indicate significant ($p < 0.05$) metabolites as labelled on the figure, where an up arrow indicated upregulation and a down arrow indicates down regulation.

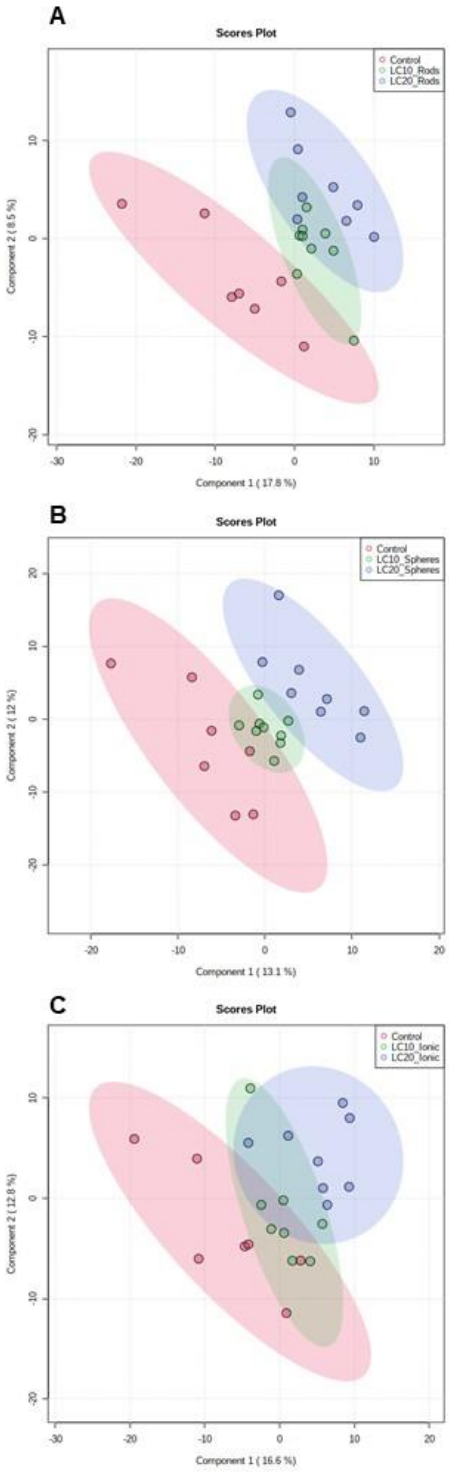

Figure 3. 9: A multivariate analysis: Partial least squares-discriminant analysis (PLS-DA) scores plots of averaged (n = 9) metabolite data sets for CTAB capped rod shaped nAu (A), citrate capped nAu (B) and ionic Au (C).

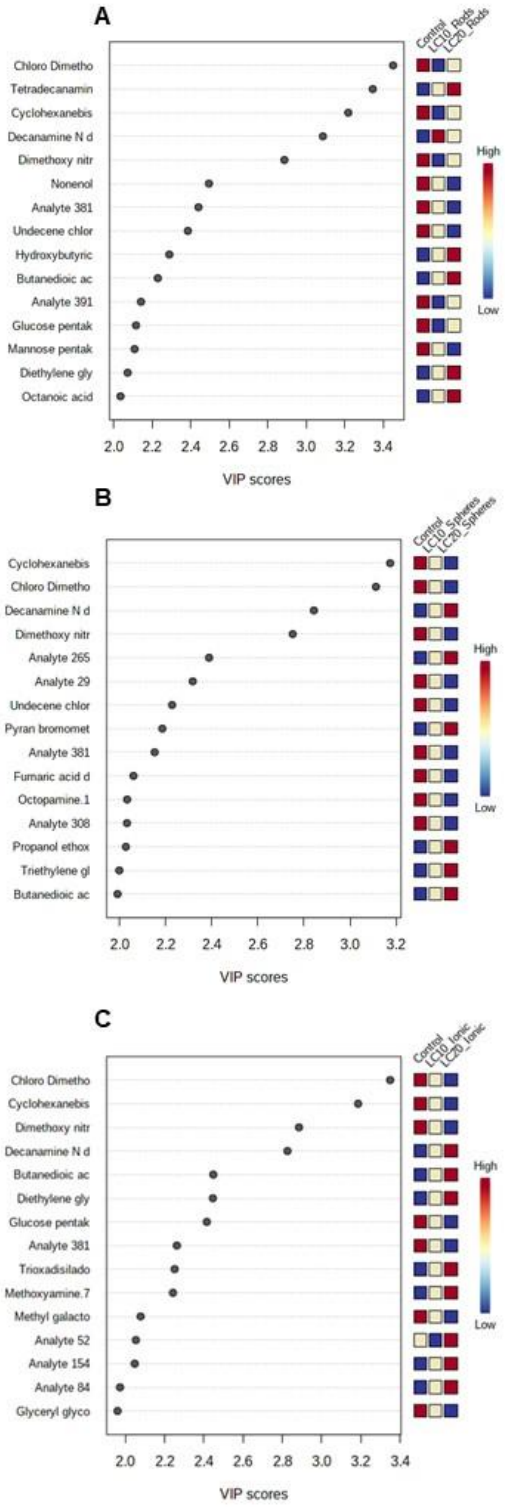

Figure 3. 10: PLS-DA scores demonstrates the variable importance in projection (VIP) and the relative concentration of the metabolites demonstrating the top 15 metabolites responsible for variance in the metabolome for CTAB capped rod shaped nAu (A), citrate capped nAu (B) and ionic Au (C).

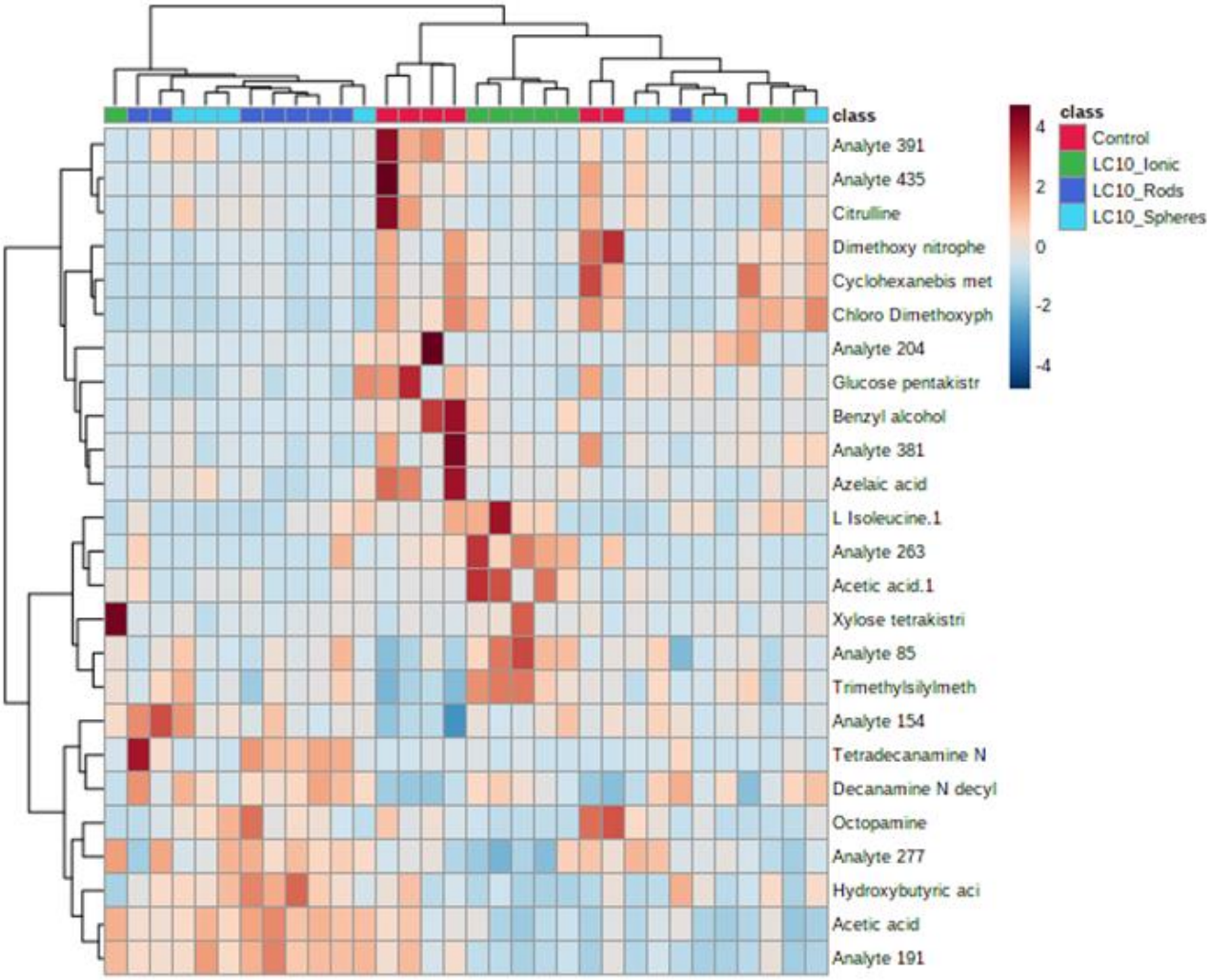

Figure 3. 11: The heat map of the top 25 metabolites differing at LC10 between CTAB capped rod shaped nAu, citrate capped nAu and ionic Au.

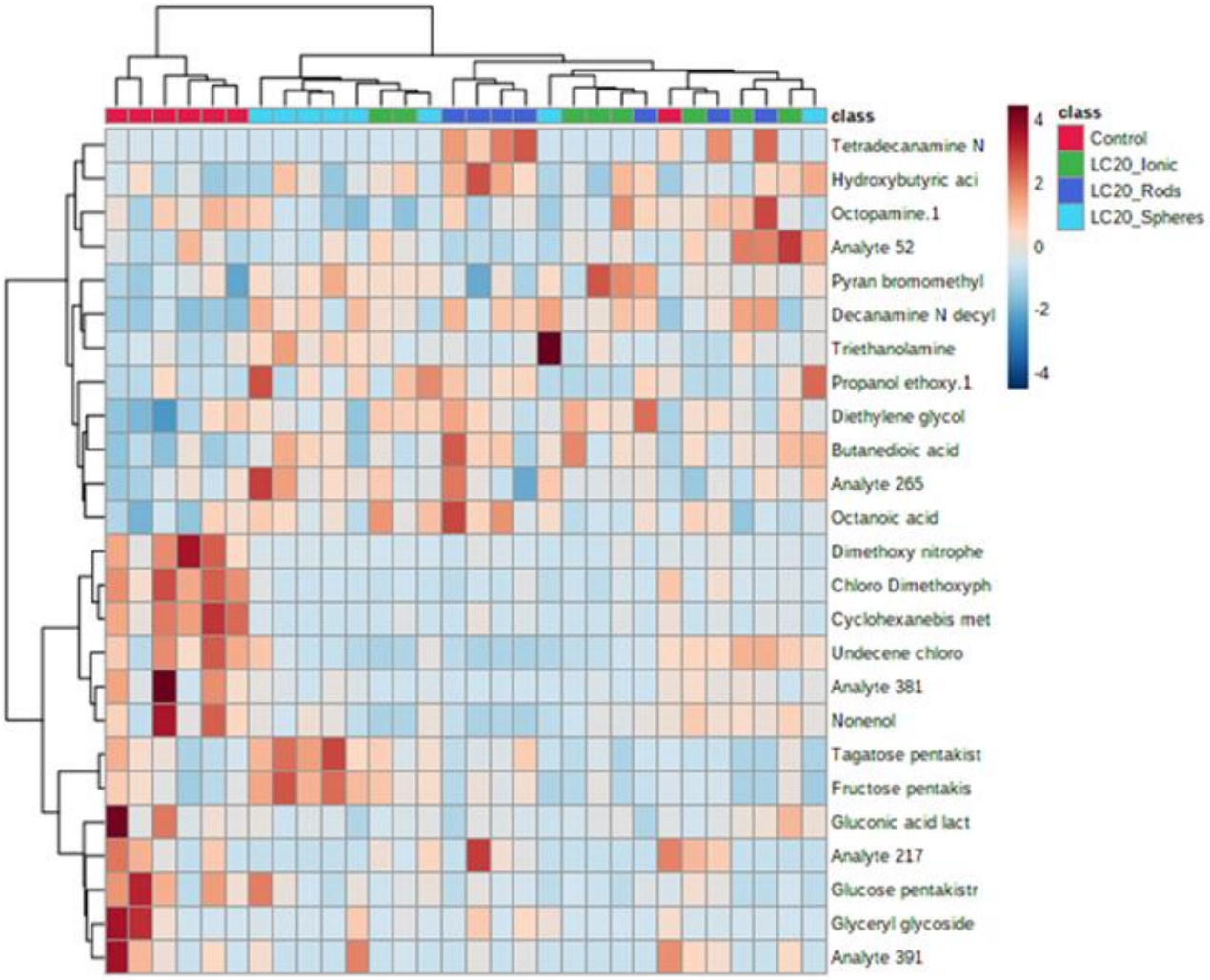

Figure 3. 12: The heat map of the top 25 metabolites differing at LC20 between CTAB capped rod shaped nAu, citrate capped nAu and ionic Au.

3.3.4. Metabolomic pathway analysis

The results suggest that CTAB capped rod shaped nAu LC10 and ionic Au LC20 shared perturbations to Sphingolipid metabolism, Glyoxylate and dicarboxylate metabolism and Glycine, serine, and threonine metabolism pathway. CTAB capped rod shaped nAu (LC10 & LC20) and ionic Au (LC10 & LC20) shared perturbations to Nicotinate and Nicotinamide Metabolism pathway (Figure 3.13 A, B and E, F). CTAB capped rod shaped nAu LC10 and ionic Au LC10 shared perturbations to Biotin metabolism (Figure 3.13 A and E). Citrate capped nAu LC10 and ionic Au LC20 shared perturbations to Tryptophan metabolism (Figure 3.13 C and F). CTAB capped rod

shaped nAu LC10, Citrate capped nAu LC10 and ionic Au LC20 shared perturbations to Glyoxylate and dicarboxylate metabolism (Figure 3.13 A, C and F).

CTAB capped rod shape nAu

The affected pathways during CTAB capped rod shape nAu LC10 are as follows: Sphingolipid metabolism; Biotin metabolism; Nicotinate and nicotinamide metabolism; Inositol phosphate metabolism; Glyoxylate and dicarboxylate metabolism; and Glycine, serine, and threonine metabolism (Figure 3.13 A). The Sphingolipid metabolism, Biotin metabolism pathway, Glyoxylate and dicarboxylate metabolism and Glycine, serine and threonine metabolism pathway serine showed significant decrease when compared to the control while the Metabolite myo-Inositol showed significant decrease when compared to the control at CTAB capped rod shape nAu LC10 in the Inositol phosphate metabolism pathway.

The affected pathways during CTAB capped rod shape nAu LC20 were as follows: Nicotinate and nicotinamide metabolism; and Phenylalanine, tyrosine, and tryptophan biosynthesis (Figure 3.13 B). Niacinamide in the Nicotinate and Nicotinamide Metabolism pathway showed significant decrease when compared to the control while tyrosine in the Phenylalanine, tyrosine and tryptophan biosynthesis pathway showed significant decrease when compared to the control.

Citrate capped nAu

The affected pathways during citrate capped nAu LC10 are as follows: beta-Alanine metabolism; Tryptophan metabolism; Citrate cycle (TCA cycle); and Glyoxylate and dicarboxylate metabolism (Figure 3.13 C). Tryptophan in the Tryptophan metabolism showed significant decrease when compared to the control. Serine showed a significant decrease in the Glyoxylate and dicarboxylate metabolism pathway while Citric acid in the Citrate cycle (TCA cycle) pathway showed significant increase when compared to the control. However, Aspartic acid in the beta-Alanine metabolism pathway showed significant decrease when compared to the control.

The affected pathways during citrate capped nAu LC20 are as follows: Insect hormone biosynthesis; and Sulfur metabolism (Figure 3.13 D). Endogenous sulfite in the Sulfur metabolism pathway showed significant increase when compared to the control, whereas cholesterol in the Insect hormone biosynthesis pathway showed significant decrease when compared to the control.

Ionic Au

The affected pathways during ionic Au LC10 are as follows: Nicotinate and Nicotinamide Metabolism; Arachidonic acid metabolism; Biotin metabolism; and D-Glutamine and D-glutamate

metabolism (Figure 3.13 E). During D-Glutamine and D-glutamate metabolism pathway glutamine showed significant decrease when compared to the control.

The affected pathways during ionic Au LC20 are as follows: Arachidonic acid metabolism; Sphingolipid metabolism; Nicotinate and nicotinamide metabolism; Glyoxylate and dicarboxylate metabolism; Tryptophan metabolism; and Glycine, serine, and threonine metabolism (Figure 3.13 F). Arachidonic acid in the Arachidonic acid metabolism pathway showed significant decrease when compared to the control.

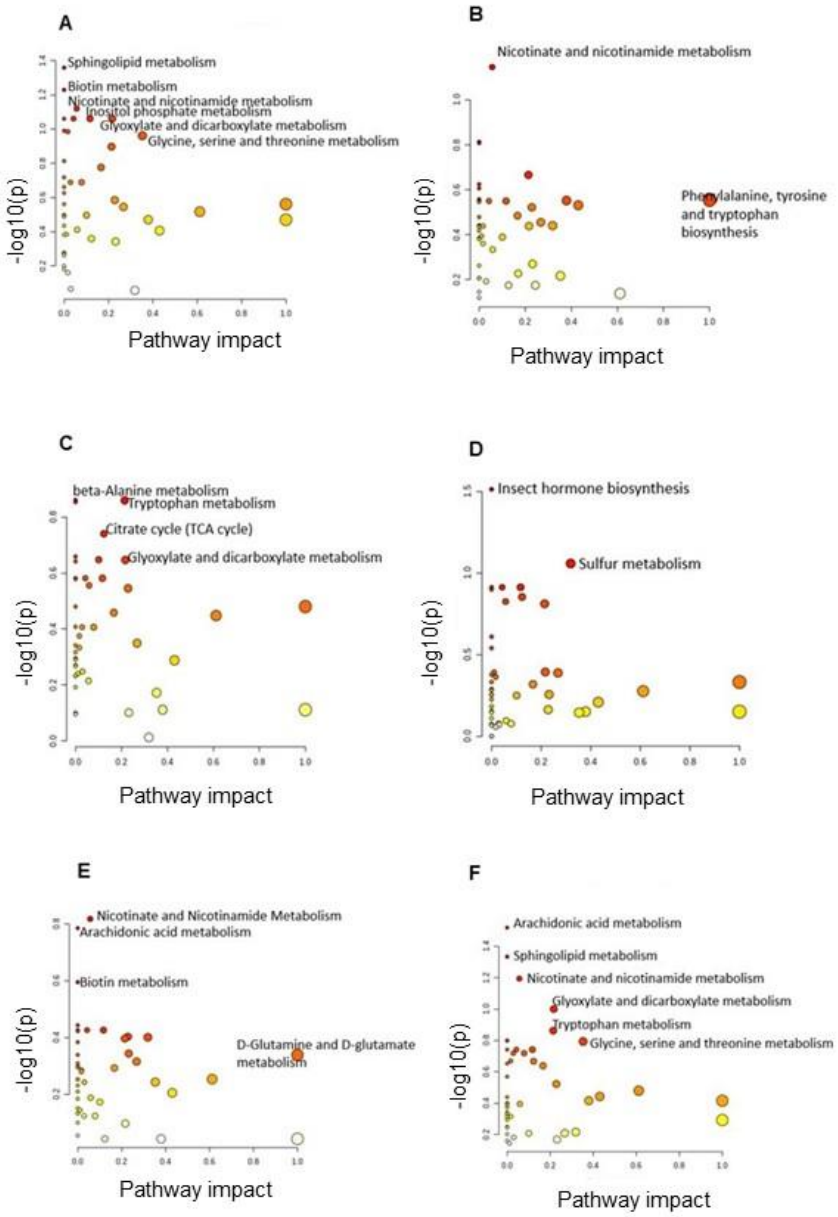

Figure 3. 13: MetaboAnalyst pathway analysis for sub-lethal exposure of *D. magna* to CTAB capped rod shaped nAu LC10 (A) and LC20 (B); citrate capped nAu LC10 (C) and LC20 (D); ionic Au LC10 (E) and LC20 (F). Pathway's analysis nodes were represented as a function of −log (p), the darker the shade of red indicates a higher pathway effect.

3.3.5 CytoViva® Hyperspectral Dark Field Imagery

The nAu particles display as bright red to maroon-coloured clusters. The control group was used as a reference to compare the accumulation of nAu (CTAB capped rod shaped nAu and citrate capped nAu) and ionic Au (Figure 3.14). To assess accumulation, the focus was on the external carapace and the different internal tissues in *D. magna.* The nAu particles were not seen near the mouth following 48 hr exposure, however after 12 hr exposure particles were observed near the mouth (micrographs not shown). In the CTAB capped rod shaped nAu, particles were observed in the gut (Figure 3.15 A), carapace (Figure 3.15 B) and antennae (Figure 3.15 C). Gold particles were observed in the gut (Figure 3.16 A), claw and spine (Figure 3.16 B) and antennae (Figure 3.16 C) of *D. magna* following exposure to citrate capped nAu. For the ionic Au exposures, particles were not observed in the gut, mouth, and antennae (Figure 3.17 A, B and C).

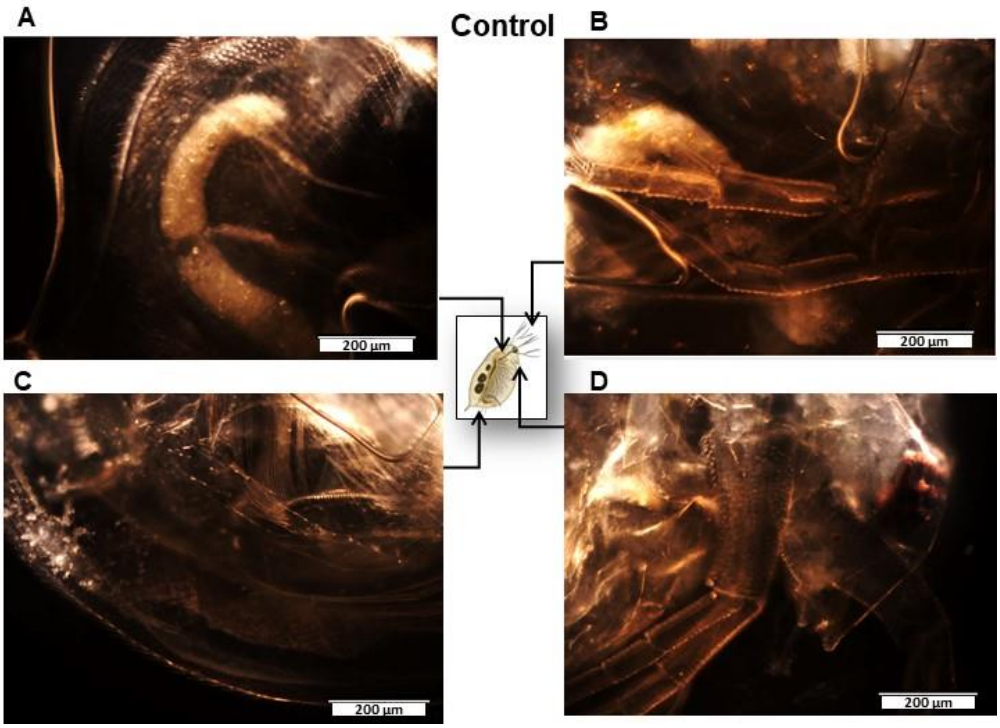

Figure 3. 14: Unexposed control *D. magna* in M7 aquatic media viewed under CytoViva®dark field hyperspectral imaging indicating A) gut, B) antennae, C) spine and claws, D) mouth parts.

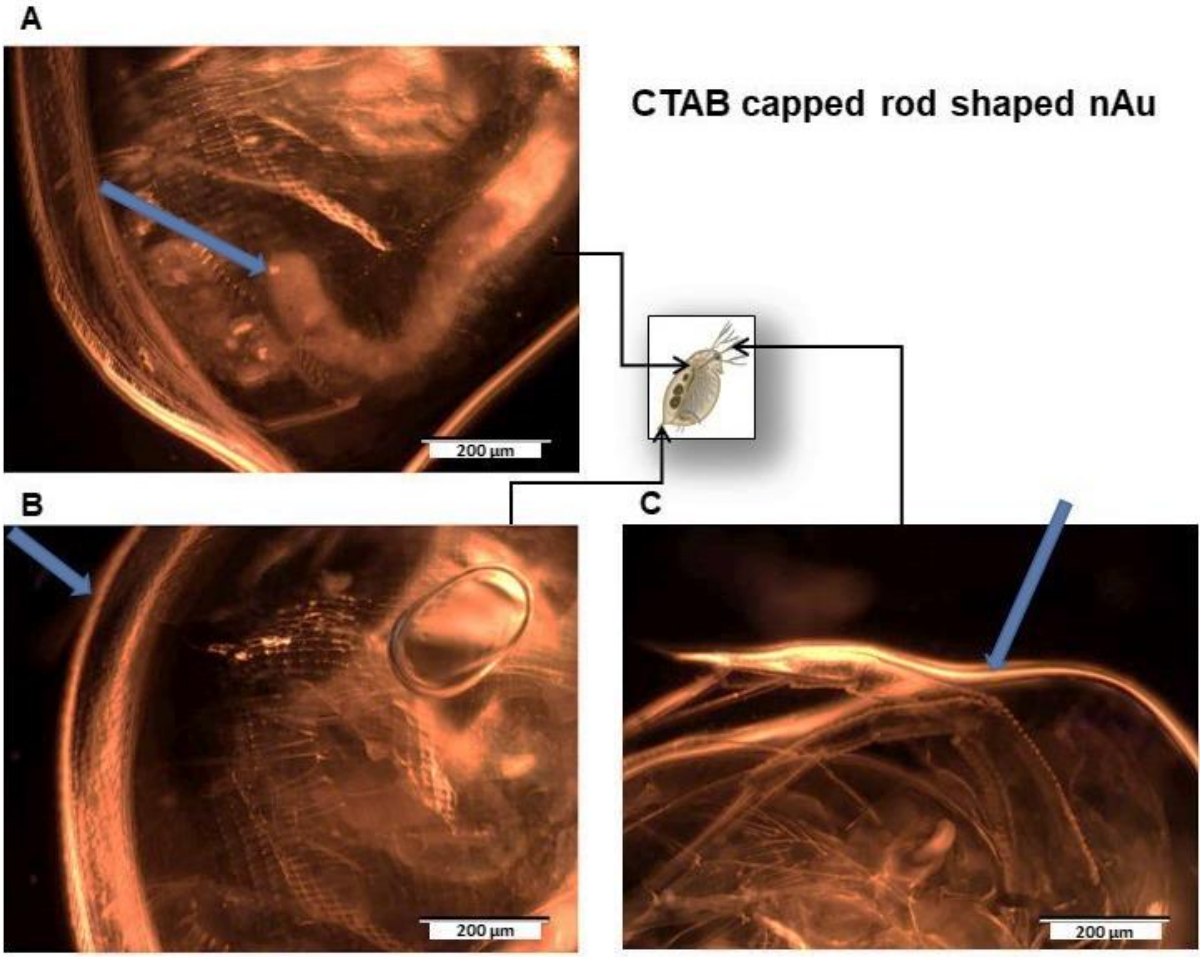

Figure 3. 15: CytoViva®dark field hyperspectral imaging of *D. magna* following 48 h exposure to CTAB capped rod shaped nAu. The arrows indicate nAu particles in the gut (A), close to the spine (B) and on the antennae (C).

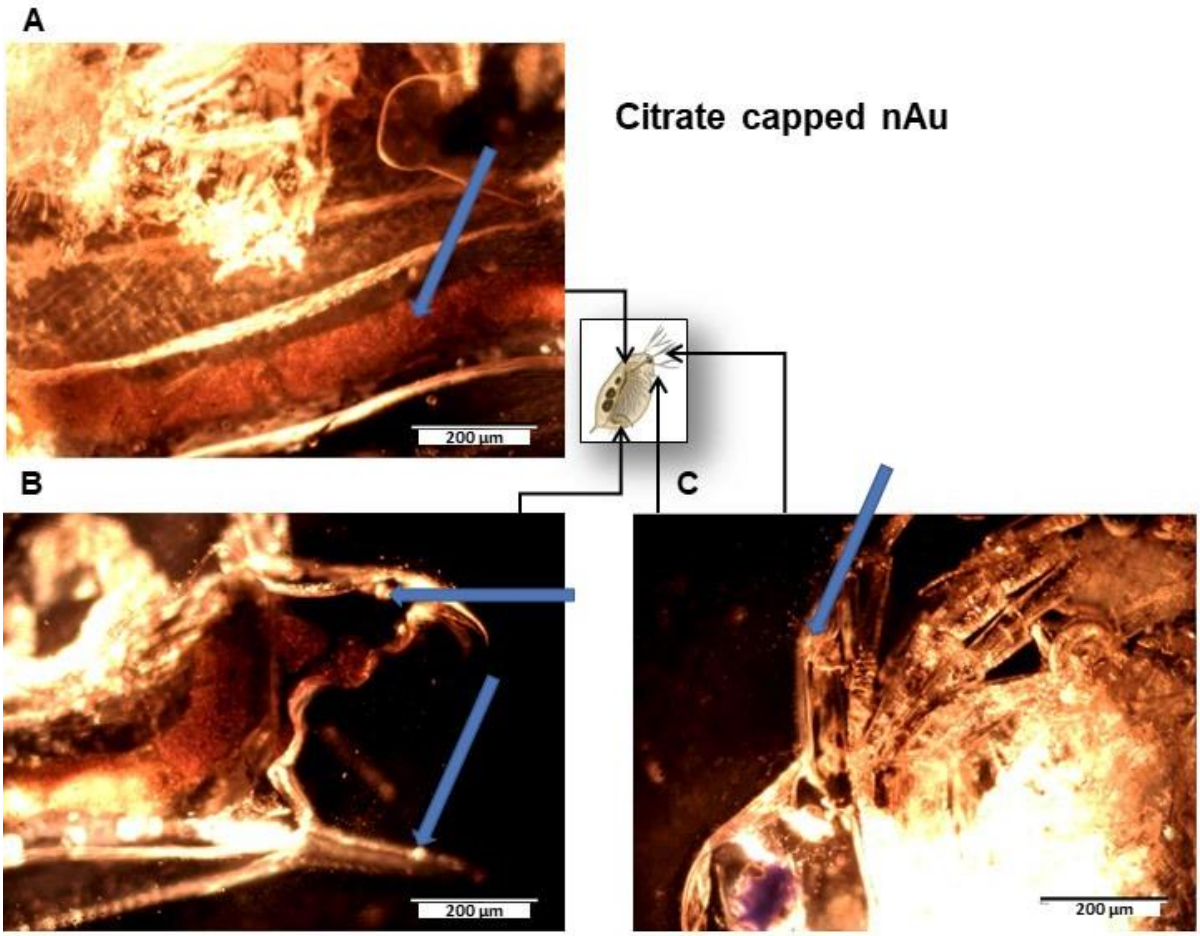

Figure 3. 16: CytoViva®dark field hyperspectral imaging of *D. magna* following 48 h exposure to citrate capped nAu. The arrows indicate nAu particles in the gut (A), close to the spine and claw (B) and on the antennae (C).

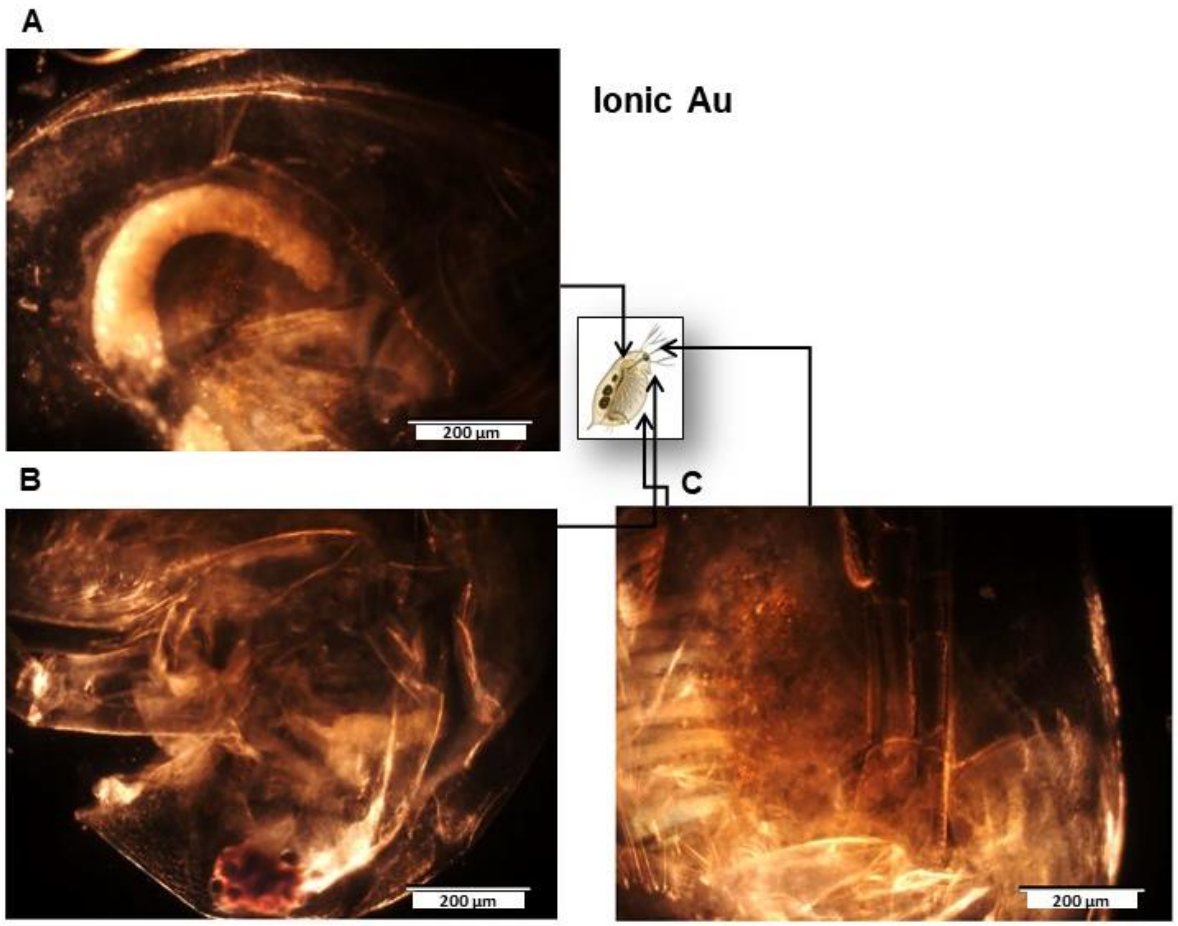

Figure 3. 17: CytoViva®dark field hyperspectral imaging of *D. magna* following 48 h exposure to ionic Au indicating (A) gut, (B) mouth parts and (C) antennae.

3.4 Discussion

Physiology is an important measure in ecotoxicology as it allows us to determine how biological responses differ when compared to normal or unexposed tissue. In this study there were alterations in the heart rate, respiration and metabolites formed after exposure to nAu and ionic Au. The metabolic rate of *D. magna* relies on the feeding current by transporting oxygenated water to the respiratory surfaces (Pirow et al., 1999a). Metabolic rate is defined as a capability of an animal to transport oxygen via the cardiovascular system with aid of cardiac output (Pirow et al., 2001). The alterations that occur during respiration can be due to increased heart rates and not increased beating rates of the appendages (Pirow et al., 2001). When the heart rate declines

it can lead to decreased oxygenated blood transportation to the tissues (Dzialowski et al., 2006). The heart rate of *D. magna* has shown to increase while the oxygen level declines (Paul et al., 1998). The effect of specific chemicals on *D. magna* heartbeat is dependent on the type of chemical (Park et al., 2019). Metaprolol, Propranolol, Acetylcholine, and caffeine result in a decrease in the heart rate of the *D. magna* (Dzialowski et al., 2006; Finn et al., 2012; Owen et al., 2007; Park et al., 2019; Stanley et al., 2006). However, there was not much of a percentage variance difference in the heart rate of daphnia in acetylcholine compared to caffeine (Dzialowski et al., 2006; Zang et al., 2019). Furthermore, lactose does influence the rate and rhythm of the heart rate of *D. pulex* causing arrhythmia heart disorder. Arrhythmia heart disorder can be observed at high concentrations with 1-2 large contractions of the heart (Campbell et al., 2004). These were mostly noted in the citrate capped nAu LC20 and ionic Au LC20, moreover ionic Au. A decrease in heart rate could be because of delayed signal transmission from nerves to heart muscle. Neuromuscular junctions were experiencing oxidative stress as noted after 24 h exposure of salicylic acid. This might be associated with increased regulation of the nervous system causing frequency in heart muscle contraction (Szabelak and Bownik, 2021).

Both NMs, quantum dots (QDs) and peptide quantum dots (gH625-QDs), exposure to daphnia showed an alteration in the heartbeat, however, there was no significant change in heart rate compared to the control (Galdiero et al., 2017). When daphnia were exposed to other NMs (Titanium Dioxide, nano-C60 and C60HxC70Hx) other physiological endpoints were altered which include changes in hopping frequency, appendage movement, and heart rate (Lovern et al., 2007). *Daphnia magna* exposed to titanium oxide, silver ion and silver nanoparticle showed a significant decrease at highest concentration in the heart rate when compared to the control for 3 h exposure by 7.3%, 4.3% and 15.0% respectively. As the duration of the exposure increased, the heart rate and movement increased when compared to a shorter exposure time (Park et al., 2021). The ionic Au LC20 and citrate capped nAu LC20 showed significant increase when compared to the control after 48 h exposure.

Changes within the heart rate can be directly linked to changes in respiration rates. Other studies assessing respiration have shown a general increase/decrease in oxygen consumption due to metabolism rates being affected. In this study the nAu increased respiration rate while ionic Au decreased respiration compared to control. Metal exposure can decrease the respiration rate due to interactions between antagonistic Magnesium ions (Carney et al., 1986; Knops et al., 2001; Pane et al., 2003). Nanomaterials showed significant increase in the CTAB capped rod nAu and citrate capped nAu when compared to the control after 48 h exposure. Thoracic limb activity plays

a crucial role in filtration and ventilation process, a decrease in thoracic limb activity could be due to weakened thoracic muscle contraction, as seen after exposure to Ketoprofen which causes dysfunctional feeding abilities and abnormal respiration (Bownik et al., 2019b; Bownik et al., 2020).

The daphnia showed no effect in the respiration rate when exposed to Cetyltrimethylammonium bromide, the capping agent used in this study (Knops et al., 2001). According to Pirow et al. (1999b), water current generated by thoracic limbs in daphnia resulted an increase in the oxygen consumption rate, but in this study that was not observed. *Daphnia magna* extracts ambient oxygen from the feeding current and gas exchange across the inner carapace wall are favourable (Pirow et al., 1999a).

Respiratory gas exchange occurs within the inner wall of the carapace of *D. magna* (Botha et al., 2016; Pirow et al., 1999a). The presence of nAu was confirmed to be accumulating in the gut. As outlined above that in the oxygen consumption rate of nAu showed a decline in respiratory rate after 48 h exposure which could be related to interferences with gaseous exchange in the gut due to nAu accumulation. Additionally, nAu was found accumulating around the thoracic limbs which play a crucial role in feeding and ventilation (Baumer et al., 2002; Bownik et al., 2019a; Lari et al., 2017; Pirow et al., 1999a). Furthermore, daphnids use antennae as a locomotory function, however, it was observed that nAu were present in the antennae in this study. Daphnids spine and claws have a protective feature, locomotory function and clean debris from the thoracic appendages but nAu accumulation was also noted in these areas which could affect physiological endpoints assessed (Botha et al., 2016).

As respiration and heart rate increases it is expected that metabolic rate will increase. This could be due to increased protein-turnover, a mechanism to cope with stressful environmental conditions (Muyssen et al., 2006).

During this study there was a decrease in *D. magna* reproduction both in nAu and ionic Au exposure. While metabolomics analysis revealed that daphnia had a decrease in eight amino acids (glutamine, serine, L-lysine, tryptophan, tyrosine, niacinamide, aspartic acid and endogenous sulfite) and an increase in citric acid. According to Wang et al. (2018) exposure of silver nanoparticles (AgNPs) to *D. similis* showed an increase in the amino acid content on the species. Further explained, an increase of amino acids can lead to decrease in fatty acids (arachidonic acid, stearidonic acid and linoleic acid). An increase in amino acids means there may be protein breakdown, which could be a release of amino acids for the requirement of energy

metabolism that the daphnids are experiencing under stressful environmental conditions (Shahid et al., 2021).

When *D. magna* was exposed to ionic Au, it showed a significant decrease in arachidonic acid. Arachidonic acid and stearidonic acid are defined as the end product of linoelaidic acid (linoleic acid). The components that derive from linoleic acid function as growth regulators and aid reproduction (Wang et al., 2018). Arachidonic acid plays a crucial role during reproduction and has potential impacts in the environmental sex determination in daphnia, causing increased female production (Ginjupalli et al., 2015). A rich diet in arachidonic acid can increase protection in some reproductive toxicants. The above-mentioned amino acid and fatty acids can be used as biomarkers (Wang et al., 2018). This is a defence mechanism for daphnia in response to AgNPs stress by conserving energy used in reproduction for growth and survival (Wang et al., 2018; Zhang et al., 2017).

It was seen that all treatment groups (CTAB capped rod shaped nAu, citrate capped nAu and ionic Au) had a common metabolic response in *D. magna*. This pattern has also been observed in Bisphenol A, Bisphenol F and Bisphenol S (Oliveira Pereira et al., 2021). Limitation in food can result in increased energy reserves causing species to have adverse effects (e.g. decline in reproduction) affecting physiological changes as outlined in physiological section. However, although daphnia were not fed in the metabolomics analysis (48 h), they were fed throughout the reproduction test. The downregulation observed in the biosynthesis of fatty acid (arachidonic acid) has the ability to disrupt the sugar and lipid metabolism. As mentioned earlier this disruption increase the release of amino acids and may result in the need to acquire a carbon source for energy (Oliveira Pereira et al., 2021; Shahid et al., 2021). With reference to the Kyoto Encyclopedia of Genes and Genomes (KEGG), it found that the influence of citrate capped nAu LC10 on citric acid involves changes in the citrate cycle (TCA cycle) (dmk00020) and LC20 changes in cholesterol mainly involves the insect hormone biosynthesis (dmk00981). The TCA cycle is an important metabolic pathway to produce energy. *Daphnia pulex* exposed to nC60 required cells to generate more energy to activate transportation of daphnia. Increased energy will require the daphnids to function as an antioxidant by preventing or slow damage to cells clearing free radicals caused by nC60 (Wang et al.,2019). Insect hormone biosynthesis is important for moulting and juvenile hormone regulation, regulating embryonic development and repressing metamorphosis in many insects (Bellés et al.,2005). There was increased moulting in daphnia therefore affecting reproduction as outlined in Chapter 2. Increased in moulting resulted in *D. magna* requiring excess energy production.

Chapter 4

Behaviour and Community responses

Chapter 4: Behaviour and Community responses

4.1 Introduction

Due to the global distribution of daphnid species in freshwater they are of ecological importance in the aquatic health of freshwater ecosystems and an effective bioindicator species in ecotoxicological studies (Bownik, 2017; Penalva-Arana et al., 2011). As a filter feeder they have the potential for high population growth rates, which play a significant ecological role in food-web dynamics. These interactions as both as a primary consumer of phytoplankton and as a key food source for secondary consumers such as fish, define it as a strong ecological interactor (Pohnert, 2019; Weiss et al., 2018). The strength of population interactions can be influenced by morphological, physiological, and behavioural changes (Miner et al., 2012).

Daphnia swimming behaviour is multifaceted, not comparable and the most sensitive biomarker of toxicity (Bownik, 2017; Bownik and Pawlik-Skowrońska, 2019; Duquesne & Küster, 2010; Simão et al., 2019). Swimming activity can be described as various behavioural swimming aspects such as immobility (inability to move or swim), depression (species can be trapped or swim at the bottom of the surface), normal swimming (there are no changes in swimming behaviour) and overactivity (species continuously spins) (Jeong et al., 2018; Miner et al., 2012; Tkaczyk et al., 2020).

Phototaxis is a vertical movement in response to changes in light and is essential for feeding behaviour and predatory avoidances. Daphnia can either move towards the source of light (positive phototaxis) or away from it (negative phototaxis). Environmental conditions, including food, light, pH, temperature, and predator cues, have an impact on stimulating the movement of daphnia in the water column (Bownik and Pawlik-Skowrońska, 2019; Chen et al., 2012; Dodson et al., 1997). Behaviour is a valuable tool to assess changes within the environment and is suitable for evaluating the effects of toxicants. Moreover, alterations of daphnia movement can be quantified through non-invasive video recordings in response to environmental pollutants (Brausch et al., 2010; Bownik, 2017; Bownik et al., 2019a).

Preliminary studies of toxicant exposure showed that all measured swimming parameters including swimming track density, hopping frequency, swimming speed, and turning ability were decreased in a time/concentration dependent manner in *D. magna* compared to the control (Bownik et al., 2019a). Any changes in behaviour can be directly related to physiological changes

within daphnia and will lead to greater community impacts due to shifts within the food web (Bownik, 2017; Bownik et al., 2019a).

Functional response is defined as the resource consumption rate related to resource density (Holling, 1959; Solomon, 1949). Functional responses are usually categorized into three types, namely: Type I, Type II and Type III. The Type I functional response can be defined as rectilinear response that is normally found in filter feeders such as daphnia. The resource consumption is not limited by handling time (Jeschke et al., 2004). The Type II functional response is defined as prey density rises; a predator's rate of prey consumption rises due to closer proximities but finally reaches a plateau as prey densities decrease. Lastly, Type III is known to be sigmoidal which is a positively density dependent response as a result of low prey density where the predator has a learning response in order to catch prey (Oaten and Murdoch, 1975). The following parameters such as attack rate, handling time and maximum feeding rates can be quantified with the above-mentioned functional response types (Juliano, 2001; Dick et al., 2013).

Organisms that have high functional response show an effect at higher attack rates, lower handling times and can be influenced by changes of behaviour of prey. Moreover, higher functional response has a higher impact potential (Bollache et al., 2008; Dick et al., 2013; Haddaway et al., 2012). Functional response analysis is an important robust assessment method which has an ecological impact by predicting and explaining several biotic and abiotic factors (Dick et al., 2014; Dick et al., 2017a; Dick et al., 2017b).

The aim of the study was to (i) evaluate the influence of sub lethal concentrations of nAu and ionic Au on *D. magna* swimming behaviour and (ii) determine the functional response of unexposed *Danio rerio* (zebrafish) preying on *D. magna* after exposure to nAu and ionic Au.

4.2 Materials and methods

4.2.1 Swimming behaviour

The stock preparation and sublethal daphnia exposure test were conducted as outlined in Section 3.2. Both the individual and community swimming behaviour was assessed in temperature controlled dedicated behavioural rooms using a Noldus DanioVison and EthoVision software (Netherlands), at the NABF. North West University (Potchefstroom campus) (Figure 4.1).

Figure 4. 1: The National Aquatic Bioassay Facility (NABF) behaviour laboratory equipment (Noldus DanioVison, Netherlands), North West University (Potchefstroom campus).

Daphnia magna individual swimming behaviour test

Swimming behaviour was assessed at both 0 h and 48 h. Adult daphnia were transferred to twelve-well flat-bottomed micro-plates (figure 4.2 A) using a plastic pipette. There were twelve replicates per group with one daphnid per well and the following exposure groups were assessed: control, CTAB capped rod shaped nAu, citrate capped nAu and ionic Au at their respective exposure concentrations for LC10 and LC20. The control consisted of clean M7 media while the exposed were measured in exposure M7 media.

The plates were digitally calibrated by physically measuring the plate diameter and updating the arena settings per plate within the software (Figure 4.2 B). At 0 h individual plates were immediately placed in a Noldus DanioVision observation chamber for a period of one hour and recordings were taken in the dark with 10-minute dark/light intervals with a video camera (Basler monochrome GigE). At 48 h the same plates were re-recorded to determine changes over exposure time. Video recordings were acquired in Ethiovision X14 software in order to determine

the following quantitative end points: distance moved, swimming speed, mobility state and turn angle. The data was then exported in excel files for further statistical analysis.

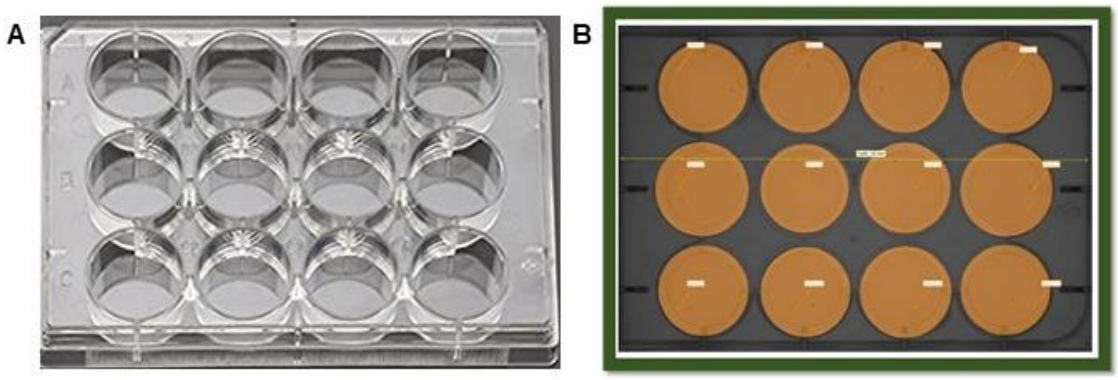

Figure 4. 2: The twelve-well flat-bottomed micro-plate used for individual swimming behaviour (A) and the digital arena settings of the 12 well plate in EthoVision (B).

Daphnia magna community swimming behaviour test

Community swimming behaviour was assessed at both 0 h and 48 h in custom-made glass tanks, with a diameter of 5 cm and 14 cm of length, filled with 140 mL of respective exposure media (Figure 4.3). A group of five daphnids were transferred to each glass tank using a plastic pipette. There were three replicates per treatment groups (n=15). The treatment groups were control, CTAB capped rod shaped nAu, citrate capped nAu and ionic Au at their respective concentrations (LC10 and LC20). The control consisted of clean M7 media with five adult *D. magna* in it while the exposed were measured in exposure M7 media. Each recording was taken using a Basler GigE camera placed in front of an infrared backlight. Recordings were taken at 25 frames per second for a duration of 30 minutes. Video files were concurrently acquired using EthoVision X14 software, data are represented as a group mean and excel files were exported to GraphPad Prism 5 for further analysis.

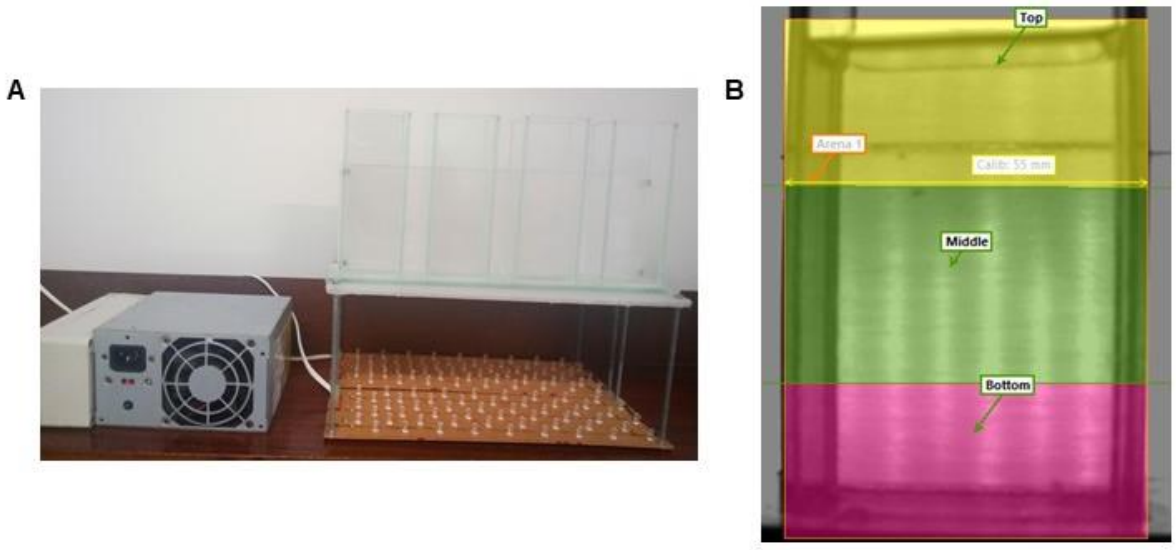

Figure 4. 3: The custom-made glass tank in front of infrared backlighting used for community swimming behaviour (A) and the digital arena settings of community swimming behaviour divided into top, middle, and bottom zones (B).

Statistical analysis

The data sets were analysed as outlined in Section 3.2 of Chapter 3.

4.2.2 Functional response

The stock preparation and sublethal 48 h daphnia exposure test were conducted as outlined in Section 3.2.

Experimental design

The prey (*D. magna*) were exposed to control, CTAB capped rod shaped nAu, citrate capped nAu and ionic Au (LC10 and LC20) for 48 h prior to the start of the test (Section 3.2). The predator used in this study was adult *D. rerio* housed at the NABF and were naïve to daphnia predation and were not exposed via media to any contaminant for the duration of the study. Predators housed at the NABF were unfed for 16-18 h prior the assessment. After the 48 h exposure test, adult daphnids were counted into densities of 1, 2, 6, 10, 15, 25, 32 and 45 in replicates of four per treatment group. The respective prey was placed in 600 mL beakers containing system water

(ISO medium) using a sieve and plastic pipette. After adding the prey there was a ten-minute acclimation period. Predators (n=3 in a fish tank) were released gently using an aquarium net into the 600 mL beaker. All prey density trials were conducted in four replicates for each of tested compounds (control, citrate capped nAu, CTAB capped rod shaped nAu and Ionic Au) and monitored for 30 minutes. After 30 minutes the predator was removed and the number of remaining preys per beaker was counted for each prey density and exposure group.

Statistical Analysis

Prey consumption

The Functional response (FR) analyses was conducted in R v.3.3.0 and R package “emmeans” was used to model FR type of *D. rerio* preying on *D. magna* (Lenth, 2018; Pritchard, 2014; Pritchard et al., 2017). A first generalized linear model (GLM) with a quasi-Poisson error distribution to account for data over dispersion was conducted to assess differentiation between the control and prey density. This was to observe the interaction among treatment and prey density as the predictor variable. A second factorial generalized linear model with a quasi-Poisson error distribution was conducted to assess the effects of concentration, exposure group and prey density on number of preys eaten. The model was first fitted with full interaction terms and then removed stepwise. Due to unbalanced observational data this was completed on the dataset with the control treatment removed.

Functional response was first tested for general Type shape via frair: frair_test, however this produced equivocal results therefore FR Type was tested manually. Functional Response Type (I, II, III) was conducted with a binomial logistic regression of the proportion of prey consumed against prey density. When non-significant terms were encountered, a scatterplot with locally weighted scatterplot smoothing (LOWESS) lines were fitted to assess the direction of proportional consumption. This was conducted to observe the shape of proportional consumption of prey at different prey densities (Pritchard et al., 2017).

Functional responses were then fitted using maximum likelihood estimation (MLE) (Bolker, 2010) and the Lambert W function (Bolker, 2008). Data were non-parametrically bootstrapped to generate bootstrapped clouds (n=2000) representing 95% confidence intervals (Barrios-O’Neill et al., 2014; Pritchard et al., 2017). This allows population level comparison of feeding responses at each different treatment, where overlapping confidence intervals are not statistically significant.

4.3 Results

Daphnia magna individual swimming behaviour

Visual observations throughout the test revealed that the daphnia in the control group were swimming just below the surface of the M7 media, the CTAB capped rod shaped nAu group were constantly spinning forward either below the surface or at the bottom of the well while the citrate capped nAu group were swimming visually at the bottom of the well (sinking). The daphnia exposed to ionic Au were swimming just below the surface and were sometimes observed spinning forward.

The quantified swimming behaviour was analysed in both dark and light phases and mean values with standard deviations are represented in the graphs and significance was when $p < 0.05$. The nAu behavioural trials were performed during the same time period while the ionic Au group was performed at a later stage and therefore had a separate control group.

Distance moved

At 0 h there were no significant differences between CTAB capped rod shaped nAu and the control (Figure 4.4 A). The citrate capped nAu group showed a significant increase in the distance moved [dark (LC10 124.35 mm & LC20 126.48 mm); light (LC10 130.32 mm & LC20 124.59 mm)] when compared to the control [dark (113.83 mm); light (112.71 mm)] at 0 h (Figure 4.4 C). The daphnia exposed to ionic Au were covering a significantly lower distance [dark (LC10 77.31 mm & LC20 82.15 mm); light (LC10 76.91 mm & LC20 74.83 mm)] when compared to the control [dark (126.95 mm); light (119.19 mm)] at 0 h (Figure 4.4 E).

After a 48 h exposure period, CTAB capped rod shaped nAu group LC20 (114.19 mm) (Figure 4.4 B) and citrate capped nAu group (LC10 146.04 mm & LC20 153.87 mm) (Figure 4.4 D) were swimming at a significantly further distance when compared to the control (114.17 mm) during the dark phase. However, during light phase CTAB capped rod shaped nAu group LC10 (Figure 4.4 B) were swimming a significantly lower distance (93.50 mm). The CTAB capped rod shaped nAu group LC20 (155.45 mm) (Figure 4.4 B) and citrate capped nAu group (LC10 167.46 mm & LC20 155.45 mm) (Figure 4. 4D) were swimming at a significantly higher distance when compared to the control in the light. The ionic Au group were swimming at a significantly higher distance [dark (LC10 213.69 mm); light (LC20 225.24 mm)] when compared to the control [dark (193.14 mm); light (188.62 mm)] at 0 h (Figure 4.4 F).

Swimming speed

During dark and light phase CTAB capped rod shaped nAu group LC10 were swimming at a significantly slower speed [dark (1.89 mm/s); light (2.10 mm/s)] when compared to the control [dark (3.23 mm/s); light (3.25 mm/s)]. However, CTAB capped rod shaped nAu group LC20 were swimming at a significantly faster speed [dark (4.49 mm/s); light (5.09 mm/s)] when compared to the control [dark (3.23 mm/s); light (3.25 mm/s)] (Figure 4.5 A) during dark and light phase. The citrate capped nAu group LC10 were swimming at a significantly slower speed (2.19 mm/s) when compared to the control (3.23 mm/s) during dark phase at 0 h (Figure 4.5 C). During dark and light phase ionic Au LC10 were swimming at a significantly slower speed [dark (9.43 mm/s); light (9.99 mm/s)] when compared to the control [dark (12.42 mm/s); light (12.38 mm/s)] at 0 h (Figure 4.5 E).

After a 48 h period, CTAB capped rod shaped nAu group LC10 were swimming at a significantly slower speed [dark (1.87 mm/s); light (1.72 mm/s)] whereas CTAB capped rod shaped nAu group LC20 [dark (3.49 mm/s); light (3.83 mm/s)] (Figure 4.5 B) and citrate capped nAu group [dark (LC10 3.65 mm/s & LC20 3.48 mm/s); light (LC10 4.35 mm/s & LC20 3.45 mm/s)] were swimming at a significantly faster when compared to the control [dark (2.50 mm/s); light (2.75 mm/s)] during dark light phase (Figure 4.5 D). During dark and light phase ionic Au LC10 were swimming at a significantly slower speed [dark (5.63 mm/s); light (5.01 mm/s)] when compared to the control [dark (6.49 mm/s); light (6.10 mm/s)] at 48 h (Figure 4.5 F).

Turn angle

In this study there was no significant differences in turn angle among nAu and ionic Au (Figure 4. 6) when compared to the control at 0-48 h across all groups tested.

Mobility state

During the dark and light phase CTAB capped rod shaped nAu group LC10 were significantly less frequently swimming [dark (2.48); light (2.71)] whereas CTAB capped rod shaped nAu group LC20 [dark (12.74); light (13.65)] (Figure 4.7 A) and citrate capped nAu group LC10 [dark (14.76); light (12.99)] (Figure 4.7 C) were significantly more frequently swimming when compared to the control [dark (7.74); light (6.43)] at 0 h. During the dark and light phase ionic Au were significantly less frequently swimming [dark (LC10 19.37 & LC20 23.82); light (LC10 21.30 & LC20 24)] when compared to the control [dark (34.64); light (34.04)] at 0 h (Figure 4.7 E).

After a 48 h period CTAB capped rod shaped nAu group LC10 were significantly swimming at a less frequency [dark (7.82); light (5.65)] whereas CTAB capped rod shaped nAu group LC20 [dark (23.56); light (23.03)] (Figure 4.3.7 B) and citrate capped nAu group [dark (LC10 25.72 & LC20 24.98); light (LC10 27.14 & LC20 24.6)] (Figure 4.7 D) were significantly swimming at a more frequency when compared to the control [dark (13.41); light (16.53)] during dark and light phase. In addition, after 48 h ionic Au LC20 were significantly swimming more frequently [dark (56.61); light (58.89)] when compared to the control [dark (49.67); light (48.68)] during dark and light phase (Figure 4.7 F).

Immobile (frequency)

CTAB capped rod shaped nAu group showed similar trend i.e., LC10 lower and LC20 higher when compared to control for the light and dark phase. LC20 (dark), LC10 (light) and both higher. During dark phase CTAB capped rod shaped nAu group LC10 (Figure 4.8 A) were significantly more frequently [dark (123.54); light (128.81)] not swimming while on the other hand, during light phase citrate capped nAu group LC20 were significantly more frequently (102.92) not swimming when compared to the control [dark (93.13); light (94.0)] at 0 h (Figure 4.8 C). During dark and light phase ionic Au LC20 were significantly less frequently [dark (40.55); light (31.17)] not swimming when compared to the control [dark (49.02); light (42.70)] at 0 h (Figure 4.8 E).

During the dark and light phase CTAB capped rod shaped nAu group LC10 were significantly less frequently [dark (63.41); light (62.54)] not swimming when compared to the control [dark (76.56); light (81.39)] at 48 h (Figure 4.8 B). During dark and light phase ionic Au LC10 were significantly more frequently [dark (93.16); light (93.75)] not swimming when compared to the control [dark (86.44); light (81.10)] at 48 h (Figure 4.8 F).

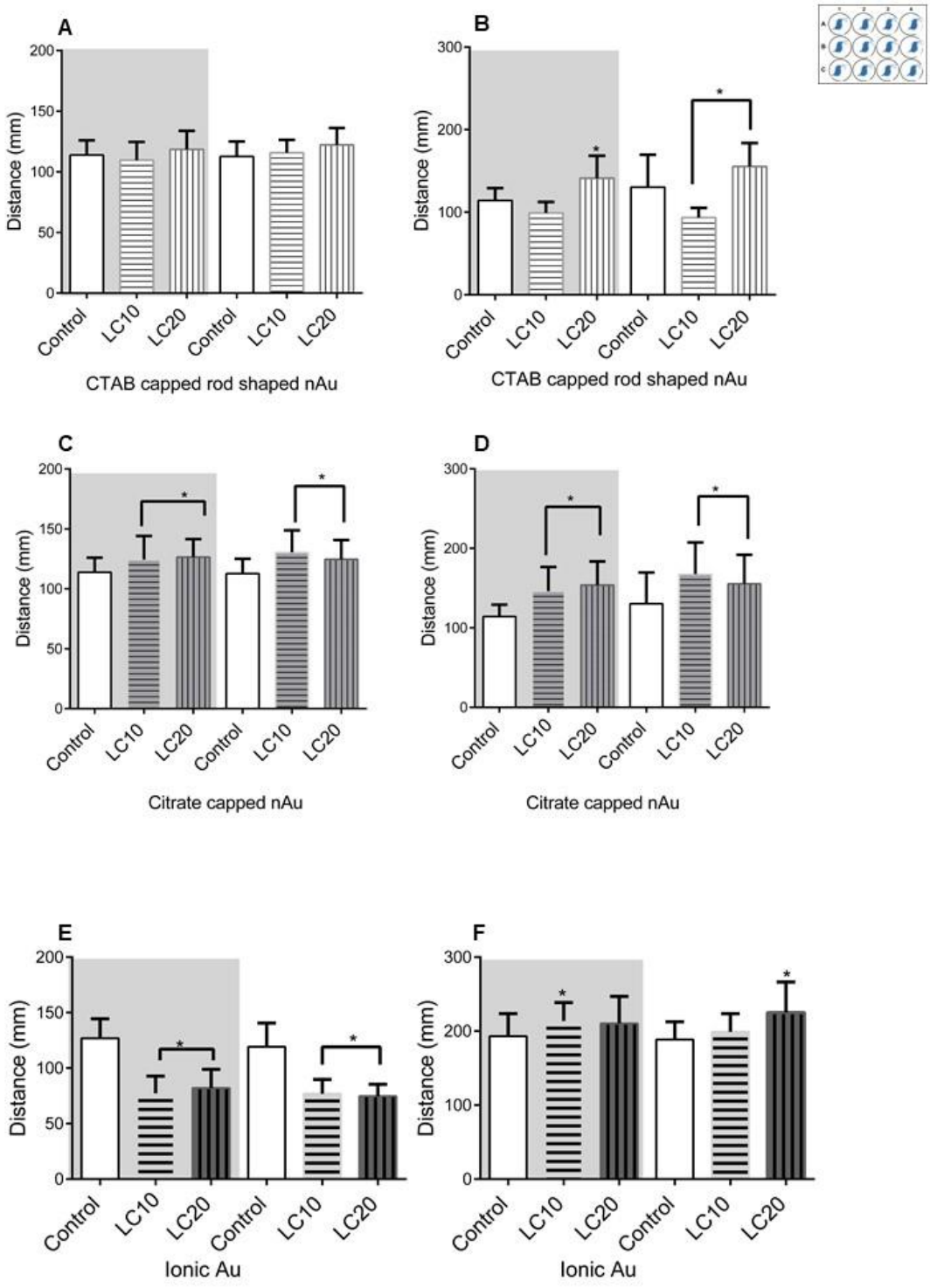

Figure 4. 4: The distance moved (mm) by *D. magna* during individual swimming behaviour trials when exposed to CTAB capped rod shaped nAu 0 h (A) and 48 h (B); citrate capped nAu 0 h (C) and 48 h (D); ionic Au 0 h (E) and 48 h (F). * indicates significance ($p < 0.05$) and shaded area indicates dark phase.

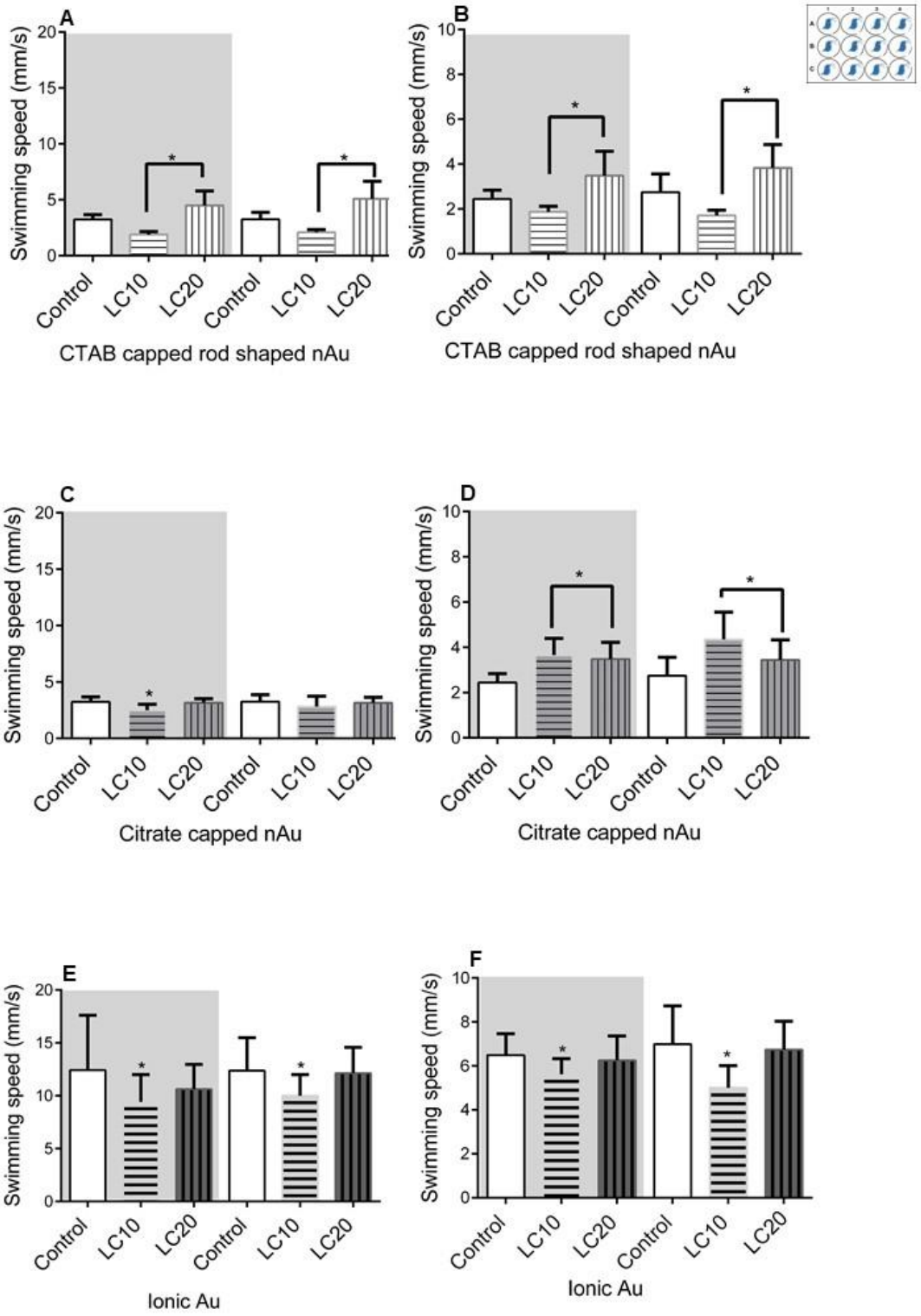

Figure 4. 5: The swimming speed (mm/s) of *D. magna* during individual swimming behaviour trials when exposed to CTAB capped rod shaped nAu 0 h (A) and 48 h (B); citrate capped nAu 0 h (C) and 48 h (D); ionic Au 0 h (E) and 48 h (F). * indicates significance ($p < 0.05$) and shaded area indicates dark phase.

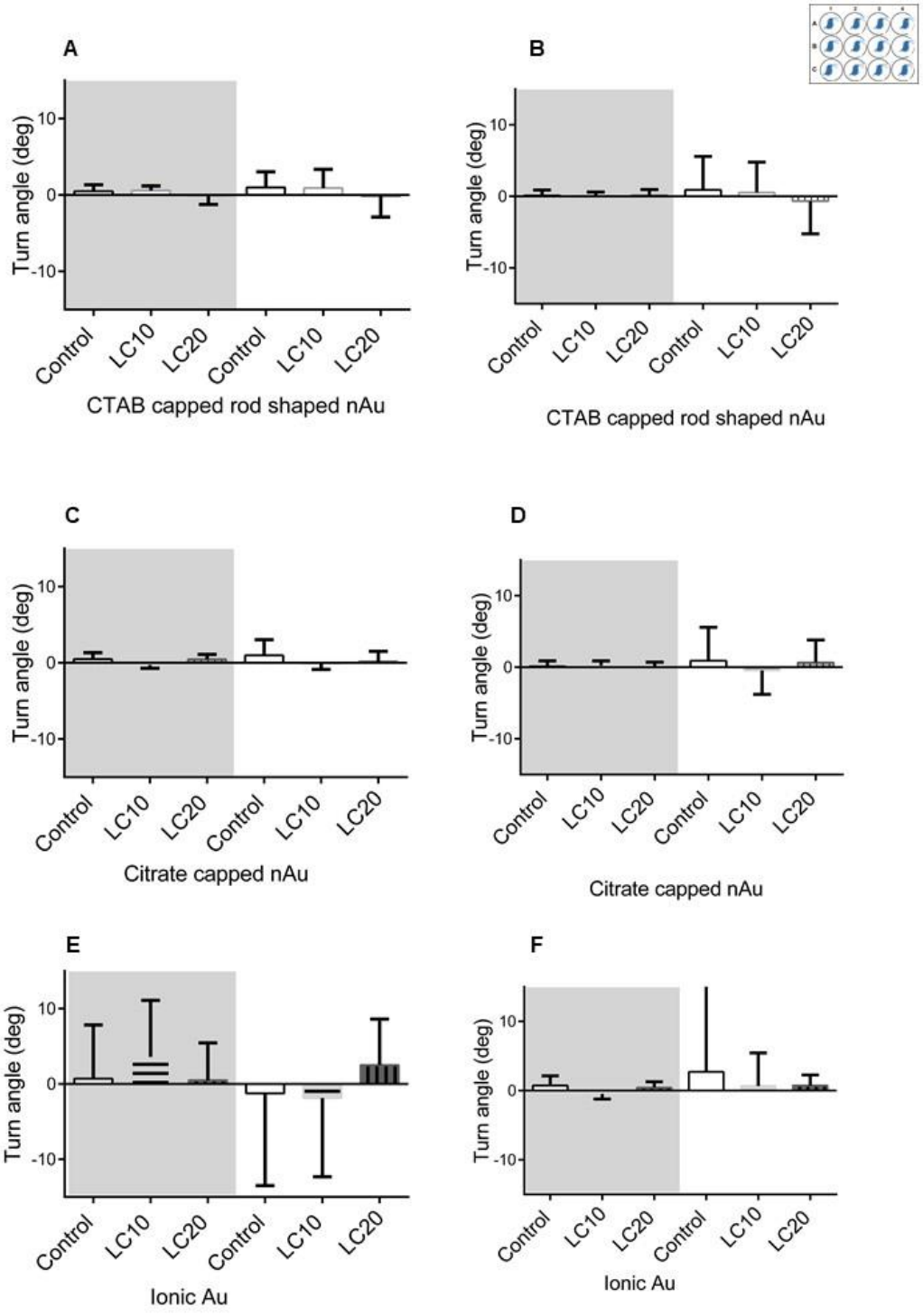

Figure 4. 6: The turn angle (degrees) of *D. magna* during individual swimming behaviour trials when exposed to CTAB capped rod shaped nAu 0 h(A) and 48 h (B); citrate capped nAu 0 h (C) and 48 h (D); ionic Au 0 h (E) and 48 h (F). Shaded area indicates dark phase.

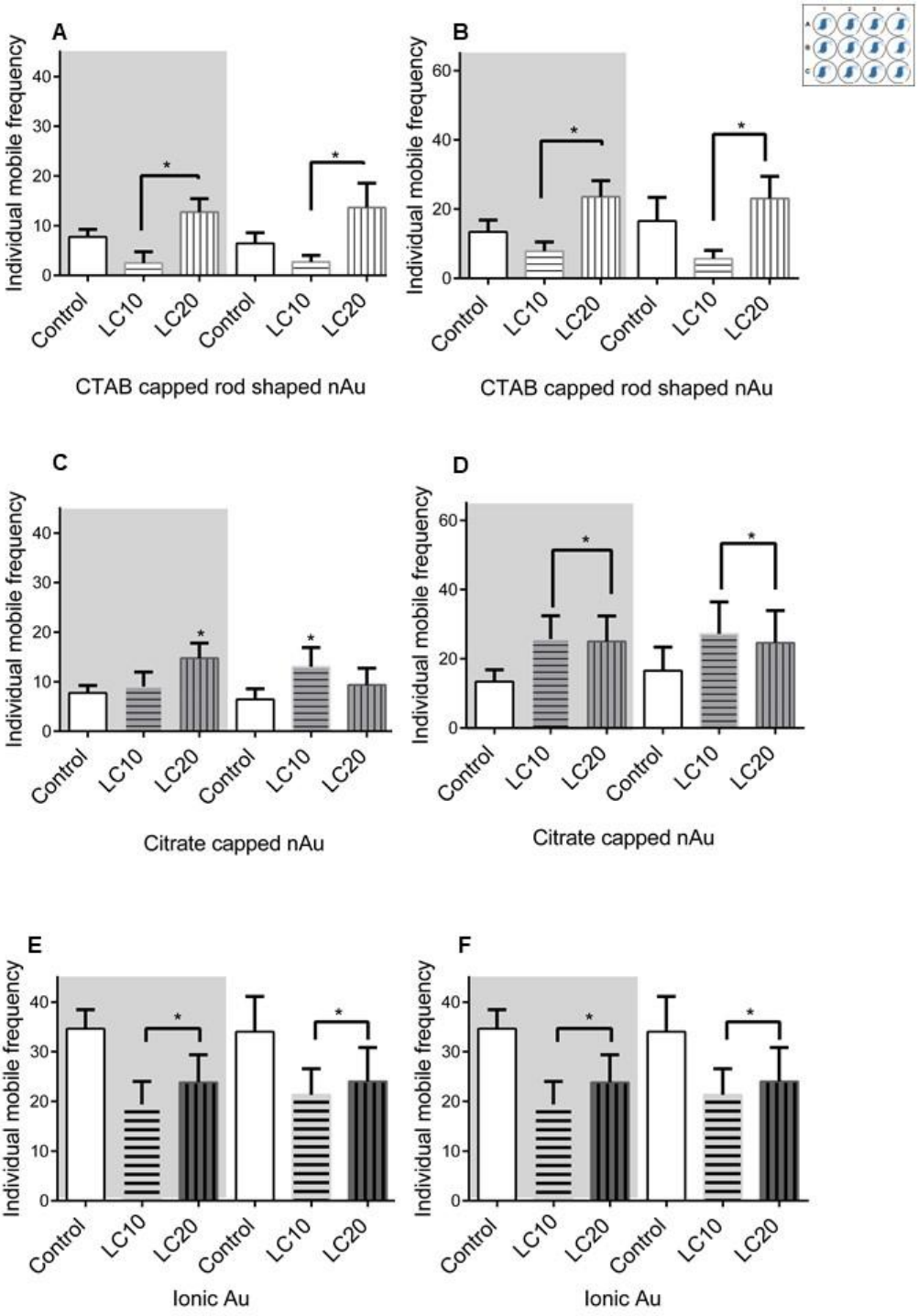

Figure 4. 7: The highly mobile frequency of *D. magna* during individual swimming behaviour trials when exposed to CTAB capped rod shaped nAu 0 h (A) and 48 h (B); citrate capped nAu 0 h (C) and 48 h (D); ionic Au 0 h (E) and 48 h (F). * indicates significance ($p < 0.05$) and shaded area indicates dark phase.

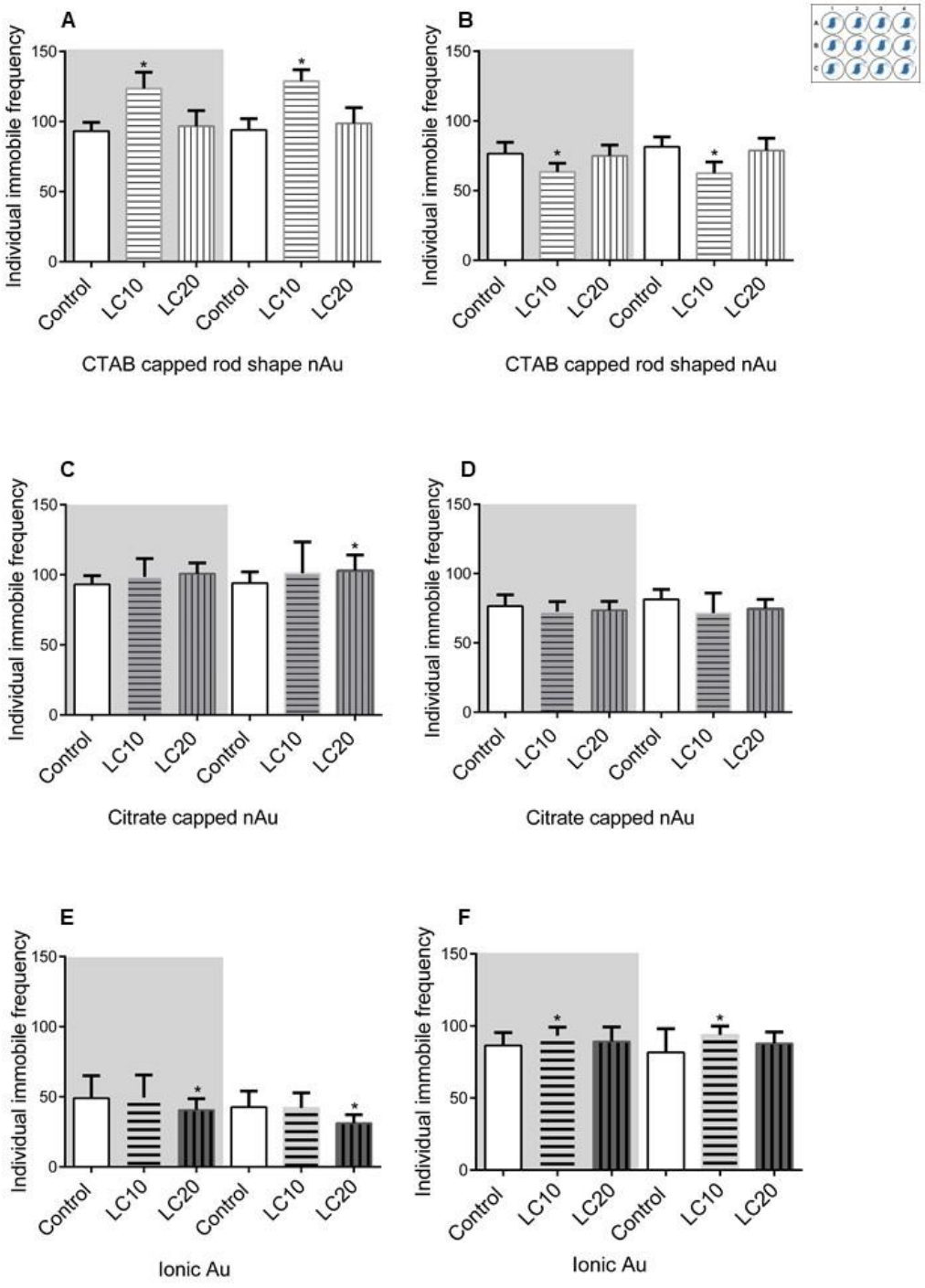

Figure 4. 8: The immobile frequency of *D. magna* during individual swimming behaviour trials when exposed to CTAB capped rod shaped nAu 0 h(A) and 48 h (B); citrate capped nAu 0 h (C) and 48 h (D); ionic Au 0 h (E) and 48 h (F). * indicates significance ($p < 0.05$) and shaded area indicates dark phase.

Daphnia magna community swimming behaviour

Distance moved

The community population of CTAB capped rod shaped nAu (LC10 2 311.96 mm & LC20 3 491.41 mm) (Figure 4.9 A) and citrate capped nAu (LC10 3 556.17 mm & LC20 2 970.66 mm) (Figure 4.9 C) showed significant decrease in distance moved when compared to the control (5 657.9 mm) at 0 h. However, ionic Au LC20 (5 704.34 mm) moved significantly at an increased distance when compared to the control (2 749.6 mm) at 0 h (Figure 4.9 E). The slow distance moved was also significantly observed in citrate capped nAu LC20 (925.95 mm) when compared to the control (2 395.25 mm) after 48 h (Figure 4.9 D).

Swimming speed

CTAB capped rod shaped nAu (LC10 2.08 mm/s & LC20 3.24 mm/s) (Figure 4.10 A) and citrate capped nAu LC20 (2.93 mm/s) (Figure 4.10 C) were significantly swimming at a slower speed when compared to the control (5.28 mm/s) at 0 h. However, ionic Au LC20 (5.47 mm/s) were significantly swimming faster when compared to the control (2.59 mm/s) at 0 h (Figure 4.10 E). After a 48 h, citrate capped nAu (LC10 1.41 mm/s & LC20 0.96 mm/s) was significantly swimming at low speed when compared to the control (2.63 mm/s) (Figure 4.10 D).

Mobility state

Daphnia population CTAB capped rod shaped nAu (LC10 146.2 & LC20 180.67) (Figure 4.11 A) and citrate capped nAu LC20 (180.33) (Figure 4.11 C) were significantly swimming at a lesser frequency when compared to the control (429.4) at 0 h. However, ionic Au LC20 (632.07) were significantly swimming at a higher frequency when compared to the control (321.33) at 0 h (Figure 4.11 E). After a 48 h period CTAB capped rod shaped nAu group LC20 (84.1) (Figure 4.11 B) and citrate capped nAu (LC10 134.5 & LC20 46.8) (Figure 4.11 D) were significantly swimming at a lesser frequency when compared to the control (277.27).

Immobile (frequency)

During 0 h ionic Au LC20 (2 610.13) were significantly more frequently not swimming when compared to the control (1 452.73) (Figure 4.12 E). After a 48 h, citrate capped nAu (nAu (LC10 754.8 & LC20 632.1) were significantly less frequently not swimming when compared to the control (1 539.27) (Figure 4.12 D).

Zone duration

CTAB capped rod shaped nAu LC20 showed a significant increase in swimming at the top zone (57.8 %) when compared to the control (33.3 %) at 0 h (Figure 4.13 A). After 48 h CTAB capped rod shaped nAu LC20 (62 %) (Figure 4.13 B) daphnids population spent most of the time swimming at the top zone. The citrate capped nAu (LC10 35.3 % & LC20 56.9 %) at 0 h (Figure 4.13 C) however, after 48 h citrate capped nAu LC20 (55 %) (Figure 4.13 D) daphnids population spent most of the time swimming at the top zone. Ionic Au (LC10 62.1 % & LC20 71.6 %) (Figure 4.13 E) spent most of the time swimming at the top zone at 0 h. The daphnia population of ionic Au (LC10 69.8 % & LC20 70 %) were significantly increasingly swimming at the top zone when compared to the control (25.9 %) (Figure 4.13 F).

During 48 h ionic Au LC10 (0 %) showed significant decrease swimming at the middle zone when compared to the control (2.4 %) (Figure 4.14 F).

CTAB capped rod shaped nAu LC10 spent most of the time swimming at the bottom zone (37.7 %) at 0 h (Figure 4.15 A). The daphnia population of ionic Au LC20 showed significant decrease swimming at the bottom zone (1.1 %) when compared to the control (29.9 %) at 0 h (Figure 4.15 E).

After 48 h, CTAB capped rod shaped nAu LC10 spent most of the time swimming at the bottom zone (41.9 %) (Figure 4.15 B). The daphnia population of citrate capped nAu LC10 were significantly increasingly swimming at the bottom zone (65.7%) when compared to the control (25.2 %) (Figure 4.15 D). The ionic Au LC20 showed significant decrease swimming at the bottom zone (2.7 %) when compared to the control (31.1 %) (Figure 4.15 F).

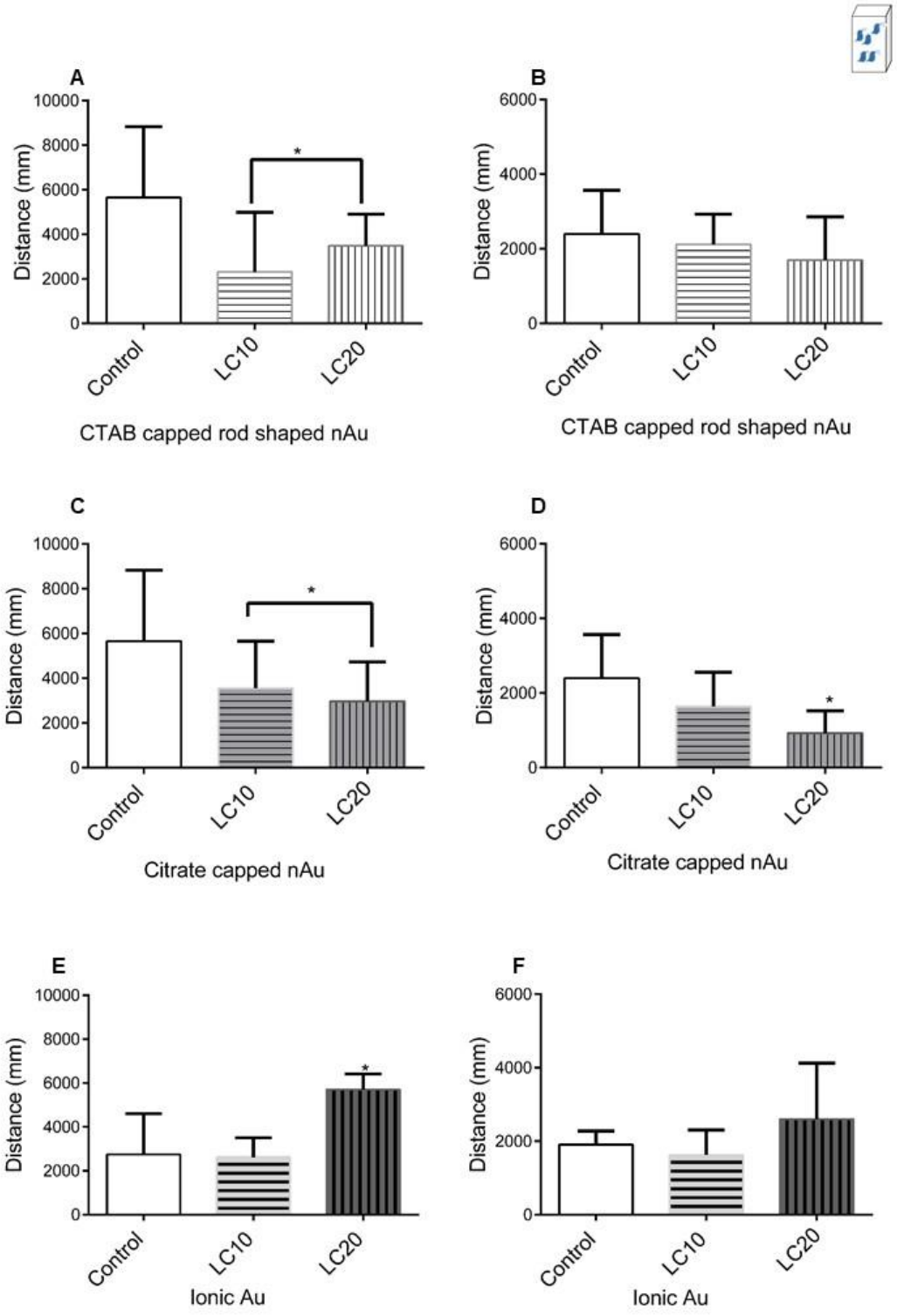

Figure 4. 9: The distance moved (mm) of *D. magna* (n= 15) during community swimming behaviour trials while exposed to CTAB capped rod shaped nAu 0 h(A) and 48 h (B); citrate capped nAu 0 h (C) and 48 h (D); ionic Au 0 h (E) and 48 h (F). * indicates significance($p < 0.05$).

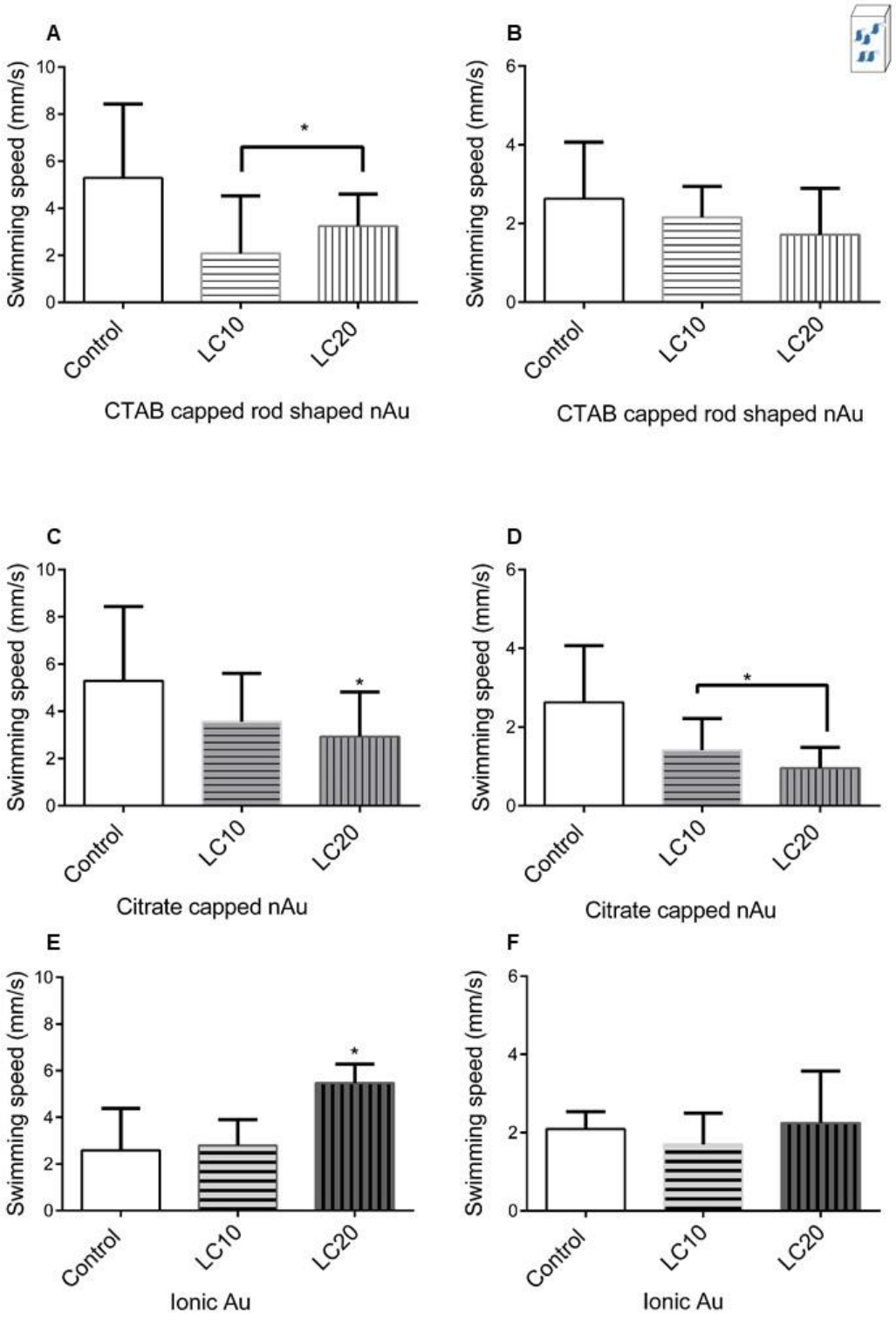

Figure 4. 10: The swimming speed (mm/s) of *D. magna* (n= 15) during community swimming behaviour trials while exposed to CTAB capped rod shaped nAu 0 h(A) and 48 h (B); citrate capped nAu 0 h (C) and 48 h (D); ionic Au 0 h (E) and 48 h (F). * indicates significance ($p < 0.05$).

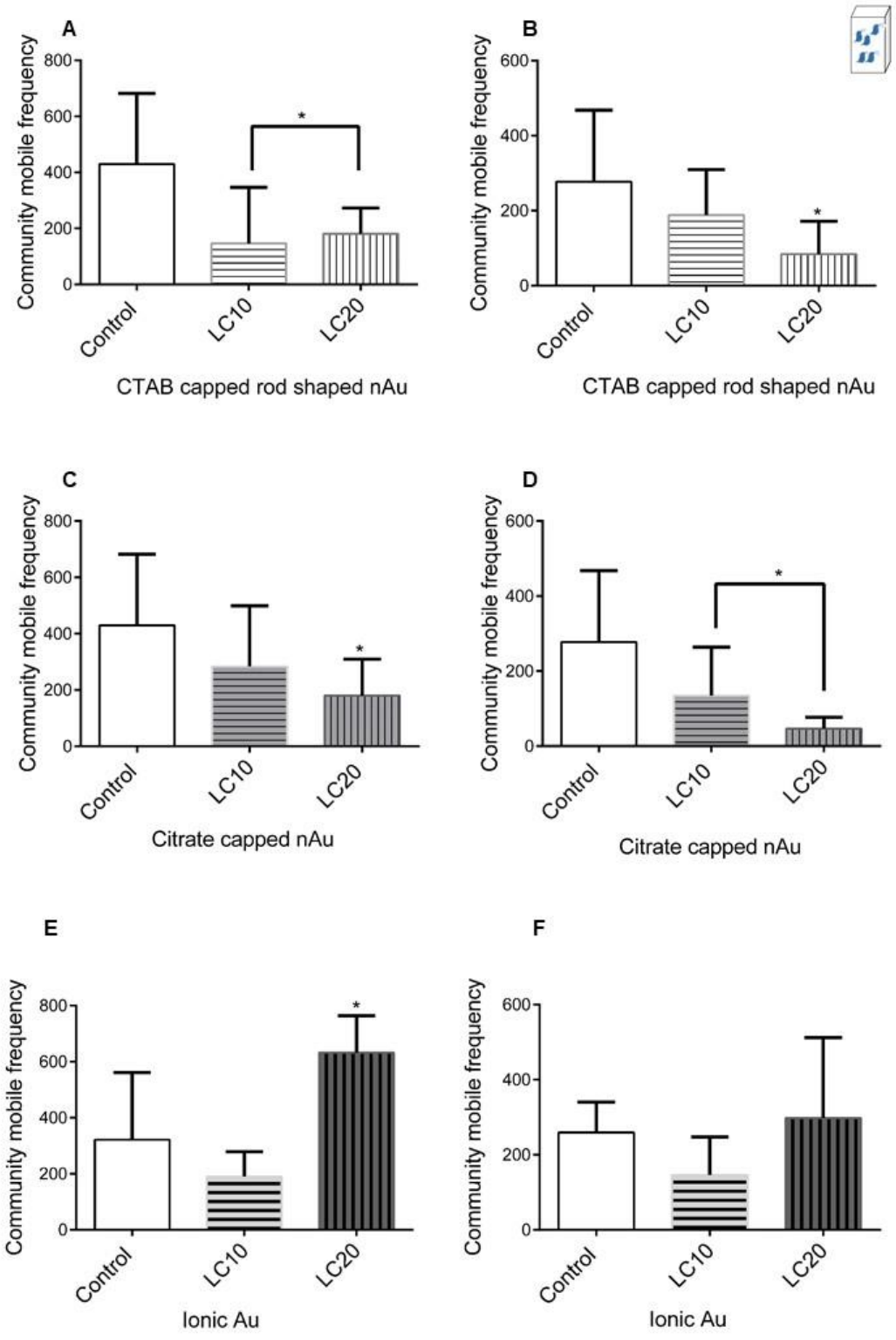

Figure 4. 11: The highly mobile frequency of *D. magna* (n= 15) during community swimming behaviour trials while exposed to CTAB capped rod shaped nAu 0 h(A) and 48 h (B); citrate capped nAu 0 h (C) and 48 h (D); ionic Au 0 h (E) and 48 h (F). * indicates significance ($p < 0.05$).

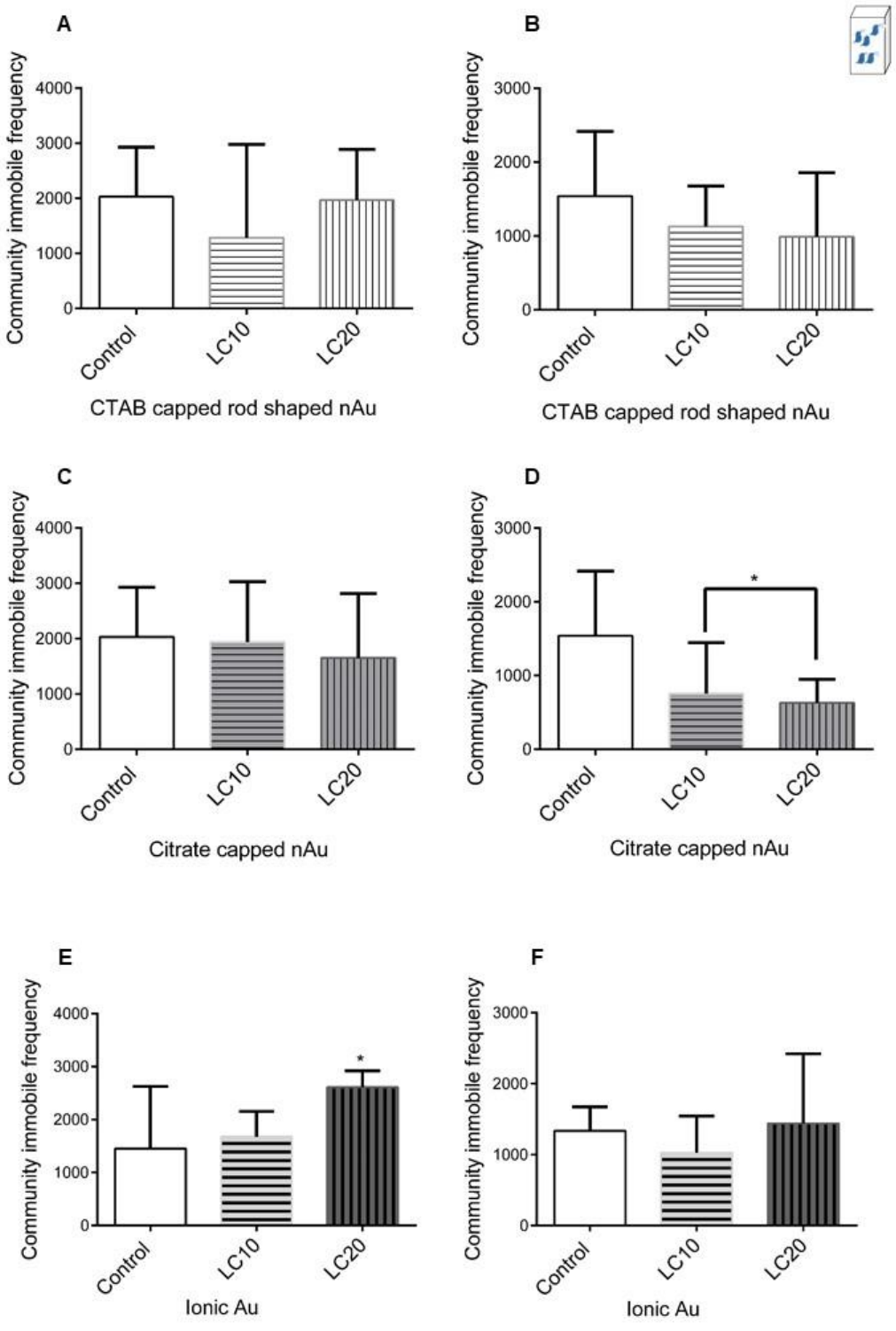

Figure 4. 12: The immobile frequency of *D. magna* (n= 15) during community swimming behaviour trials while exposed to CTAB capped rod shaped nAu 0 h(A) and 48 h (B); citrate capped nAu 0 h (C) and 48 h (D); ionic Au 0 h (E) and 48 h (F). * indicates significance ($p < 0.05$).

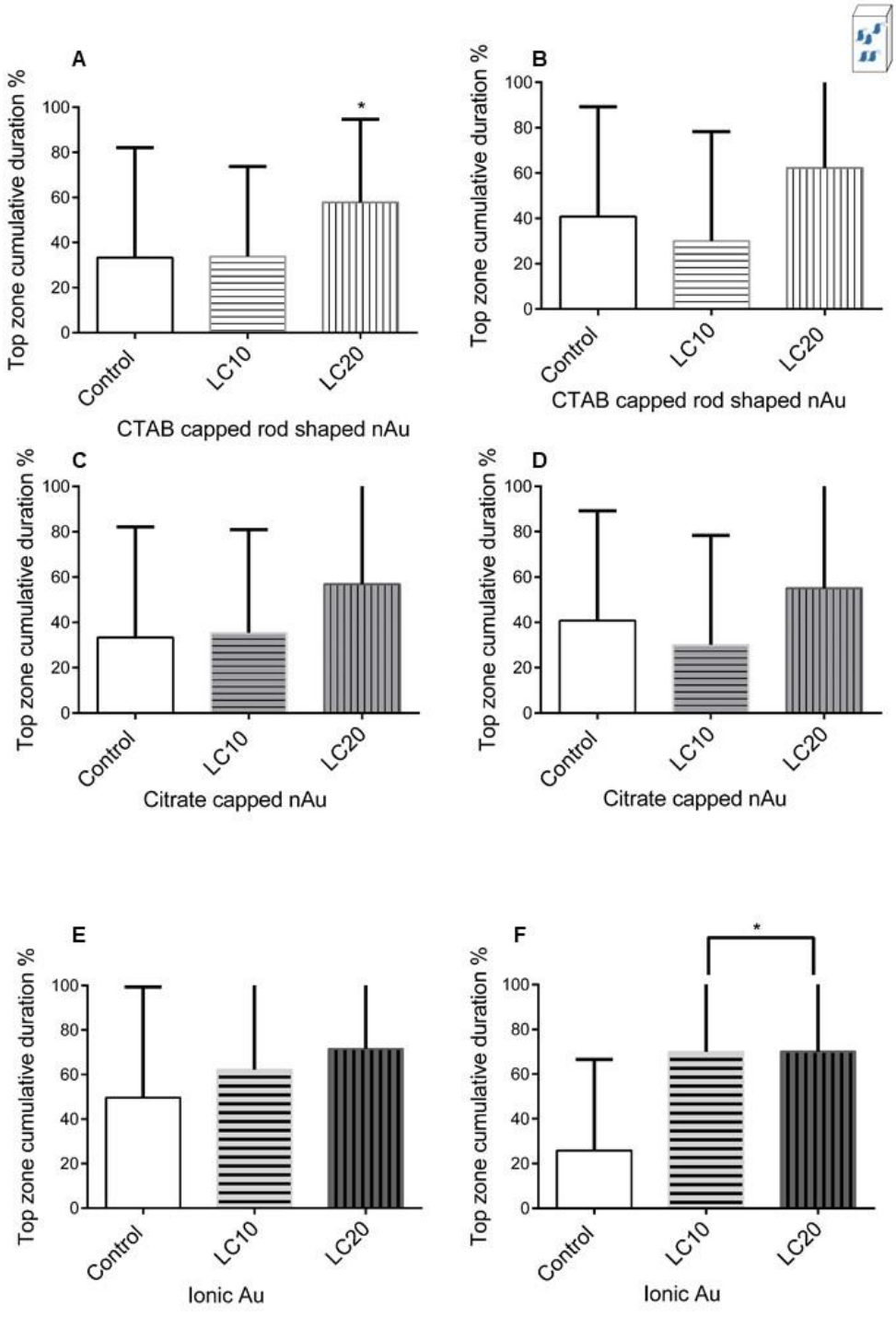

Figure 4. 13: The top zone cumulative duration of *D. magna* (n= 15) during community swimming behaviour trials while exposed to CTAB capped rod shaped nAu 0 h(A) and 48 h (B); citrate capped nAu 0 h (C) and 48 h (D); ionic Au 0 h (E) and 48 h (F). * indicates significance ($p < 0.05$).

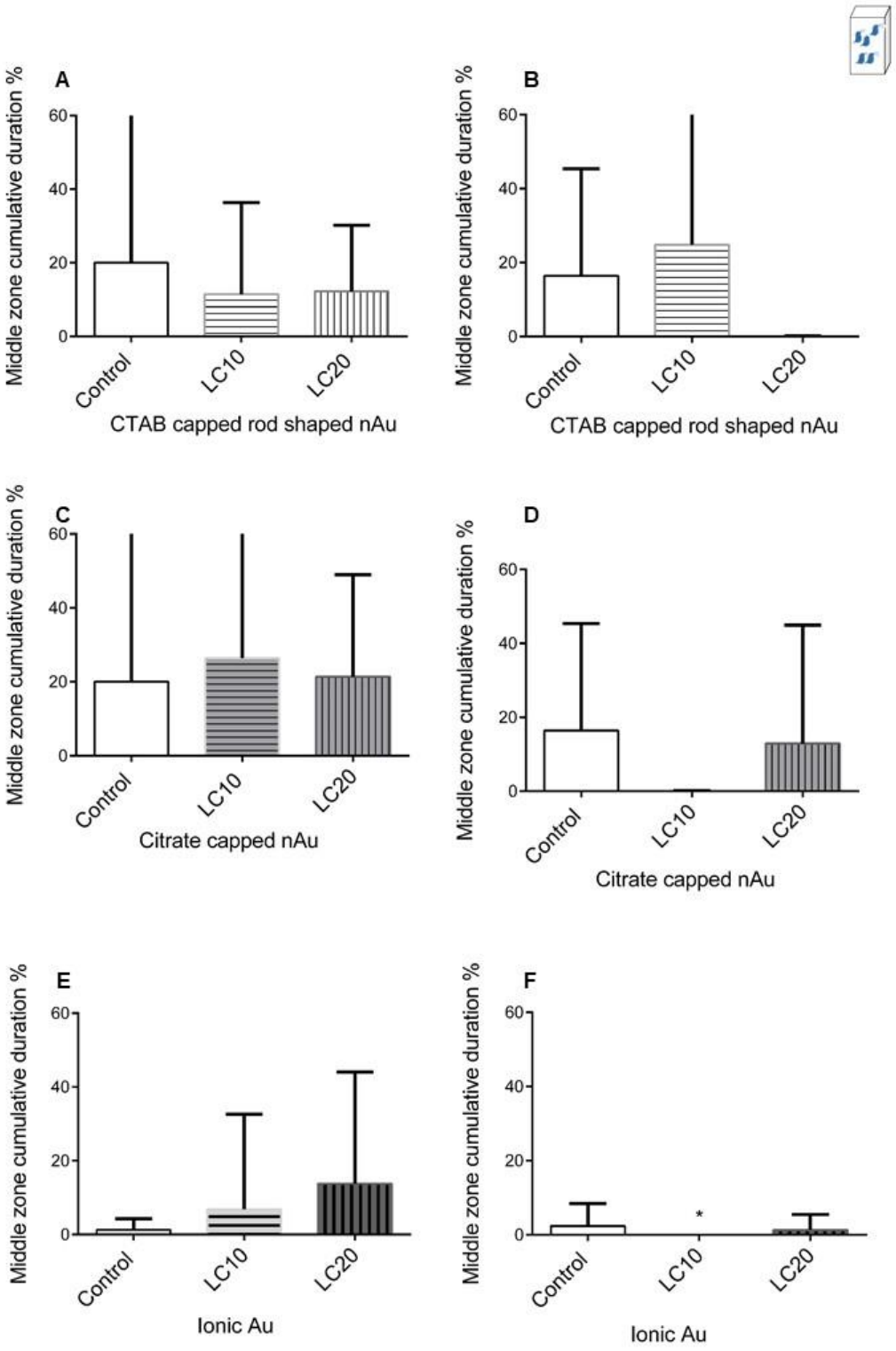

Figure 4. 14: The middle zone cumulative duration of *D. magna* (n= 15) during community swimming behaviour trials while exposed to CTAB capped rod shaped nAu 0 h(A) and 48 h (B); citrate capped nAu 0 h (C) and 48 h (D); ionic Au 0 h (E) and 48 h (F). * indicates significance ($p < 0.05$).

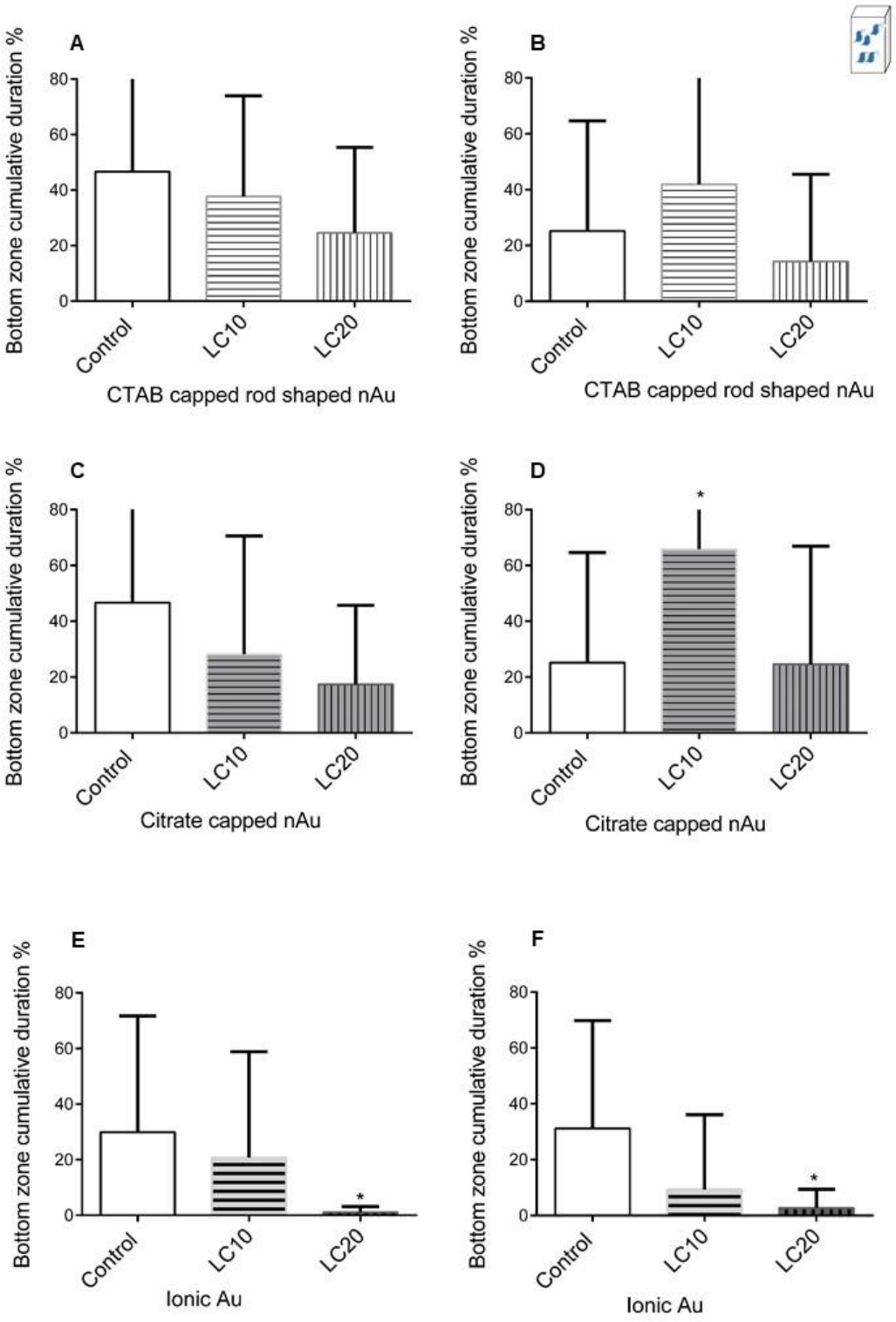

Figure 4. 15: The bottom zone cumulative duration of *D. magna* (n= 15) during community swimming behaviour trials while exposed to CTAB capped rod shaped nAu 0 h(A) and 48 h (B); citrate capped nAu 0 h (C) and 48 h (D); ionic Au 0 h (E) and 48 h (F). * indicates significance ($p < 0.05$).

Functional response

After 30 minutes of feeding, Zebrafish were aggressive when removed from the glass beakers. There was no interaction between treatment and prey density, and no main effect of treatment when compared to the control. There was a main effect of prey density which was expected, and these differences are dealt with in the FR analysis (Figure 4.16). The number of preys eaten was significantly affected by LC and density treatments when compared to the nanoparticle but not by shape of the particles, there were significantly fewer prey that were consumed at LC20 than LC10 (Table 4.1) (z=1.96, p=0.05) (Table 4.2). Treatment as a factor doesn't have an overall effect on number of preys consumed. However, when considering treatment conditions, LC20 caused less consumption overall than LC10. All of the FR types were intermediate between Type II/III. Although the ionic Au treatments don't differ from the control in terms of FR curve, with an increasing trend of consumption (see max feeding estimate, 1/h (Table 4.3). CTAB capped rod shaped nAu LC20 had a lower feeding rate when compared to the control. The citrate capped nAu differed from the control at intermediate prey densities indicating a difference in predator response compared to control. Although not significant, the ionic Au made daphnia more susceptible to predation which could cause a decline in daphnia populations. The CTAB capped rod shaped nAu and citrate capped nAu however have a trend of decreasing prey consumption compared to control which indicate a decoupling of the trophic interactions (Figure 4.16 and Figure 4. 17).

Table 4. 1: The first generalized linear models assessing differences from control.

LR	**Chisq**	**Df**	**Pr(>Chisq)**
Treatment	4.6	6	0.59
Density	9 784.3	7	<0.0002 ***
Treatment: density	31.7	42	0.88

Table 4. 2: Second generalized linear models testing for differences between exposure groups Analysis of Deviance Table (Type II tests). Response: eaten

LR	**Chisq**	**Df**	**Pr(>Chisq)**
Shape	4.0	2	0.14
LC	3.8	1	0.05 *
Density	7 723.1	7	< 0.0002 ***

Table 4. 3: Functional response types determined from logistic regression and first and second order terms reported for all treatments and replacement and non-replacement trials of *D. magna.*

Treatment	**First order term**	**Second order term**	**Scaling exponent (q), FR Type**	**Attack (b), p**	**Handling (h), p**	**1/h**
Control	-0.134, <0.05	0.002, <0.05	0.5, II/III	0.89 <0.001	0.014, <0.001	71.4
CTAB capped rod shaped nAu						
LC10	-0.001, 0.96	-0.00017, 0.77	0.4, II/III	0.90, <0.001	0.016, <0.001	62.5
LC20	-0.188, <0.001	0.002, <0.01	0.6, II/III	0.96, <0.001	0.028, <0.001	35.7
Citrate capped nAu						
LC10	-0.153, <0.001	0.002, <0.01	0.5, II/III	0.86, <0.001	0.023, <0.001	43.5
LC20	-0.116, <0.001	0.002, <0.001	0.3, II/III	1.35, <0.001	0.019, <0.001	52.6
Ionic Au						
LC10	-0.007, 0.07	0.001, 0.05	0.4, II/III	0.87, <0.001	0.012, <0.001	83.3
LC20	-0.133, <0.001	0.002, <0.001	0.3, II/III	0.88, <0.001	0.010, <0.001	100

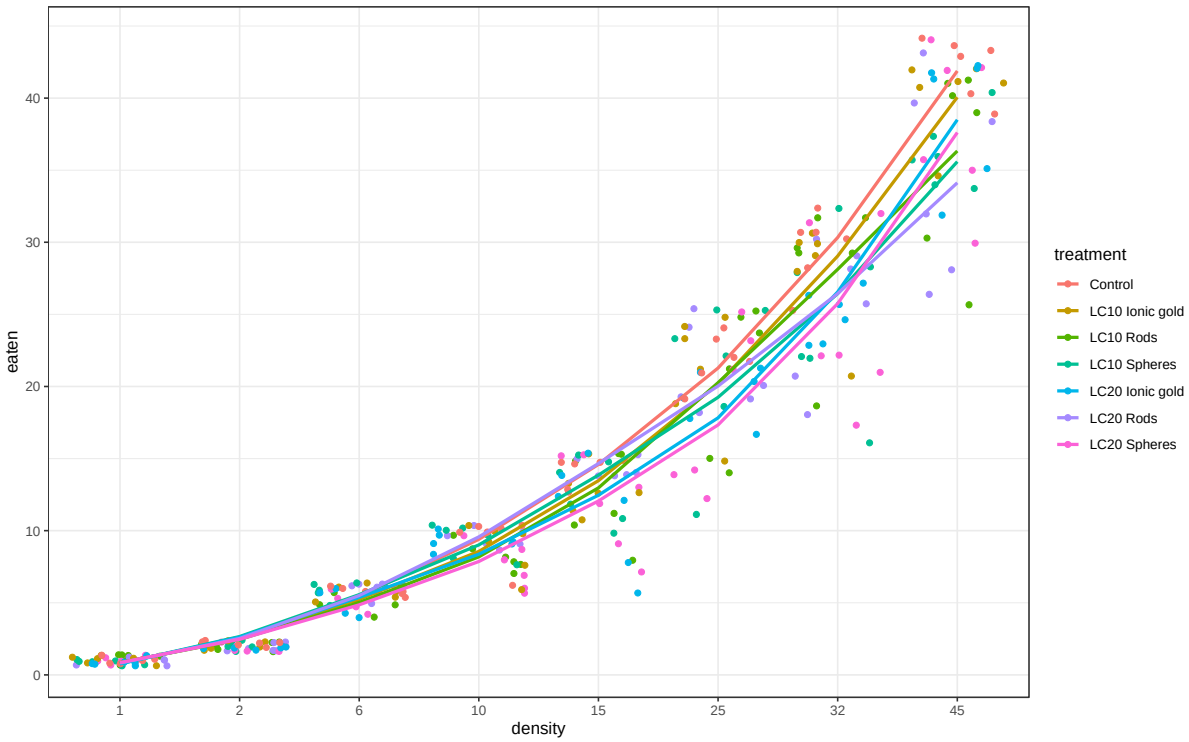

Figure 4. 16: The number of prey (*D. magna*) consumed per density supplied to the predator (*D. rerio*) after exposure to CTAB capped rod shaped nAu, citrate capped nAu and ionic Au.

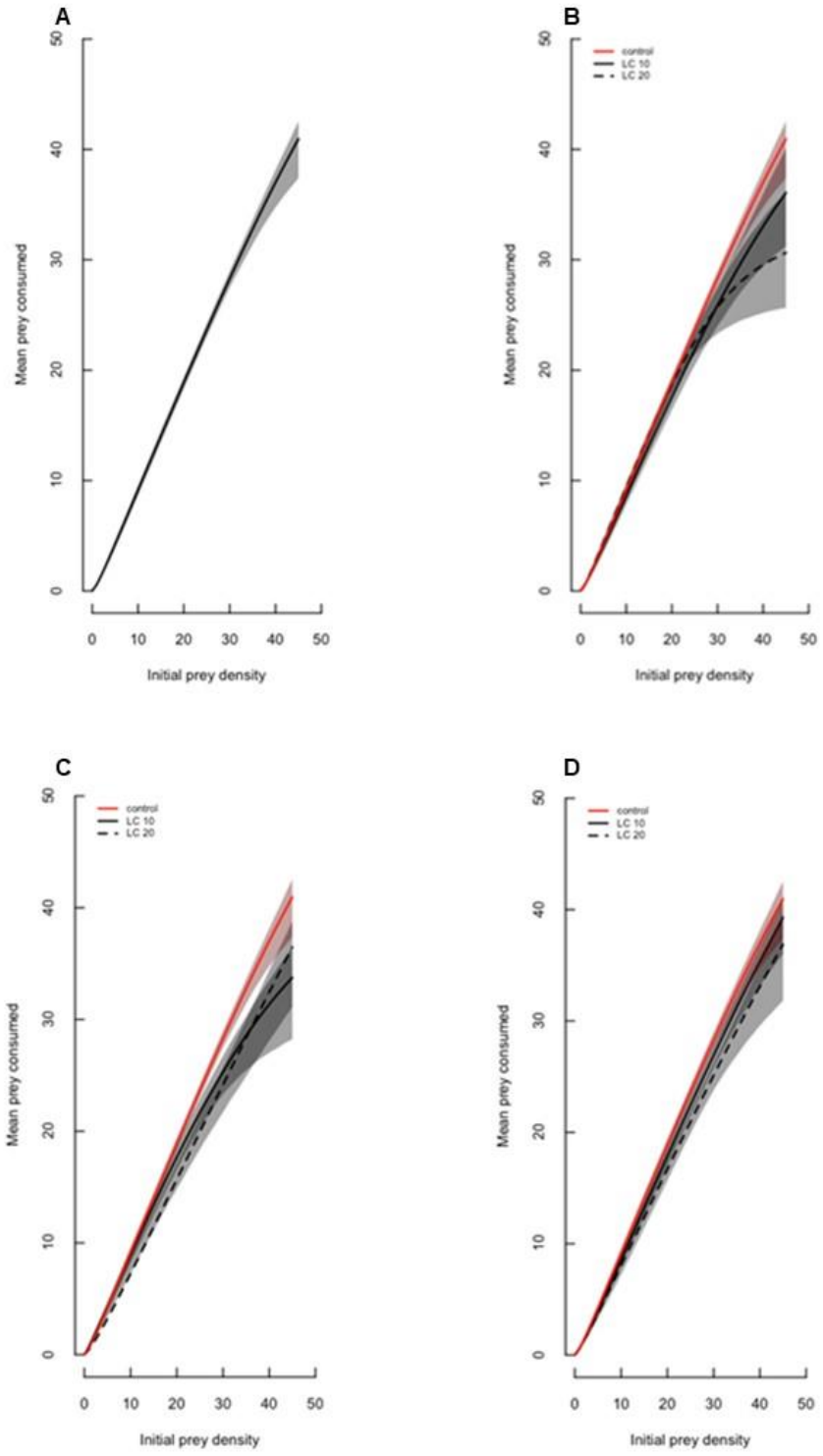

Figure 4. 17: Functional response curves (±SE.) of *D. rerio* preying on *D. magna* for each treatment (Control (A), CTAB capped rod shaped nAu (B), citrate capped nAu (C) and ionic Au (D)). , 95% c.i. bootstrapped values for each curve (darker areas indicate overlap).

4.4 Discussion

The swimming behaviour of daphnia is mostly associated with effective metabolism and ecological parameters like food intake, reproduction, and escape from predators. In this study all daphnia swimming behaviour was differentially affected after exposure to CTAB capped rod shaped nAu, citrate capped nAu and Ionic Au. The way behaviour was affected was dependent on the type of contaminant. The control group were swimming throughout all the zones spending slightly more time in the top zone, the CTAB capped rod shaped nAu group were constantly spinning forward and spent a significant amount of time in the top zone while the citrate capped nAu group were swimming visually and significantly more at the bottom zone (sinking). Ionic Au were swimming significantly (>62 %) below the surface in the top zone and were sometimes spinning. Changes in swimming behaviour patterns were noted once daphnids moulted, showing slow and nearly heavy movements to normal movements affecting their energy uptake, storage, and effective metabolism (Artells et al, 2013). This implies that they tried to maintain their swimming capability even though the absorption or accumulation of nanoparticles on their carapace restricted their locomotion. This results in an increase in moulting and alteration in reproduction, therefore affecting swimming behaviour (Botha et al., 2016).

Other studies assessing NM exposure and daphnia swimming behaviour showed reduced swimming speed and mobility state of *Daphnia spp.* when exposed to NM cerium dioxide and multiwalled carbon nanotubes (Artells et al*.,* 2013, Stanley et al., 2016). This decrease in swimming ability was also found in other toxicant exposure studies other than NM- such as salicylic acid, ketoprofen and procaine penicillin (Szabelak and Bownik, 2021; Bownik et al., 2019b).

Typically, the individuals may be exhibiting a variety of behaviours, such as swimming in any direction (at a variety of speeds) or sinking, and populations at different depths may be behaving differently. There are several possible ways daphnia might move downward. *Daphnia magna* in this study displayed a large increase in spinning, a downward-directed head-down fast swimming, also observed by Bownik (2017). This behaviour is highly unusual during normal swimming (with no changes in light intensity), as observed in citrate capped nAu and ionic Au. This characteristic behaviour means daphnia exposed to stressful agents are not swimming out of free will (Dodson et al, 1995b). This is a continuous escape response exacerbated by high concentration of toxicants causing an imbalance of body reactions because of neurotoxic changes. This can influence changes in movement frequency, swimming speed and direction (Bownik, 2017)-

swimming at a fast rate to ascend when light conditions change (as observed after 48h). Swimming behaviour would enable daphnia to find patches of algae and remain in them (Stearns, 1975), as feeders they have a capacity to ingest nAu (Artells et al., 2013; Lovern et al., 2008) and changes could be due to excessive nanomaterials adhering onto the carapace and accumulating in the gut (García-Cambero et al., 2013).

Normal daphnia swimming behaviour is in a horizontal motion (Dodson et al., 1997). However, daphnia do swim upward and downward to remove excessive particulate matter and feed within the water column (Harris, 1953; Ringelberg and Servass, 1971). This sinking phenomenon has been noted in other studies when *D. magna* were exposed to titanium dioxide nanoparticles (Bownik, 2017). The sinking rate of these species could be associated with decreased swimming velocity when exposed to NM.

Daphnia magna respond to both positive phototaxis under 'homogeneous light' and 'heterogeneous light' at high level of food availability, therefore, the distribution of light influences aggregation between daphnia (Jensen et al., 1999). Once light conditions are disturbed, as when exposed to a predator, they can easily escape- this change in light causes a response to danger and could be delayed in the exposed groups (Pijanowska and Kowalczewski, 1997; Ringelberg, 1991b; Ringelberg, 1991a).

The exposure period has an impact on the behavioural effects from early exposure and *D. magna* become more active after a certain stabilization period (Park et al., 2021). Prey species that are structurally small-bodied use most of their energy trying to escape which decreases their swimming speed making them more susceptible to predatory attack (Dell et al., 2011; Dell et al., 2013). In this instance the prey was disadvantaged due to the predator experiencing favourable condition (no toxicant exposure) with decreased swimming performance in exposed groups. The above-mentioned behaviour may cause changes in predator response at high prey densities (Ariyomo and Watt, 2015). During low prey densities the rate of attack increases which creates unstable prey populations (South and Dick, 2017). Attack rate indicates rapid successful search, thus increasing resource consumption at low density. However, as the density of predators increase there might be alterations in resource consumption at high prey densities. This can be caused by motivational state of changes in handling time. Handling time can be described as time taken to eat and digest prey's item (Englund et al., 2011; Jeschke et al., 2002; South and Dick, 2017).

The functional response showed a type II/III curve which is suitable to the predator species used in this study (Watts et al., 2012; Watts et al., 2016). Zebrafish have superior mouth type and feed better on the surface (Watts et al., 2012; Watts et al., 2016). As density increased, a significant shift was noted in the FR indicating that the predator was unable to catch all the prey; however, when exposed the exposure concentrations and the type of exposure group, there was an effect on the ability of the predator to consume prey. This can be related to the different types of swimming behaviour observed by daphnia within this study- citrate capped nAu would be found towards the bottom of the beaker while both CTAB capped rod shaped nAu and ionic Au gold would be found on the surface where the predator feeds. Further exacerbated by the spinning behaviour observed in daphnia which could affect the handling time of the predator causing a shift within the FR. There was a shift within predator-prey interactions in this study as observed in other studies exposed to toxicants (South et al., 2019).

Chapter 5

Conclusions and Recommendations

Chapter 5: Conclusions and recommendations

5.1 Conclusions

Adverse Outcome Pathway development is relatively new for NMs and this study is one of the first to report findings on the adverse effects of nAu (CTAB capped rod shaped nAu and citrate capped nAu) and their ionic bulk elemental Au on *D. magna* using different endpoints. Both Aim 1 and Aim 2 and the associated objectives (Chapter 1.6) were achieved to realize the exposure concentrations and the necessary endpoints to develop the AOPs. Therefore, the data from this study support the general alternative hypothesis that the AOP framework is suitable to determine the effect of two different nAu (CTAB capped rod shaped nAu and citrate capped nAu) and ionic Au in the aquatic ecosystems using *D. magna*.

The first event in an AOP is the molecular initiating event (MIE) which in this study was metabolomic analysis. The collective KEs measured following an OECD protocol, utilized organisms' physiological responses (heart rate, respiration, uptake, and behaviour). The AO might be hindered by species homeostatic mechanisms approach, as it was seen throughout the effect of metabolism response in *D. magna*. The AOs in this study influenced reproduction and the ecological predator-prey interactions. The main factors that affect dissolution of the particle might be the surface area of the particles, however less than one percent dissolution was observed. There is an interaction of complex media used in this study with the particles resulting in agglomeration or aggregation, thus changing the size of the nAu. Moreover, the response of the daphnia could be the result of increased agglomeration or aggregation in the media. After all, the functional group and shape that the particle consist of, plays a huge factor on how the particle itself behaves. Any changes within the nAu can change the impact it has on the organism and the environment.

CTAB capped rod shaped nAu with an LC50 of 12.1 µg/L was most toxic compared to citrate capped nAu which showed low acute toxicity. CTAB capped rod shaped with size of ± 40 nm showed to have less than 1% dissolution after 48h. There was an increase in agglomeration and at 0 h the zeta potential was already negative. *Daphnia magna* showed uptake of CTAB capped rod shaped nAu to adhere at the external carapace resulting in an increase in respiration, thus the inability to maintain oxygen at both at LC10 and LC20. Adhesion of CTAB capped rod shaped nAu onto the carapace affected the behavioural performance of daphnids. Daphnids were

constantly spinning (face forward in a circular motion) and constantly migrating at the top zone. This could be due to physiological stress of the heart rate as indicated by an increase at LC20. Swimming behaviour being affected showing an AO that their escape response declined over time. The highlighted metabolism pathways at the MIE showed decrease in the amino acids such as serine, L-lysine, tryptophan, and niacinamide. The daphnids constantly migrating at the top zone using increased energy the release of the above-mentioned amino acid such as serine, L-lysine, tryptophan resulting to protein decline. Specifically, niacinamide composite important compounds such as Nicotinamide adenine dinucleotide (NAD) and nicotinamide adenine dinucleotide phosphate (NADP). The NAD and NADP are crucial for electron transportation. They act as decision makers between life and death at the cellular level. When Daphnia migrated at the top zone, it required the use of reserved energy resulting, reduced oxygen consumption at LC10. This species moulted less with no recovery and in some case showed no moulting, resulting in mortality. Therefore, adverse outcomes caused a decline in the reproduction rate (Figure 5.1).

Citrate capped nAu with a LC50 >100 mg/L with size of ± 20 nm showed to have less than 0.68 % dissolution after 48h. There was an increase in agglomeration and at 0 h the zeta potential was already negative as it was observed in CTAB capped rod shaped nAu. *Daphnia magna* showed uptake of citrate capped nAu to adhere to the external carapace and accumulating in the gut resulting in an increase in respiration, thus inability to maintain oxygen at both at LC10 and LC20. This is because of an increase physiological stress of heart rate at LC20. Adhesion of citrate capped nAu onto the carapace affected the behavioural performance of daphnids as it was seen in CTAB capped rod shaped nAu. As they were constantly observed at the bottom zone experiencing difficultly to swim as the citrate capped nAu adhere to the external carapace. This observed behaviour makes daphnids to be susceptible to predator prey interaction causing a decline in the escape response mechanism. The highlighted metabolism pathways at the MIE showed decrease in the amino acids such as serine, tryptophan, and cholesterol. The above-mentioned metabolites except cholesterol, were observed at CTAB rod capped shaped nAu. The insect hormone biosynthesis plays a major role in moulting hormone. This biosynthesis is important for regulating embryonic development and repress metamorphosis in many species, however, adverse outcomes in reproduction reduced production of juveniles. This could be due to increased moulting as seen in this study, resulting in increased mortality and a reduced daphnids population rate due to energy reserves being depleted (Figure 5.2).

Ionic Au with a LC50 of 57 µg/L, was found to be highly toxic compared to CTAB capped rod shaped nAu and citrate capped nAu. The stress response metabolism levels of ionic Au reduced

during respiration at LC10 and LC20, even though daphnids were constantly migrating at the top zone with no possibility of particle accumulation on their surface hindering movement and respiration. However, their escape response was reduced due to a decreased distance travelled immediately after exposure. Nor was it challenging for them when migrating to the top zone, some spinning was observed which requires energy and daphnids utilize reserved energy for regulation purposes. The highlighted metabolism pathways at the MIE showed decrease in the amino acids such as L-lysine, arachidonic acid, serine, tryptophan, and niacinamide. The above-mentioned five amino acids were observed at CTAB capped rod shaped nAu and citrate capped nAu. Arachidonic acid metabolism showed AO by reducing reproduction rate. Arachidonic acid is crucial for reproduction and environmental sex determination. Daphnids did not only require energy reserves to migrate at the top zone but also for moulting which occurred less when compared to the control and nAu. Since moulting would not rid the daphnia of the ionic Au exposure it probably occurred less (Figure 5.3).

There was metabolite overlap between treatment groups: CTAB capped rod shaped nAu LC10 and ionic Au LC20 shared perturbations to Sphingolipid metabolism, Glyoxylate and dicarboxylate metabolism as well as the Glycine, serine, and threonine metabolism pathway. CTAB capped rod shaped nAu and ionic Au shared perturbations to Nicotinate and Nicotinamide Metabolism pathways. CTAB capped rod shaped nAu LC10 and ionic Au LC10 shared perturbations to Biotin metabolism. Citrate capped nAu LC10 and ionic Au LC20 shared perturbations to Tryptophan metabolism. CTAB capped rod shaped nAu LC10, Citrate capped nAu LC10 and ionic Au LC20 shared perturbations to Glyoxylate and dicarboxylate metabolism. This means there was an oxidative stress response involved utilizing reserved energy for the regulation of metabolism in response to a stressor. However, citrate capped nAu, CTAB capped rod shaped nAu, and ionic Au also had different metabolite, physiological and adverse responses. Thus, there is specific nano/ionic stressor response observed. The Ho is rejected. The HA is accepted that the AOP framework is suitable to determine the effect of two different nAu (CTAB capped rod shaped nAu and citrate capped nAu) and ionic Au in aquatic ecosystems using *D. magna*.

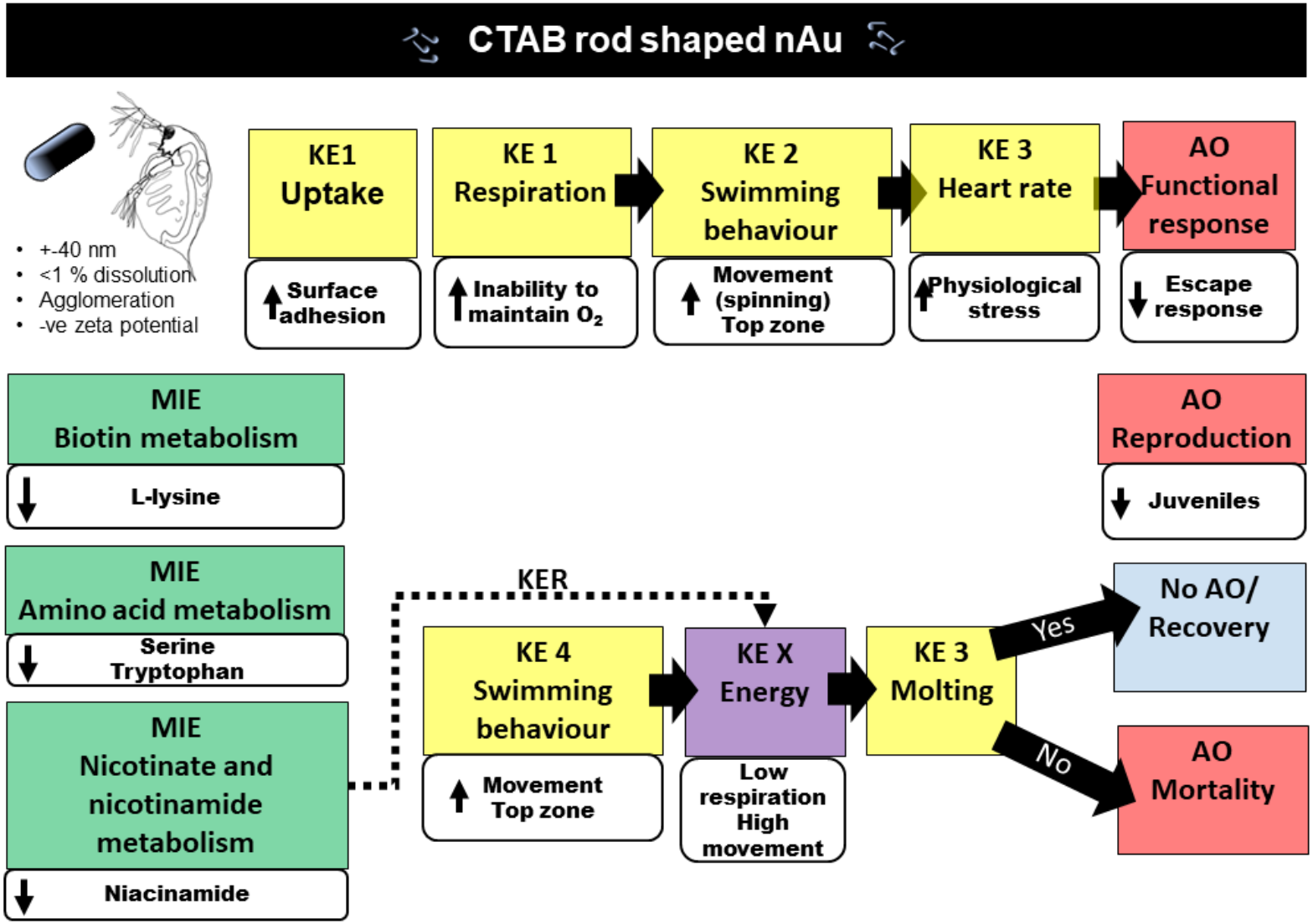

Figure 5. 1: The proposed Adverse outcome pathway of CTAB capped rod shaped nAu after exposure to *D. magna*.

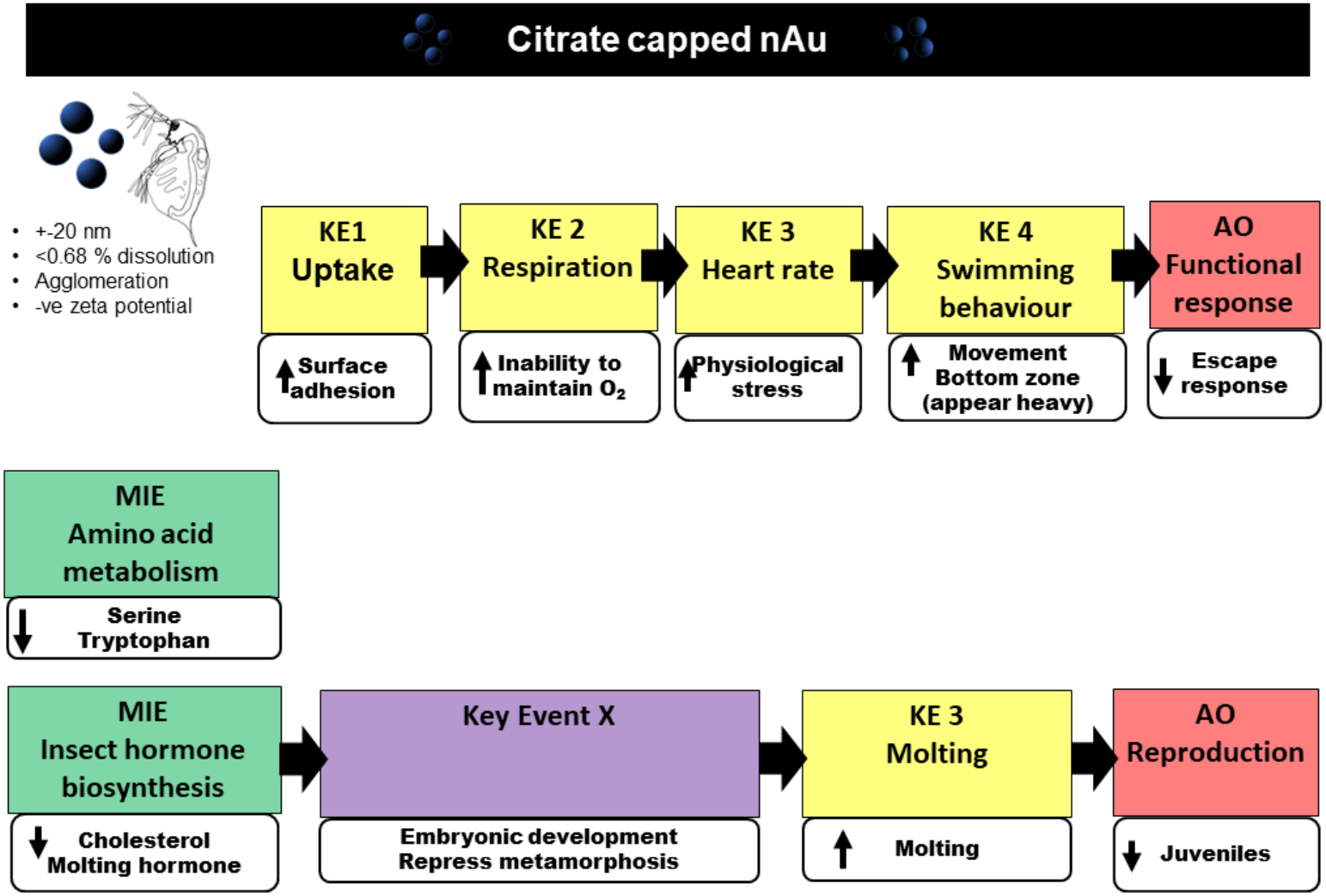

Figure 5. 2: The proposed Adverse outcome pathway of citrate capped nAu after exposure to *D. magna.*

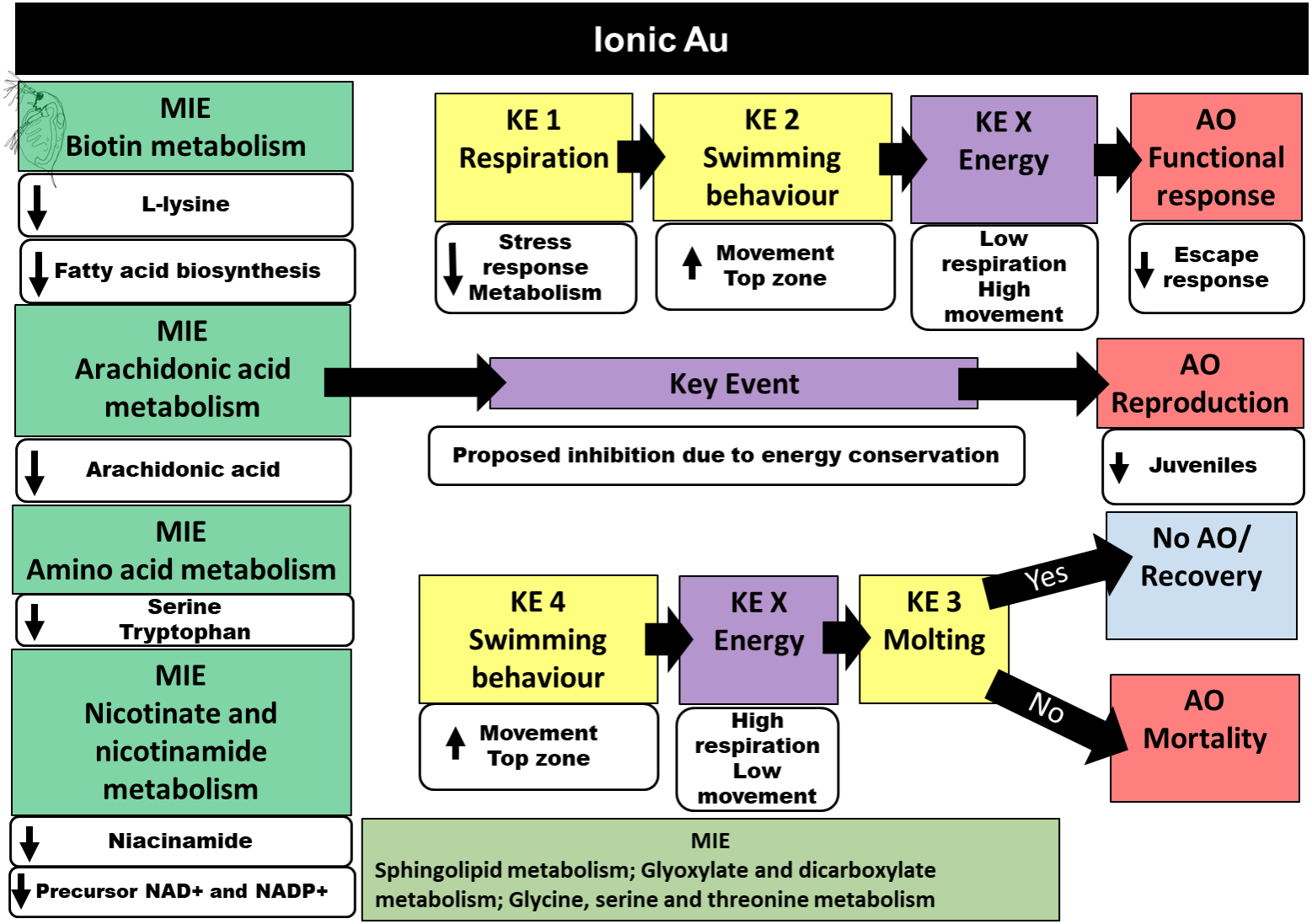

Figure 5. 3: The proposed Adverse outcome pathway of ionic Au after exposure to *D. magna.*

5.2 Recommendations

Based on the results of this study the following recommendations can be made for future studies:

- Assessing the sub-cellular and physiological endpoints after a shorter exposure period (e.g. 6, 12, 24 h) to understand the hermetic and adaptation responses that may take place.
- The AOPs show that there are some missing links between MIEs for the KEs observed and therefore it is recommended to utilise other omic's tools such as toxicogenomics or proteonomics for future studies. This will provide more detailed information regarding gene up or down regulation and protein expression.
- To address the unknown KEs that were proposed for the MIEs – thus undertake suitable endpoint measurements for those KE-Xs that were identified.

Chapter 6

References

Chapter 6: References

6.1 References

Anderson, B.G. & Jenkins, J.C. 1942. A time study of event in the life span of *Daphnia magna*. *Journal of Biological Bulletin*, 83: 260-272.

Ankley, G.T., Bennett, R.S., Erickson, R.J., Hoff, D.J., Hornung, M.W., Johnson, R.D., Mount, D.R., Nichols, J.W., Russom, C.L., Schmieder, P.K., Serrrano, J.A., Tietge, J.E., & Villeneuve, D.L. 2010. Adverse outcome pathways: a conceptual framework to support ecotoxicology research and risk assessment. *Environmental Toxicology and Chemistry*, 29: 730-741.

Ankley, G.T. & Edwards, S.W. 2018. The adverse outcome pathway: a multifaceted framework supporting 21st century toxicology. *Current Opinion in Toxicology,* 9**:** 1-7.

Allen, M., Aguirre, M., Chesley, S., Sroczynski, M. & Reeves, S. 2019. CBD Water and Nicotine: The Effects on *Daphnia magna's* Neurogenic Pacemaker Not What You May Expect. *Journal of Undergraduate Biology Laboratory Investigations*, 1-4.

Ariyomo, T.O. & Watt, P.J. 2015. Effect of hunger level and time of day on boldness and aggression in the zebrafishDanio rerio. *Journal of Fish Biology*, 86(6): 1852–1859.

Artells, E., Issartel, J., Auffan, M., Borschneck, D., Thill, A., Tella, M., Brousset, L., Rose, J., Bottero, J. & Thi′Ery, A. 2013. Exposure to Cerium Dioxide Nanoparticles Differently Affect Swimming Performance and Survival in Two Daphnid Species. *Nanomaterials*, 8: 1-11.

Banta, A.M. 1939. *Studies on the physiology, genetics, and evolution of some Cladocera*. Carnegie Institution of Washington. Publ. No. i513. Washington, D.C. pp. 106-130.

Barreto, A., Carvalhoa, A., Camposb, A., Osórioc, H., Pinto, E., Almeida, A., Trindade, T., Soaresa, A.M.V. M., Hyllandh, K., Loureiroa, S. & Oliveira, M. 2020. Effects of gold nanoparticles in gilthead seabream—A proteomic approach. *Aquatic Toxicology,* 221: 1-12.

Barreto, A., Luis, L.G., Girão, A.V., Trindade, T., Soares, A.M.V.M. & Oliveira, M. 2015. Behavior of colloidal gold nanoparticles in different ionic strength media. *Nanoparticles Research,* 17: 1–13.

Barrios-O'Neill, D., Dick, J.T.A., Emmerson, M.C., Ricciardi, A. & MacIsaac, H.J. 2014. Predator-free space, functional responses and biological invasions. *Functional Ecology*, 29(3): 377–384.

Baumer, C., Pirow, R. & Paul, R.J. 2002. Circulatory oxygen transport in the water flea *Daphnia magna*. *Comparative Physiology Part B: Biochemical, Systemic, and Environmental Physiology*, 172: 275-285.

Bekker, J.M. & Krijgsman, B.J. 1951. Myogenic heart in Daphnia. *Journal of Physiology*, 115: 249-257.

Bellés, X., Martín, D. & Piulachs, M.-D. 2005. The Mevalonate Pathway And The Synthesis Of Juvenile Hormone In Insects. *Annual Review of Entomology*, 50(1): 181–199.

Beukes D., Du Preez, I. & Loots, D.T. 2019. Total Metabolome Extraction from Mycobacterial Cells for GC-MS Metabolomics Analysis. In: Baidoo E. (eds) Microbial Metabolomics. Methods in Molecular Biology, vol 1859. Humana Press, New York, NY.

Bino, R.J., Hall, R.D., Fiehn, O., Kopka, J., Saito, K., Draper, J., Nikolau, B.J., Mendes, P., Roessner-Tunali, U., Beale, M.H., Trethewey, R.N., Lange, B.M., Wurtele, E.S. & Sumner, L.W. 2004. Potential of metabolomics as a functional genomics tool. *Trends Plant Science*, 9 (9): 418–25.

Brausch, K.A., Anderson, T.A., Smith, P.N. & Maul, J.D. 2010. The effect of fullerenes and functionalized fullerenes on *Daphnia magna* phototaxis and swimming behaviour. *Environmental Toxicology and Chemistry*, 30 (4): 878–884.

Bodar, C., Voogt, P. & Zandee, D. 1990. Ecdysteroids in *Daphnia magna*: Their role in moulting and reproduction and their levels upon exposure to cadmium. *Aquatic Toxicology*, 17: 339–350.

Bohrer, R.N. & Lampert, W. 1988. Simultaneous Measurement of the Effect of Food Concentration on Assimilation and Respiration in *Daphnia magna Straus*. *British Ecological Society*, 2 (4): 463-471.

Bollache, L., Dick, J.T., Farnsworth, K.D. & Montgomery, W.I. 2008. Comparison of the functional responses of invasive and native amphipods. *Biology Letters*, 4(2): 166–169.

Bolker, B.M. 2008. *emdbook: ecological models and data in R.* Princeton University press, Princeton, New Jersey, USA.

Bolker, B.M. 2010. Bbmle: tools for general maximum likelihood estimation. R Package. http://www.cran.rproject.org/

Bonvallot, N., Tremblay-Franco, M., Chevrier, C., Canlet, C., Debrauwer, L., Cravedi, J.-P. & Cordier, S. 2014. Potential Input from Metabolomics for Exploring and Understanding the Links Between Environment and Health. *Toxicology and Environmental Health*, Part B, 17(1): 21–44.

Borgert, C.J., Quill, T.F., Mccarty, L.S. & Mason, A.M. 2004. Canmodeof action predict mixture toxicity for risk assessment? *Toxicological Applied Pharmacology,* 201: 85–96.

Bossuyt, B.T.A, & Janssen, C.R. 2005. Copper regulation and homeostasis of *Daphnia magna* and *Pseudokirchneriella subcapitata*: influence of acclimation. *Environmental Pollution*, 136(1): 135-144.

Botha, T.L., Boodhia, K. & Wepener, V. 2016. Adsorption, uptake and distribution of gold nanoparticles in *Daphnia magna* following long term exposure. *Aquatic Toxicology,* 170: 104–111.

Botha, T.L., James, T.E. & Wepener, V. 2015. Comparative Aquatic Toxicity of Gold Nanoparticles and Ionic Gold Using a Species Sensitivity Distribution Approach. *Nanomaterials*: 1-17.

Bownik, A. 2017. Daphnia swimming behaviour as a biomarker in toxicity assessment: A review. *Science of the Total Environment*: 194–205.

Bownik, A., Jasieczek, M. & Kosztowny, E. 2020. Ketoprofen affects swimming behavior and impairs physiological endpoints of *Daphnia magna*. *Science of the Total Environment*, 725: 1-7.

Bownik, A., Ślaska, B., Bochra, J., Gumieniak, K. & Gałek, K. 2019a. Procaine penicillin alters swimming behaviour and physiological parameters of *Daphnia magna*. *Environmental Science and Pollution Research*, 26:18662–18673.

Bownik, A., Ślaska, B. & Dudka, J. 2019b. Cisplatin affects locomotor activity and physiological endpoints of *Daphnia magna*. *Journal of Hazardous Materials*, 384:121259.

Bownik, A. & Pawlik-Skowrońska, B. 2019. Early indicators of behavioral and physiological disturbances in *Daphnia magna* (Cladocera) induced by cyanobacterial neurotoxin anatoxin-a. *Science of Total Environment,* 695:133913.

.

Bozich, J.S., Lohse, S.E., Torelli, M.D., Murphy, C.J., Hamers, R.J. & Klaper, R.D. 2014. Surface chemistry, charge and ligand type impact the toxicity of gold nanoparticles to *Daphnia magna*. *Environmental Science: Nano*, 1 (3): 260-270.

Campbell, A.K., Wann, K.T. & Matthews, S.B. 2004. Lactose causes heart arrhythmia in the water flea *Daphnia pulex*. *Comparative Biochemistry and Physiology Part B*, 139: 225–234.

Carney, G.C., Shore, P., Chandra, H., 1986. The uptake of cadmium from a dietary and soluble source by the crustacean *Daphnia magna*. *Environmental Research*, 39 (2): 290-298.

Carpenter, S.R., Kitchell, J.F., Hodgson, J.R., Cochran, P.A., Elser, J.J., Elser, M.M., Lodge, D.M., Kretchmer, D., He, X. & Vonende, C.N. 1987. Regulation of Lake Primary Productivity by Food Web Structure. *Ecology,* 68: 1863- 1876.

Castillo, S., Gopalacharyulu, P., Yetukuri, L. & Orešič, M. 2011. Algorithms and tools for the preprocessing of LC–MS metabolomics data. *Chemometrics and Intelligent Laboratory Systems*, 108(1): 23–32.

Chapman, A.A., Venter, E.A. & Pearson, H. 2011. Aquatic toxicity testing in South Africa: Guideline for the accreditation of routine aquatic toxicity testing laboratories. No.TT504/11, ToxSolutions, Kits & Services. Pretoria.

Chen, L., Fu, X., Zhang, G., Zeng, Y. & Ren, Z. 2012. Influences of temperature, turbidity on the behavioural responses of *Daphnia magna* and Japaneese (*Oryzias latipes*) in the biomonitor. *Procedia Environmental Sciences*, 13: 80–86.

Chong, J., Soufan, O., Li, C., Caraus, I., Li, S., Bourque, G., Wishart, D.S. & Xia, J. 2018a. MetaboAnalyst 4.0: towards more transparent and integrative metabolomics analysis. *Nucleic Acids Research*, 46(W1): W486–W494.

Chong, J., Wishart, D.S. & Xia, J. 2019. Using MetaboAnalyst 4.0 for Comprehensive and Integrative Metabolomics Data Analysis. *Current Protocols in Bioinformatics*, 68(1): 86.

Chong, J. & Xia, J. 2018b. MetaboAnalystR: an R package for flexible and reproducible analysis of metabolomics data. *Bioinformatics*, 1-3.

Dabrunz, A., Duester, L., Prasse, C., Seitz, F., Rosenfeldt, R., Schilde, C., Schaumann, G.E. & Schulz, R. 2011. Biological Surface Coating and Molting Inhibition as Mechanisms of TiO2 Nanoparticle Toxicity in *Daphnia magna*. *PLoS ONE*, 6: e20112.

Das, M., Shim, K.H., An, S.S.A. & Yi, D.K. 2011. Review on Gold Nanoparticles and Their Applications. *Toxicology and Environmental Health Sciences*, 3:193–205.

Dell, A.I., Pawar, S. & Savage, V.M. 2011. Systematic variation in the temperature dependence of physiological and ecological traits. *Proceedings of the National Academy of Sciences*, 108(26): 10591–10596.

Dell, A.I., Pawar, S. & Savage, V.M. 2013. Temperature dependence of trophic interactions are driven by asymmetry of species responses and foraging strategy. *Animal Ecology*, 83(1): 70–84.

Dewey, J.E. & Parker, B.L. 1964. Mass rearing of *Daphnia magna* for insecticide bioassay. *Economic Entomology*, 57: 821-825.

Dick, J.T.A., Alexander, M.E., Jeschke, J.M., Ricciardi, A., MacIsaac, H.J., Robinson, T.B., Kumschick, B., Weyl, O.L.F., Dunn, A.M., Hatcher, M.J., Paterson, R.A.,

Farnsworth, K.D. & Richardson, D.M. 2014. Advancing impact prediction and hypothesis testing in invasion ecology using a comparative functional response approach. *Biological Invasions*, 16: 735–753.

Dick, J.T.A., Alexander, M.E., Ricciardi, A., Laverty, C., Downey, P.O., Xu, M., Jeschke, J.M., Saul, W-C., Hill, M.P., Wasserman, R., Barrios-O'Neill, D., Weyl, O.L.F. & Shaw, R.H. 2017b. Functional responses can unify invasion ecology. *Biological Invasions*, 19(5): 1667–1672.

Dick, J.T.A., Gallagher, K., Avlijas, S., Clarke, H.C., Lewis, S.E., Leung, S., Minchin, D., Caffrey, J., Alexander, M.E., Maguire, C., Harrod, C., Reid, N., Haddaway, N.R., Farnsworth, K.D., Penk, M. & Ricciardi, A. 2013. Ecological impacts of an invasive predator explained and predicted by comparative functional responses. *Journal of Biological Invasions*, 15: 837–846.

Dick, J.T.A., Laverty, C., Lennon, J.J., Barrios-O'Neill, D., Mensink, P.J., Britton, J.R., Medoc, V., Boets, P., Alexander, M.E., Taylor, N.G., Dunn, A.M., Hatcher, M.J., Rosewarne, P.J., Crookes, S., MacIsaac, H.J., Xu, M., Ricciardi, A., Wasserman, R.J., Ellender, B.R., Weyl, O.L.F., Lucy, F.E., Banks, P.B., Dodd, J.A., MacNeil, C., Penk, M.R., Aldridge, D.C. & Caffrey, J.M. 2017a. Invader Relative Impact Potential: a new metric to understand and predict the ecological impacts of existing, emerging and future invasive alien species. *Applied Ecology*, 54(4): 1259–1267.

Dodson, S.I. & Frey, D.G. 1991. The Cladocera and other Branchiopoda. In Thorpe, J.H. & A.P. Covich (eds), Ecology and Systematics of North American Freshwater Invertebrates. Academic Press, San Diego.

Dodson, S.I. & Hanazato, T. 1995a. Commentary on Effects of Anthropogenic and Natural Organic- Chemicals on Development, Swimming Behavior, and Reproduction of Daphnia, a Key Member of Aquatic Ecosystems. *Environmental Health Perspectives,* 103: 7-11.

Dodson, S.I., Hanazato, T. & Gorski, P.R. 1995b. Behavioral responses of *Daphnia pulex* exposed to carbaryl and Chaoborus kairomone. *Environmental Toxicological Chemistry*, 14: 43–50.

Dodson, S.I., Tollrian, R. & Lampert, W. 1997. Daphnia swimming behavior during vertical migration. *Plankton Research*, 19 (8): 969-978.

Duquesne, S. & Küster, E. 2010. Biochemical, metabolic, and behavioural responses and recovery of *Daphnia magna* after exposure to an organophosphate. *Ecotoxicological Environmental Safety*, 73 (3): 353–359.

Dzialowski, E.M., Turner, P.K. & Brooks, B.W., 2006. Physiological and reproductive effects of beta adrenergic receptor antagonists in *Daphnia magna*. *Archives of Environmental Contamination of Toxicology*, 50 (4): 503–510.

Ebert, D. 2005. *Ecology, Epidemiology, and Evolution of Parasitism in Daphnia*. Bethesda (MD): National Library of Medicine (US), National Center for Biotechnology.

Englund, G., Öhlund, G., Hein, C.L. & Diehl, S. 2011. Temperature dependence of the functional response. *Ecology Letters*, 14(9): 914–921.

European Centre For Ecotoxicology And Toxicology Of Chemicals (ECETOC). 2007. Intelligent testing strategies in ecotoxicology: Mode of action approach for specifically acting chemicals. Technical Report 102, Brussels, Belgium.

Fiehn, O. 2002. Metabolomics: the link between genotypes and phenotypes. *Plant Molecular Biology*, 48(1-2): 155–71.

Finn, J., Hui, M., Li, V., Lorenzi, V., de la Paz, N., Cheng, S.H., Lai-Chan, L. & Schlenk, D. 2012. Effects of propranolol on heart rate and development in Japanese medaka (*Oryzias latipes*) and zebrafish (*Danio rerio*). *Aquatic Toxicology*, 122: 214-221.

Frens, G. 1973. Controlled Nucleation for the Regulation of the Particle Size in Monodisperse Gold Suspensions. *Nature Physics,* 241: 20-22.

Galdiero, E., Falanga, A., Siciliano, A., Maselli, V., Guida, M., Carotenuto, R., Tussellino, M., Lombardi, L., Benvenuto, G. & Galdiero, S. 2017. *Daphnia magna* and *Xenopus laevis* as in vivo models to probe toxicity and uptake of quantum dots functionalized with gH625. *International Journal of Nanomedicine*, 12: 2717–2731.

García-Cambero, J.P., García, M.M., López, G.D., Herranz, A.L., Cuevas, L., Pérez-Pastrana, E., Cuadal, J.S., Castelltort, M.R. & Calvo, A.C. 2013. Converging

hazard assessment of gold nanoparticles to aquatic organisms. *Chemosphere*, 93: 1194–1200.

Ginjupalli, G.K., Gerard, P.D. & Baldwin, W.S. 2015. Arachidonic acid enhances reproduction in *Daphnia magna* and mitigates changes in sex ratios induced by pyriproxyfen. *Environmental Toxicological Chemistry*, 34(3): 527-535.

Gökçe, D., Köytepe, S. & Özcan, I. 2018. Effects of nanoparticles on *Daphnia magna* population dynamics. *Chemistry and Ecology*, 34(4): 301-323.

Gole, A. & Murphy, J.C. 2004. Seed-Mediated Synthesis of Gold Nanorods: Role of the Size and Nature of the Seed. *Chemistry Matter*, 16: 3633-3640.

Gomez-Casati, D.F., Grisolía, M. & Busi, M.V. 2016. The Significance of Metabolomics in Human Health. *Medical and Health Genomics*: 89–100.

Gomez-Casati, D.F., Zanor, M.I., & Busi, M.V. 2013. Metabolomics in Plants and Humans: Applications in the Prevention and Diagnosis of Diseases. *BioMed Research International*, 2013: 1–11.

Greene, M., Pitts, W. & Dewprashad, B. 2017. Using Videography to Study the Effects of Stimulants on *Daphnia magna*. *The American Biology Teacher*, 79 (1): 35–40.

Griffitt, R.J., Luo, J., Gao, J., Bonzongo, J.C. & Barber, D.S. 2008. Effects of particle composition and species on toxicity of metallic nanomaterials in aquatic organisms. *Environmental Toxicology and Chemistry*, 27 (9): 1972–1978.

Griffin, J.L. & Shockcor, J.P. 2004. Metabolic profiles of cancer cells. *Nature Review Cancer*, 4(7): 551–561.

Haddaway, N.R.,Wilcox, R.H., Heptonstall, R.E., Griffiths, H.M., Mortimer, R.J.G., Christmas, M. & Dunn, A.M. 2012. Predatory functional response and prey choice identify predation differences between native/invasive and parasitised/unparasitised crayfish. *PLoS One*, 7(2):e32229.

Hall, R., Beale, M., Fiehn, O., Hardy, N., Sumner, L. & Bino, R. 2002. Plant metabolomics: the missing link in functional genomics strategies. *Plant Cell*, 14(7): 1437–1440.

Han, G.H., Hur, H.G. & Kim, S.D. 2006. Ecotoxicological Risk of Pharmaceuticals from Wastewater Treatment Plants in Korea: Occurrence and Toxicity to *Daphnia magna*. *Environmental Toxicology and Chemistry*, 25(1): 265-271.

Handy, R.D., Eddy, F.B. & Romain, G. 1989. In vitro evidence for the ionoregulatory role of rainbow trout mucus in acid, acid/aluminium and zinc toxicity. *Journal of Fish Biology*, 35: 737-747.

Harris, J.E. 1953. Physical Factors involved in the Vertical Migration of Plankton. *Microscopical Science*, 94 (4): 537-550.

Hartmann, S., Louch, R., Zeumer, R., Steinhoff, B., Mozhayeva, D., Engelhard, C., Schönherr, H., Schlechtriem, C. & Witte, K. 2019. Comparative multi-generation study on long-term effects of pristine and wastewater-borne silver and titanium dioxide nanoparticles on key lifecycle parameters in *Daphnia magna*. *NanoImpact*, 14: 1-13.

Hassan, P.A., Rana, S. & Verma, G. 2015. Making Sense of Brownian Motion: Colloid Characterization by Dynamic Light Scattering. *Langmuir*, 31 (1): 3-12.

Heckmann, L.H., Sibly, R.M., Connon. R., Hooper, H.L., Hutchinson, T.H., Maund, S.J., Hill, C.J., Bouetard, A. & Callaghan, A. 2008. Systems biology meets stress ecology: linking molecular and organismal stress responses in *Daphnia magna*. *Genome Biology*, 9(2): R40.

Holling, C.S. 1959. Some Characteristics of Simple Types of Predation and Parasitism. *The Canadian Entomologist*, 91(07): 385–398.

Hu, X., Zhang, Y., Ding, T., Liu, J. & Zhao, H. 2020. Multifunctional Gold Nanoparticles: A Novel Nanomaterial for Various Medical Applications and Biological Activities. *Frontiers in Bioengineering and Biotechnology*, 8: 990.

Idle, J.R., & Gonzalez, F.J. 2007. Metabolomics. *Cell Metabolism*, 6(5): 348–351.

Ignace, D.D., Dodson, S.I. & Kashian, D.R. 2010. Identification of the critical timing of sex determination in *Daphnia magna* (Crustacea, Branchiopoda) for use in toxicological studies. *Hydrobiologia,* 668: 117–123.

Iswarya, V., Manivannan, J., De, A., Paul, S., Roy, R., Johnson, J.B., Kundu, R., Chandrasekaran, N., Mukherjee, A. & Mukherjee, A. 2016. Surface capping and

size-dependent toxicity of gold nanoparticles on different trophic levels. *Environmental Science of Pollution Research,* 23: 4844–4858.

Jansen, M., Coors, A., Stoks, R. & De Meester, L. 2011. Evolutionary ecotoxicology of pesticide resistance: a case study in Daphnia. *Ecotoxicology*, 20(3): 543–551.

Jensen, T.C. & Hessen, D.O. 2007. Does excess dietary carbon affect respiration of Daphnia*? Journal of Oecologia*, 152: 191-200.

Jensen, K.H., Kleiven, O.T. & Jakobsen, P.J. 1999. How important is light in the aggregation behaviour of *Daphnia pulex* (Cladocera: Crustacea)? *Hydrobiologia*, 411: 13–18.

Jeong, T.-Y., Yoon, D., Kim, S., Kim, H.Y. & Kim, S.D. 2018. Mode of action characterization for adverse effect of propranolol in *Daphnia magna* based on behavior and physiology monitoring and metabolite profiling *Environmental Pollution*, 233: 99-108.

Jeong, T.-Y. & Simpson, M.J. 2019. *Daphnia magna* metabolic profiling as a promising water quality parameter for the biological early warning system. *Water Research*, 166: 115033-115042.

Jeong, T.-Y. & Simpson, M.J. 2020. Time-dependent biomolecular responses and bioaccumulation of perfluorooctane sulfonate (PFOS) in *Daphnia magna*. *Comparative Biochemistry and Physiology Part D: Genomics and Proteomics*, 35: 100701-100707.

Jeschke, J. M., Kopp, M. & Tollrian, R. 2002. Predator Functional Responses: Discriminating between Handling and Digesting Prey. *Ecological Monographs*, 72(1): 95-112.

Jeschke, J.M., Kopp, M. & Tollrian, R. 2004. Consumer-food systems: why type I functional responses are exclusive to filter feeders. *Biological Reviews*, 79(2): 337–349.

Juliano, S.A. 2001. Nonlinear curve fitting: predation and functional response curves. In: Scheiner SM, Gurevitch J (eds) Design and analysis of ecological experiments. Oxford University Press, Oxford, pp 178–196.

Kabir, E., Kumar, V., Kim, K., Yip, A.C.K. & Sohn, J.R. 2018. Environmental impacts of nanomaterials. *Journal of Environmental Management,* 146: 261–271.

Karatzas, P., Melagraki, G., Ellis, L-J.A., Lynch, I., Varsou, D-D, Afantitis, A., Tsoumanis, A., Doganis, P., & Sarimveis, H. 2020. Development of Deep Learning Models for Predicting the Effects of Exposure to Engineered Nanomaterials on *Daphnia magna*. *Nano-micro small Journal*, 2001080: 1-12.

Kaas, B., Krishnarao, K., Marion, E., Stuckey, L. & Kohn, R. 2009. Effects of melatonin and ethanol on the heart rate of *Daphnia magna*. *The Premier Journal for Undergraduate Publications in the Neurosciences*, 1-8.

Kapoore, R.V. & Vaidyanathan, S. 2016. Towards quantitative mass spectrometry-based metabolomics in microbial and mammalian systems. *Philosophical Transactions of the Royal Society A: Mathematical, Physical and Engineering Sciences*, 374 (2079): 20150363.

Kelpsiene, E., Torstensson, O., Ekvall, M.T., Hansson, L.-A. & Cedervall, T. 2020. Long-term exposure to nanoplastics reduces life-time in *Daphnia magna*. S*cientific Reports*, 10: 59-79.

Kish, A. 2017. The Impact of Round Up® on *Daphnia Magna*. AAAS Annual Meeting.

Khan, A.K., Rashid, R., Murtaza, G. & Zahra, A. 2014. Gold Nanoparticles: Synthesis and Applications in Drug Delivery. *Tropical Journal of Pharmaceutical Research*, 13 (7): 1169-1177.

Khan, I., Saeed, K. & Khan, I. 2019. Nanoparticles: Properties, Applications and Toxicities. *Arabian Journal of Chemistry*, 12(7): 908-931.

Kim, I., Lee, B., Kim, H., Kim, K., Kim, S.D. & Hwang, Y. 2015. Citrate coated silver nanoparticles change heavy metal toxicities and bioaccumulation of *Daphnia magna*. *Chemosphere*, 99–105.

Knops, M., Altenburger, R. & Segner, H. 2001. Alterations of physiological energetics, growth, and reproduction of *Daphnia magna* under toxicant stress. *Aquatic Toxicology*, 53: 79-90.

Kovacevic, V., Simpson, A.J. & Simpson, M.J. 2016. 1 H NMR-based metabolomics of *Daphnia magna* responses after sub-lethal exposure to triclosan, carbamazepine

and ibuprofen. *Comparative Biochemistry and Physiology Part D: Genomics and Proteomics*, 19: 199–210.

Kozanoglu, D., Apaydin, D.H., Cirpan, A. & Esenturk, E.N. 2013. Power conversion efficiency enhancement of organic solar cells by addition of gold nanostars, nanorods, and nanospheres. *Organic Electronics*, 14 (7): 1720-1727.

Lari, E., Steinkey, D., Morandi, G., Rasmussen, J.B., Giesy, J.P. & Pyle, G.G. 2017. Oil sands process-affected water impairs feeding by *Daphnia magna*. *Chemosphere*, 175: 465-472.

Leatherman, A.K., Pirlamarla, B.P., Rogman, S., Yodice, D.S. & Kohn, R.E. 2009. The Neurophysiological Effects of Guarana and Ethanol Intake on *Daphnia magna*. *The Premier Journal for Undergraduate Publications in the Neurosciences*, 1-8.

Lee, B.T. & Ranville, J.F. 2012. The Effect of Hardness on the Stability of Citrate-Stabilized Gold Nanoparticles and Their Uptake by *Daphnia Magna*. *Hazardous Materials*, 213–214: 434–439.

Lei, Z., Huhman, D.V. & Sumner, L.W. 2011. Mass spectrometry strategies in metabolomics. *Biological Chemistry*, 286(29): 25435–42.

Lenth, R. 2018. emmeans: Estimated Marginal Means, aka Least-Squares Means. R package version1.1.3. https://CRAN.R-project.org/package=emmeans. 2018.

Li, T., Albee, B., Alemayehu, M., Diaz, R., Ingham, L., Kamal, S., Rodriguez, M & Bishnoi, S.W. 2010. Comparative toxicity study of Ag, Au, and Ag–Au bimetallic nanoparticles on *Daphnia magna*. *The journal of Anal Bioanal Chemistry*, 689–700.

Li, S., Zhang, L., Wang, T., Li, L., Wang, C. & Su, Z. 2015. The facile synthesis of hollow Au nanoflowers for synergistic chemo-photothermal cancer therapy. *Chemical Commununication*, 51: 14338–14341.

Liu, S., Cui, M., Li, X., Thuyet, D.Q. & Fan, W. 2019. Effects of hydrophobicity of titanium dioxide nanoparticles and exposure scenarios on copper uptake and toxicity in *Daphnia magna*. *Water Research*, 154: 162-170.

Lorke, D. 1983. A new approach to practical acute toxicity testing. *Archives of Toxicology*, 54(4): 275–287.

Lovern, S.B., Strickler, J.R. & Klaper, R. 2007. Behavioral and physiological changes in *Daphnia magna* when exposed to nanoparticle suspensions (titanium dioxide, nano-C60, and C60HxC70Hx). *Environmental Sciences & Technology*, 41: 4465–4470.

Lovern, S.B., Owen, H.A. & Klaper, R. 2008. Electron microscopy of gold nanoparticle intake in the gut of *Daphnia magna*. *Nanotoxicology*, 2(1): 43-48.

Mattsson, K., Aguilar, R., Torstensson, O., Perry, D., Bernfur, K., Linse, S., Hansson, L.A., Åkerfeldt, K.S. & Cedervall, T. 2018. Disaggregation of gold nanoparticles by *Daphnia magna*. *Nanotoxicology*, 12 (8): 885-900.

Miner, B.E., De Meester, L., Pfrender, M.E., Lampert, W. & Hairston, N.G. 2012. Linking genes to communities and ecosystems: Daphnia as an ecogenomic model. *Proceedings of the Royal Society B: Biological Sciences*, 279 (1735): 1873–1882.

Mohammadpour, R., Dobrovolskaia, M.A., Cheney, D.L., Greish, K.F. & Ghandehari, H. 2019. Subchronic and chronic toxicity evaluation of inorganic nanoparticles for delivery applications. *Advanced Drug Delivery Reviews*, 144: 112-132.

Murphy, C.J., Gole, A.M., Stone, J.W., Sisco, P.N., Alkilany, A.M., Goldsmith, E.C. & Baxter, S.C. 2008. Gold Nanoparticles in Biology: Beyond Toxicity to Cellular Imaging. *Accounts of Chemical Research,* 41 (12): 1721-1730.

Muyssen, B.T.A., De Schamphelaere, K.A.C. & Janssen, C.R. 2006. Mechanisms of chronic waterborne Zn toxicity in *Daphnia magna*. *Aquatic Toxicology*, 77: 393–401.

Nasser, F., Davis, A., Valsami-Jones, E. & Lynch, I. 2016. Shape and Charge of Gold Nanomaterials Influence Survivorship, Oxidative Stress and Moulting of *Daphnia magna*. *Nanomaterials*, 6 (12): 222–234.

Nehl, C.L., Liao, H. & Hafner, J.H. 2006. Optical Properties of Star-Shaped Gold Nanoparticles. *Nano letters*, 6 (4): 683-688.

Oaten, A. & Murdoch, W.W. 1975. Functional Response and Stability in Predator-Prey Systems. *The American Naturalist*, 109 (967): 289–298.

OECD, 2004. OECD Guideline for the Testing of Chemicals. Guideline 202: *Daphnia magna* Acute Immobilisation Test. Organisation for EconomicCo-operation and Development, France.

OECD, 2012. OECD Guideline for the Testing of Chemicals. Guideline 211: *Daphnia magna* Reproduction Test. Organisation for Economic Co-operation and Development, France.

OECD, 2020. OECD Guideline for testing of chemicals. No.97, Series on the Safety of Manufactured Nanomaterials. Paris: OECD.

Oleszczuk, P., Jośko, I. & Skwarek, E. 2015. Surfactants decrease the toxicity of ZnO, TiO2 and Ni nanoparticles to *Daphnia magna*. *Ecotoxicology*, 24(9): 1923–1932.

Oliveira-Pereira, E.A., Labine, L.M., Kleywegt, S., Jobst, K.J., Simpson, A.J. & Simpson, M.J. 2021. Metabolomics Reveals That Bisphenol Pollutants Impair Protein Synthesis-Related Pathways in *Daphnia magna*. *Metabolites*, 11: 666.

Owen, S.F., Giltrow, E., Huggett, D.B., Hutchinson, T.H., Saye, J., Winter, M.J. & Sumpter, J.P. 2007. Comparative physiology, pharmacology and toxicology of bblockers: mammals versus fish. *Aquatic Toxicology*, 82: 145-162.

Pacheco, A., Martins, A. & Guilhermino, L. 2018. Toxicological interactions induced by chronic exposure to gold nanoparticles and microplastics mixtures in *Daphnia magna*. *Science of the Total Environment*, 628–629: 474–483.

Pane, E.F., Smith, C., McGeer, J.C. & Wood, C.M. 2003. Mechanisms of acute and chronic waterborne nickel toxicity in the freshwater cladoceran, *Daphnia magna*. *Environmental Science & Technology*, 37: 4382-4389.

Pang, Z., Chong, J., Li, S. & Xia, J. 2020. MetaboAnalystR 3.0: Toward an Optimized Workflow for Global Metabolomics. *Journal of Metabolites*, 10(5): 186.

Park, S., Jo, A., Choi, J., Kim, J., Zoh, K. & Choi, K. 2019. Rapid screening for ecotoxicity of plating and semiconductor wastewater employing the heartbeat of *Daphnia magna*. *Ecotoxicology and Environmental Safety*, 186: 1-7.

Park, J., Park, C.P., Sung, B., Lee, Y-O., Ryu, C.S., Ja Young Park, J-Y. & Kim, Y.J. 2021. Acute Adverse Effects of Metallic Nanomaterials on Cardiac and Behavioral Changes in *Daphnia magna*. *Research Square*, 18: 1-21.

Paul, R.J., Colmorgen, M., Pirow, R., Chen, Y.H. & Tsai, M.C. 1998. Systemic and metabolic responses in *Daphnia magna* to anoxia. *Comparative Biochemistry and Physiology Part A: Molecular Integrative Physiology*, 120: 519-530.

Paul, R.J., Zeis, B., Lamkemeyer, T., Seidl, M. & Pirow, R. 2004. Control of oxygen transport in the microcrustacean Daphnia: regulation of haemoglobin expression as central mechanism of adaptation to different oxygen and temperature conditions. *Acta Physiologica Scandinavica*, 182: 259-275.

Penalva-Arana, D.C., Forshay, K., Johnson, P.T.J., Strickler, J.R. & Dodson, S.I. 2011. Chytrid infection reduces thoracic beat and heart rate of *Daphnia pulicaria*. *Hydrobiologia*, 668: 147-154.

Pijanowska, J. & Kowalczewski, A. 1997. Predators can induce swarming behaviour and locomotory responses in Daphnia. *Freshwater Biology*, 37: 649–656.

Pirow, R., Bäumer, C. & Paul, R.J. 2001. Benefits of haemoglobin in the cladoceran crustacean *Daphnia magna*. *Experimental Biology*, 204: 3425–3441.

Pirow, R., Bäumer, C. & Paul, R.J. 2004. Crater landscape: two-dimensional oxygen gradients in the circulatory system of the microcrustacean *Daphnia magna*. *Experimental Biology*, 204: 4393-4405.

Pirow, R., Wollinger, F. & Paul, R.J. 1999a. The sites of respiratory gas exchange in the planktonic crustacean *Daphnia magna*: an in vivo study employing blood haemoglobin as an internal oxygen probe. *Experimental Biology*, 202: 3089–3099.

Pirow, R., Wollinger, F. & Paul, R.J., 1999b. The importance of the feeding current for oxygen uptake in the water flea *Daphnia magna*. *Experimental Biology*, 202: 553-562.

Pissuwan, D., Camilla, G., Mongkolsuk, S. & Cortie, M.B. 2019. Single and multiple detections of foodborne pathogens by gold nanoparticle assays. *WIREs Nanomedicine and Nanobiotechnology*, 12: 1584.

Pohnert, G. 2019. Kairomones: Finding the fish factor. *Journal of eLife*, 48459: 1-3.

Postmes, T.J., Nacken, G. & Nelissen, R.G. 1973. An electronic method for measuring the heart frequency of the water flea: *Daphnia pulex*. *Experientia*, 30: 1478– 1480.

Pritchard, D.W. 2014. frair: Functional response analysis in R. R package version 0.4.

Pritchard, D.W., Paterson, R.A., Bovy, H.C. & Barrios-O'Neill, D. 2017. Frair: an R package for fitting and comparing consumer functional responses. responses. *Methods in Ecology and Evolution*, 8(11): 1528–1534.

Qiao, L., Wanga, D., Zuo, L., Ye, Y., Qian, J., Chen, H. & He, S. 2011. Localized surface plasmon resonance enhanced organic solar cell with gold nanospheres. *Journal of Applied Energy*, 88 (3): 848-852.

Ramalingam, V. 2019. Multifunctionality of gold nanoparticles: plausible and convincing properties. . *Advances in Colloid and Interface Science*, 271: 101989.

Riediker, M., Zink, D., Kreyling, W., Oberdörster, G., Elder, A., Graham, U., Lynch, I., Duschl, A., Ichihara, G., Ichihara, S., Kobayashi, T., Hisanaga, N., Umezawa, M., Cheng, T., Handy, R., Gulumian, M., Tinkle, S. & Cassee, F. 2019. Particle toxicology and health - where are we? *Particle and Fibre Toxicology*, 1-33.

Ringelberg, J. & Servass, H. 1971. Circadian Rhythm in *Daphnia magna*. *Oecologia*, 6: 289-292.

Ringelberg, J. 1991a. Enhancement of the phototactic reaction in *Daphnia hyalina* by a chemical mediated by juvenile perch (*Perca fluviatilis*). *Plankton Research*, 13 (1): 17-25.

Ringelberg, J. 1991b. A mechanism of predator-mediated induction of diel vertical migration in *Daphnia hyaline*. *Plankton Research*, 13 (1): 83-89.

Robison, A.L., Chapman, T. & Bidwell, J.R. 2018. Predation cues influence metabolic rate and sensitivity to other chemical stressors in fathead minnows (*Pimephales promelas*) and *Daphnia pulex*. Ecotoxicology, 27: 55-68.

Römer, I., Gavin, A.J., White, T.A., Merrifield, R.C., Chipman, J.K., Viant, M.R. & Lead, J.R. 2013. The critical importance of defined media conditions in *Daphnia magna* nanotoxicity studies. *Toxicology letters*, 103-108.

Rusilowicz, M., Dickinson, M., Charlton, A., O'Keefe, S. & Wilson, J. 2016. A batch correction method for liquid chromatography–mass spectrometry data that does not depend on quality control samples. *Metabolomics*, 12(3): 56-66.

Sarma, S.S.S. & Nandini, S. 2006. Review of Recent Ecotoxicological Studies on Cladocerans. *Environmental Science and Health*, Part B, 41(8): 1417–1430.

Schmoker, C. & Hernández -León, S. 2003. The effect of food on the respiration rates of *Daphnia magna* using a flow-through system. *Scientia Marina*, 67 (3): 361-365.

Shah, M., Badwaik, V., Kherde, Y., Waghwani, H.K., Modi, T., Aguilar, Z.P., Rodgers, H., Hamilton, W., Marutharaj, T., Webb, C., Lawrenz, M.B. & Dakshinamurthy, R. 2014. Gold nanoparticles: various methods of synthesis and antibacterial applications. *Frontiers in Bioscience*, 19: 1320-1344.

Shahid, N., Rolle-Kampczyk, U., Siddique, A., von Bergen, M. & Liess, M. 2021. Pesticide-induced metabolic changes are amplified by food stress. *of Science of the Total Environment*, 792: 148350.

Simão, F.C., Martínez-Jerónimo, F., Blasco, V., Moreno, F., Porta, J.M., Pestana, J.L., Soares, A.M.V.M., Raldúa, D. & Barata, C. 2019. Using a new high-throughput video-tracking platform to assess behavioural changes in *Daphnia magna* exposed to neuro-active drugs. *Science of the Total Environment,* 662 (20): 160-167.

Solomon, M.E. 1949. The natural control of animal popula- tions. *Animal Ecology*, 18:1–35.

South, J., Botha, T.L., Wolmarans, N.J., Wepener, V. & Weyl, O.L.F. 2019. Assessing predator-prey interactions in a chemically altered aquatic environment: the effects of DDT on *Xenopus laevis* and *Culex sp*. larvae interactions and behaviour. *Ecotoxicology*, 28 (7): 771-780.

South, J. & Dick, J.T.A. 2017. Effects of acute and chronic temperature changes on the functional responses of the dogfish *Scyliorhinus canicula* (Linnaeus, 1758) towards amphipod prey *Echinogammarus marinus* (Leach, 1815). *Environmental Biology of Fishes*, 100(10): 1251–1263.

Southam, A.D., Lange, A., Hines, A., Hill, E.M., Katsu, Y., Iguchi, T., Tyler, C.R. & Viant, M.R. 2011. Metabolomics Reveals Target and Off-Target Toxicities of a Model Organophosphate Pesticide to Roach (*Rutilus rutilus*): Implications for Biomonitoring. *Environmental Science & Technology*, 45(8): 3759–3767.

Spratlin, J.L., Serkova, N.J. & Eckhardt, S.G. 2009. Clinical Applications of Metabolomics in Oncology: A Review. *Clinical Cancer Research*, 15(2): 431–440.

Stanier, R.Y. & Cohen-Bazire, G. 1977. Phototrophic prokaryotes: the cyanobacteria. *Annual Review of Microbiology*, 31: 225-274.

Stanley, J.K., Laird, J.G., Kennedy, A.J. & Steevens, J.A. 2016. Sublethal effects of multiwalled carbon nanotube exposure in the invertebrate *Daphnia magna*. *Environmental Toxicological Chemistry*, 35: 200–204.

Stanley, J.K., Ramirez, A.J., Mottaleb, M., Chambliss, C.K. & Brooks, B.W. 2006. Enantiospecific toxicity of the b-blocker propranolol to *Daphnia magna* and *Pimephales promelas*. *Environmental Toxicology and Chemistry*, 25: 1780-1786.

Stearns, C.S. 1975. Light responses of *Daphnia pulex*. *Limnology and Oceanography*, 20 (4): 564-570.

Stitt, M. & Fernie, A.R. 2003. From measurements of metabolites to metabolomics: an 'on the fly' perspective illustrated by recent studies of carbon–nitrogen interactions. *Current Opinion Biotechnology*, 14(2): 136–44.

Stross, R.G. & Hill, J.C. 1965. Diapause induction in Daphnia requires two stimuli. *Science*, 150: 1462-1464.

Sun, X. & Weckwerth, W. 2012. COVAIN: a toolbox for uni- and multivariate statistics, time-series and correlation network analysis and inverse estimation of the differential Jacobian from metabolomics covariance data. *Metabolomics*, 8(S1), 81–93.

Szabelak, A. & Bownik, A. 2021. Behavioral and physiological responses of *Daphnia magna* to salicylic acid. *Chemosphere*, 270: 128660.

Tessier, A.J., Leibold, M.A. & Tsao, J. 2000. A Fundamental trade -off in resource exploitation by Daphnia and consequences to plankton communities. *Ecology,* 81: 826- 841.

Tkaczyk, A., Bownik, A., Dudka, J., Kowal, K. & Ślaska, B. 2020. *Daphnia magna* model in the toxicity assessment of pharmaceuticals: A review. *Science of the Total Environment*, 763: 1-57.

Truter, E. 1994. Methods of estimating the Chronic Toxicity of a chemical or water sample to the Cladoceran *Daphnia pulex*, Department of Water Affairs and Forestry, Department of Water Affairs & Forestry, Pretoria.

Verma, H.N., Singh, P. & Chavan, R.M. 2014. Gold nanoparticle: synthesis and characterization. *Veterinary World*, 7(2): 72-77.

Vicky, V.M., Rodney, S., Ajay, S. & Hardik, R. 2010. Introduction to Metallic nanoparticles. *J Pharmacy and Bioallied Sciences*, 2(4): 282-289.

Villegas-Navarroa, A., Rosas-L, E. & Reyes, J.L. 2003. The heart of *Daphnia magna*: effects of four cardioactive drugs. *Comparative Biochemistry and Physiology Part C*, 136: 127–134.

Villeneuve, D.L., Crump, D., Garcia-Reyero, N., Hecker, M., Hutchinson, T.H., Lalone, C.A., Landesmann, B., Lattieri, T., Munn, S., Nepelska, M., Ottinger, M.A., Vergauwen, L. & Whelan, M. 2014. Adverse outcome pathway (AOP) development 1: strategies and principles. *Toxicological Sciences,* 142 (2): 312–320.

Walum, E. 1998. Acute oral toxicity. *Environmental Health Perspectives*, 106 (2): 497-503.

Wang, ,L., Jiang, X., Ji, Y., Bai, R., Zhao, Y., Wu, X. & Chen, C. 2013. Surface chemistry of gold nanorods: origin of cell membrane damage and cytotoxicity. *Nanoscale*, 5: 8384- 8391.

Wang, P., Ng, Q.X., Zhang, H., Zhang, B., Ong, C N. & He, Y. 2018. Metabolite changes behind faster growth and less reproduction of *Daphnia similis* exposed to low-dose silver nanoparticles. *Ecotoxicology and Environmental Safety*, 163: 266–273.

Wang, P., Ng, Q., Zhang, B., Wei, Z., Hassan, M., He, Y. & Ong, C.N. 2019. Employing multi-omics to elucidate the hormetic response against oxidative stress exerted by nC60 on *Daphnia pulex*. *Environmental Pollution*, 251: 22–29.

Ward, H.B. & Whipple, G.C. 1959. *Fresh-water Biology 2nd edition*. W.T. Edmondson, ed. John Wiley & Sons, Inc. New York. 1248 pp.

Watts, S.A., Lawrence, C., Powell, M. & D'Abramo, L.R. 2016. The Vital Relationship Between Nutrition and Health in Zebrafish. *Zebrafish*, 13 (1): 1299-103.

Watts, S.A., Powell, M. & D'Abramo, L.R. 2012. Fundamental Approaches to the Study of Zebrafish Nutrition. *ILAR Journal*, 53(2): 144–160.

Weckwerth W. 2003. Metabolomics in systems biology. *Annual Review Plant Biology*, 54 (1): 669–689.

Weider, L.J. & Lampert, W. 1985. Differential response of Daphnia genotypes to oxygen stress: respiration rates, hemoglobin content and low-oxygen tolerance. *Oecologia*, 65: 487-491.

Weinberg, H., Galyean, A. & Leopold, M. 2011. Evaluating engineered nanoparticles in natural waters. *rends in Analytical Chemistry*, 30 (1): 72–83.

Weiss, L.C., Albada, B., Becker, S.M., Meckelmann, S.W., Klein, J., Meyer, M., Schmitz, O.J., Sommer, U., Leo, M., Zagermann, J., Metzler-Nolte, N. & Tollrian, R. 2018. Identification of Chaoborus kairomone chemicals that induce defences in Daphnia. *Nature Chemical Biology*, 14:1133–1139.

Wetzel, R.G. 1975. *Limnology*. W.B. Saunders Co. Philadelphia, PA. 743 pp.

Woermann, M. & Sures, B. 2020. Ecotoxicological effects of micropollutant-loaded powdered activated carbon emitted from wastewater treatment plants on *Daphnia magna*. *Science of the Total Environment*, 746: 141104-141112.

Wong, B. & Ward, F.J. 1972. Size Selection of *Daphnia pulicaria* by Yellow Perch (Perca flavescens) Fry in West Blue Lake, Manitoba. *Journal of the Fisheries Research Board of Canada*, 29(12): 1761–1764.

Wray, A.T. & Klaine, S.J. 2015. Modeling The Influence of Physicochemical Properties on Gold Nanoparticle Uptake And Elimination by *Daphnia magna*. *Environmental Toxicology and Chemistry, 34 (4)*: 860–872.

Wu, Y. & Li, L. 2016. Sample normalization methods in quantitative metabolomics. *Chromatography A*, 1430: 80–95.

Xiao, T., Huang, J., Wang, D., Meng, T. & Yang, X. 2019. Au and AuBased nanomaterials: synthesis and recent progress in electrochemical sensor applications. *Talanta*, 206: 120210.

Yang, X., Yang, M., Pang, B., Vara, M. & Xia, Y. 2015. Gold Nanomaterials at Work in Biomedicine. *Chemical Reviews*, 115 (19): 10410-10488.

Zang, C., Laia, N., Abigail Gruse, A., Comfort, C. & Felder, M. 2019. Caffeine and acetylcholine decrease *Daphnia magna* heart rate. *Undergraduate Biology Laboratory Investigations*, 278: 1-5.

Zhang, B., Zhang, H., Du, C., Ng, Q.X., Hu, C., He, Y. & Ong, C.N. 2017. Metabolic responses of the growing *Daphnia similis* to chronic AgNPs exposure as revealed by GC-Q-TOF/MS and LC-Q-TOF/MS. *Water Research*, 114: 135–143.

Appendix A

NWU®
INTERNATIONAL UNIVERSITY
NOORDWES-UNIVERSITEIT
YUNIBESITI YA BOKONE BOPHIRIMA

Private Bag X1290, Potchefstroom
South Africa 2520
Tel: 018 299-1111/2222
Fax: 018 299-4910
Web: http://www.nwu.ac.za

Senate Committee for Research Ethics
Tel: 018 299-4849
Email: nkosinathi.machine@nwu.ac.za

ETHICS APPROVAL LETTER OF STUDY

Based on the review by the **Faculty of Natural and Agricultural Sciences Ethics Committee (FNASREC)**, the Committee hereby clears your study as no ethical risk. This implies that the FNASREC grants permission that, provided the general conditions specified below are met, the study may be initiated, using the ethics number below.

Study title: Application of Adverse Outcome Pathway framework in assessing nanogold exposure to Daphnia magna
Study Leader/Supervisor: Dr TL Botha
Student: A Mbangatha

Ethics number: N | W | U | - | 0 | 1 | 4 2 5 - 2 0 - A 9
Institution | Study Number | Year | Status

Status: S = Submission; R = Re-Submission; P = Provisional Authorisation; A = Authorisation

Application type: Single **Risk Category:** **No Risk**

Commencement date: 01/02/2020
Expiry date: 01/10/2022

General conditions:
The following general terms and conditions apply:

- *The commencement date indicates the date when the study may be started.*
- *In the interest of ethical responsibility, the NWU-SCRE and FNASREC reserves the right to:*
  - *request access to any information or data at any time during the course or after completion of the study;*
  - *to ask further questions, seek additional information, require further modification or monitor the conduct of your research or the informed consent process;*
  - *withdraw or postpone approval if:*
    - *any unethical principles or practices of the study are revealed or suspected;*
    - *it becomes apparent that any relevant information was withheld from the FNASREC or that information has been false or misrepresented;*
    - *submission of the annual (or otherwise stipulated) monitoring report, the required amendments, or reporting of adverse events or incidents was not done in a timely manner and accurately; and / or*
    - *new institutional rules, national legislation or international conventions deem it necessary.*
- *FNASREC can be contacted for further information or any report templates via Roelof.Burger@nwu.ac.za 018 299 4269*

The FNASREC would like to remain at your service as scientist and researcher, and wishes you well with your study. Please do not hesitate to contact the FNASREC or the NWU-SCRE for any further enquiries or requests for assistance.

Yours sincerely,

Prof Roelof Burger
Chairperson Faculty of Natural and Agricultural Sciences Ethics Committee (FNASREC)

File reference: 9.1.5.4.2

Page 1 of 1

Appendix B

The physico-chemical water parameters over the duration of the test.

Treatment groups	Conductivity (µs)	TDS (mg /L)	Temperature(◦C)	pH
CTAB capped rod shaped nAu	600.1 ± 17	425.1 ± 12.1	19 ± 0.1	7.9 ± 0.1
Citrate capped nAu	599 ± 17.0	420.3 ± 12.3	19 ± 0.1	7.9 ± 0.1
Ionic Au	619 ± 17.3	427.4 ± 12.8	19 ± 0.1	7.9 ± 0.2